Fall 2016

Event-sampled direct adaptive neural network control of uncertain strict-feedback system with application to quadrotor unmanned aerial vehicle

Nathan Szanto

Follow this and additional works at: https://scholarsmine.mst.edu/masters_theses

Part of the Electrical and Computer Engineering Commons

Department:

Recommended Citation

EVENT-SAMPLED DIRECT ADAPTIVE NEURAL NETWORK CONTROL OF

UNCERTAIN STRICT-FEEDBACK SYSTEM WITH APPLICATION TO

QUADROTOR UNMANNED AERIAL VEHICLE

by

NATHAN SZANTO

A THESIS

Presented to the Graduate Faculty of the

MISSOURI UNIVERSITY OF SCIENCE AND TECHNOLOGY

In Partial Fulfillment of the Requirements for the Degree

MASTER OF SCIENCE

in

ELECTRICAL ENGINEERING

2016

Approved by

Dr. Jagannathan Sarangapani, Advisor
Dr. Levent Acar
Dr. Joe Stanley

PUBLICATION THESIS OPTION

This thesis has been prepared in the form of two papers. It has been formatted in accordance with the specifications provided by the Missouri University of Science and Technology.

Paper I. Pages 5-53 have been submitted to 2016 IEEE Transactions on Neural Networks.

Paper II. Pages 54-109 are intended for submission to 2016 IEEE Transactions on Control Systems Technology. The second paper in this thesis has been augmented to include hardware results.

ABSTRACT

Neural networks (NNs) are utilized in the backstepping approach to design a control input by approximating unknown dynamics of the strict-feedback nonlinear system with event-sampled inputs. The system state vector is assumed to be unknown and an observer is used to estimate the state vector. By using the estimated state vector and backstepping design approach, an event-sampled controller is introduced. As part of the controller design, first, input-to-state-like stability (ISS) for a continuously sampled controller that has been injected with bounded measurement errors is demonstrated and, subsequently, an event-execution control law is derived such that the measurement errors are guaranteed to remain bounded. Lyapunov theory is used to demonstrate that the tracking errors, the observer estimation errors, and the NN weight estimation errors for each NN are locally uniformly ultimately bounded (UUB) in the presence bounded disturbances, NN reconstruction errors, as well as errors introduced by event-sampling. Simulation results are provided to illustrate the effectiveness of the proposed controllers.

Subsequently, the output-feedback neural network (NN) controller that was presented above is considered for an underactuated quadrotor UAV application. The flexibility for the control of a quadrotor UAV is extended by incorporating notions of event-sampling and by designing an appropriate event-execution law. First, the continuously sampled controller is considered in the presence of bounded measurement errors and it is shown that the system generates a local ISS-like Lyapunov function. Next, by designing an appropriate event-execution law, the measurement errors that result from event-sampling are shown to be bounded for all time. Finally, the effectiveness of the proposed event-sampled controller is demonstrated with simulation results.

ACKNOWLEDGMENTS

TABLE OF CONTENTS

SECTION

LIST OF ILLUSTRATIONS

LIST OF TABLES

SECTION

1 INTRODUCTION

1.1 BACKGROUND

Given their inherent approximation properties, neural networks (NNs) have become popular in real-world applications that include unknown dynamics. In addition, due to the fact that many dynamic systems can be expressed in the strict-feedback form, the incorporation of NNs in a backstepping design has become a natural approach in controller design. In strict-feedback systems that have unknown nonlinearities, subsystems are considered separately from one another and NNs are implemented in approximating the unknown part of each subsystem's virtual control law. A general control scheme for this approach is presented by Ge and Wang in [1]. However, the effort [1] requires full knowledge of the state vector, a provision that is not always guaranteed.

The need for full-knowledge of the state vector can be easily avoided with the implementation of a NN observer. As an example, the work in [2] models a quadrotor UAV system in strict-feedback form and circumvents the need for velocity sensors with an observer. In general, designing an output-feedback controller with backstepping is an approach that has been implemented in a number of different applications [3]-[6].

The previous works [1]-[6] on this class of systems assume a continuous sampling paradigm wherein the control law is executed at a fixed frequency. An alternative to the traditional sampling scheme, event-based sampling, is introduced by Tabuada in [7]: With event-sampling, the control is updated only when an event occurs. The immediate advantage to this is that the number of computations is reduced; furthermore, if all design parameters are appropriately selected, it can be shown that the reduction of computations can be achieved without compromising the fidelity of the controller.

The work in [7] introduces basic concepts of event-sampling and applies them to a general control system with known dynamics. Since then, a significant amount of work has been done in the development of event-based controllers and they have been discussed in various contexts, such as input-state stability [8], sensor/actuator networks [9], state-

and output-feedback systems [10][11], and trajectory tracking applications [12]. In these works [7]-[12], the dynamics are assumed to be known and the use of NNs becomes unnecessary; for this reason, the extent to which their results can be implemented in real-world applications is somewhat restrictive. Finally, the work in [13] extends the notions of event-based sampling to incorporate unknown dynamics in an NN-based controller for an affine nonlinear system. In any work presenting results in event-sampling, the derivation of an event-execution law is a necessary provision; a particularly useful conclusion given in [13] is the presentation of an execution law in the presence of NN approximations.

However, the degree to which the results [13] can be applied in practical applications is limited to affine systems. Moreover, the execution law presented relies on having knowledge of the NN weight estimates at the event-triggering mechanism. This necessitates "mirror estimators" that synchronously provide NN weight estimates at both the controller and at the event-triggering mechanism.

Additionally, the efforts in event-sampling [7]-[13] primarily consider generalized systems and do not make substantial contributions to the incorporation of intermittent sampling in real-world applications. To this effect, the works [14] and [15] make efforts to implement event-sampling in the context of real-world dynamics. In [14], an event-sampled approach is used in a vibration analysis for pneumatic tires; the work in [15] incorporates event-sampling with an observer-based controller and it considers the results in the context of a servoing control system. However, the efforts presented in [14] and [15] only consider dynamics that are simple enough to where it is unecessary to implement advanced adaptive methods. The incorporation of event-sampling in robotic applications that require extensive use of NNs is a topic which has not received much attention.

This thesis extends the applicability of event-sampling to situations which have not been previously explored. First, a general strict-feedback system will be considered. The Lyapunov method will be used to develop an event-sampled direct adaptive NN output-feedback controller for an uncertain nonlinear strict-feedback system. Subsequently, the

modified strict-feedback dynamics of an under-actuated quadrotor UAV will be considered in the derivation of an event-sampled NN-based output-feedback controller. The effectiveness of the proposed controllers will be illustrated with simulation results and it will be shown how the number of samples can be reduced without having to sacrifice controller performance.

1.2 OBJECTIVE

The primary objective of this thesis is to design two event-sampled controllers. First, an event-sampled output-feedback controller is derived for a general nonlinear uncertain strict-feedback system such that the output follows a desired trajectory. Next, an under-actuated quadrotor UAV system is considered. The derivation for an event-sampled output-feedback controller is derived such that the UAV follows a desired trajectory while maintaining stable flight.

1.3 ORGANIZATION

This thesis begins with this introductory section which is followed by two papers. The first paper, "Event-Sampled Direct Adaptive NN Output- and State-Feedback Control of Uncertain Strict-Feedback System," will show the derivation for the event-sampled controller for a general strict-feedback system. The primary contribution of the first paper is an output-feedback controller that utilizes an observer and relaxes the need for full knowledge of the state vector; the state-feedback case is presented as a corollary. The second paper, "Event-Sampled Control of Quadrotor UAV," presents the derivation for an event-sampled output-feedback control for a quadrotor UAV. Here, too, the need for additional sensors is avoided with the inclusion of an observer.

After the second paper, a final conclusion for the thesis will be given. The conclusion will discuss the work that has been completed as well as possible opportunities for future research.

1.4 CONTRIBUTIONS

The primary contribution of this thesis is the development of an event-sampled controller for both a general as well as a specific system, both of which are characterized by uncertain nonlinearities. For the general case, the results from previous works were limited by the assumptions that were invoked in the analyses. In particular, many of the efforts assumed either full knowledge of the state vector, full knowledge of the system dynamics, or both. With the incorporation of NNs, these assumptions can be relaxed. Moreover, the use of NNs with event-sampling is a topic which has been explored, however, the results are largely limited to affine systems; moreover, the use of mirror estimators in the event-execution law that was presented requires greater computational effort. In the derivations presented in this work, a strict-feedback system is considered, giving a greater degree of flexibility for real-world applications. Additionally, it is shown how the Lyapunov method can be used to derive an event-execution law that does not rely in mirror estimators while ensuring the boundedness of the measurement errors that are introduced with the intermittent sampling.

For the specific case, the dynamics of an under-actuated output-feedback quadrotor UAV in a modified strict-feedback form is considered. Here, too, it will be shown how the Lyapunov method can be used to design an event-execution law that guarantees bounded measurement errors and stable performance. Simulation results will be given in order to demonstrate the effectiveness of the proposed event-sampled controller and it will be illustrated how a reduction in computations can be achieved without having to sacrifice controller performance.

PAPER

I. EVENT-SAMPLED DIRECT ADAPTIVE NN OUTPUT- AND STATE-FEEDBACK CONTROL OF UNCERTAIN STRICT-FEEDBACK SYSTEM

Abstract

In this paper, neural networks (NNs) are utilized in the backstepping approach to design a control input by approximating unknown dynamics of the strict-feedback nonlinear system with event-sampled inputs. The system state vector is assumed to be unknown and an observer is used to estimate the state vector. By using the estimated state vector and backstepping design approach, an event-sampled controller is introduced. As part of the controller design, first, input-to-state-like stability (ISS) for a continuously sampled controller that has been injected with bounded measurement errors is demonstrated and, subsequently, an event-execution control law is derived such that the measurement errors are guaranteed to remain bounded. Lyapunov theory is used to demonstrate that the tracking errors, the observer estimation errors, and the NN weight estimation errors for each NN are locally uniformly ultimately bounded (UUB) in the presence bounded disturbances, NN reconstruction errors, as well as errors introduced by event-sampling. Simulation results are provided to illustrate the effectiveness of the proposed controllers.

1 INTRODUCTION

Given their inherent approximation properties, neural networks (NNs) have become popular in real-world applications that include unknown dynamics. In addition, due to the fact that many dynamic systems can be expressed in the strict-feedback form, the incorporation of NNs in a backstepping design has become a natural approach in controller design. In strict-feedback systems that have unknown nonlinearities, subsystems are considered separately from one another and NNs are implemented in approximating the unknown part of each subsystem's virtual control law. A general control scheme for this approach is presented by Ge and Wang in [1] and the work in [2] is able to use the concepts in a hypersonic flight vehicle application. However, the efforts [1] and [2] require full knowledge of the state vector, a provision that is not always guranteed.

In situations where the state vector is not available, an additional NN can be used as an observer to estimate the unknown states. As an example, the work in [3] models a quadrotor UAV system in strict-feedback form and circumvents the need for velocity sensors with an observer. In general, designing an output-feedback controller with backstepping is an approach that has been implemented in a number of different applications [4]-[7].

The previous works [1]-[7] on this class of systems assume a continuous sampling paradigm wherein the control law is executed at a fixed frequency. An alternative to the traditional sampling scheme, event-based sampling, is introduced by Tabuada in [8]: With event-sampling, the control is updated only when an event occurs. The immediate advantage to this is that the number of computations is reduced; furthermore, if all design parameters are appropriately selected, it can be shown that the reduction of computations can be achieved without compromising the fidelity of the controller.

The work in [8] introduces basic concepts of event-sampling and applies them to a general control system with known dynamics. Since then, a significant amount of work has been done in the development of event-based controllers and they have been discussed

in various contexts, such as input-state stability [9], sensor/actuator networks [10], state-and output-feedback systems [11, 12], and trajectory tracking applications [13]. In these works [9]-[13], the dynamics are assumed to be known and the use of NNs becomes unnecessary; for this reason, the extent to which their results can be implemented in real-world applications is somewhat restrictive. Finally, the work in [14] extends the notions of event-based sampling to incorporate unknown dynamics in an NN-based controller for an affine nonlinear system. In any work presenting results in event-sampling, the derivation of an event-execution law is a necessary provision; a particularly useful conclusion given in [14] is the presentation of an execution law in the presence of NN approximations.

However, the degree to which the results [14] can be applied in practical applications is limited to affine systems. Moreover, the execution law presented relies on having knowledge of the NN weight estimates at the event-triggering mechanism. This necessitates "mirror estimators" that synchronously provide NN weight estimates at both the controller and at the event-triggering mechanism.

To our knowledge, the inclusion of event-sampling in a NN-based backstepping controller design for a strict-feedback nonlinear continuous-time system has not yet been presented. Additionally, the incorporation of NNs in these systems allows the controller to achieve a greater degree of flexibility in that the requirement for complete knowledge of the system dynamics is relaxed. Moreover, the number of applications for which a controller could be employed can be further increased with the inclusion of an observer, alleviating the need for full knowledge of the states.

As part of the controller design, first, input-to-state stability (ISS) for a continuously sampled controller that has been injected with bounded measurement errors is demonstrated and, subsequently, an event-execution control law is derived such that the measurement errors are guaranteed to remain bounded. Lyapunov theory is used to demonstrate that the tracking errors, the observer estimation errors, and the NN weight estimation errors for each NN are locally uniformly ultimately bounded (UUB) in the presence bounded

disturbances, NN reconstruction errors, as well as errors introduced by event-sampling. Simulation results are provided to illustrate the effectiveness of the proposed controllers.

The main contribution of this paper is the derivation of an event-sampled, strict-feedback controller that operates in the presence of unknown nonlinearities without needing full knowledge of the state vector. In tandem, an event-execution law that does not rely on mirror estimators is presented, providing a more computationally efficient approach to what was given in [14]. Finally, whereas the primary contribution in this work is the derivation of an output-feedback controller, the state-feedback case is briefly presented as a corollary.

The remainder of this paper will be organized as follows: Section 2 will provide background information and the problem statement; Section 3 will present details for the output-feedback controller design and briefly give results for the state-feedback case; Section 4 will provide simulation results as well a discussion comparing event-sampled results with time-sampled results; finally, conclusions will be given in Section 5.

2 BACKGROUND AND PROBLEM STATEMENT

In this section, an introduction on the notations used in this paper will be given, a brief background on backstepping design with NNs will be provided, and the class of strict-feedback system considered in this work will be defined.

2.1 NOTATIONS

The partial state vector is denoted by $\bar{x}_i = [x_1, \ldots, x_i]^T$, $i \leq n$. It will become necessary to make a distinction between estimated values and actual values; in this work, estimated values will be denoted by a hat. Furthermore, the error between estimated values and actual values will be denoted by a tilde, specifically $(\tilde{\cdot}) = (\hat{\cdot}) - (\cdot)$. In general, for sake of brevity, the terms by which a function is defined will not be explicitly written; as an example, $f_1(x_1)$ will simply be written as f_1. Finally, in this work, $\|\cdot\|$ will be used as the Euclidean vector norm; for matrices, $\|\cdot\|$ will be understood to be the Frobenius norm [15].

2.2 BACKSTEPPING CONTROLLER DESIGN WITH NNs

In this work, each subsystem in the strict-feedback system is defined in terms of unknown nonlinear functions and, as a result, the virtual control laws consist, in part, of unknown constituents. The *universal approximation property* [15] of NNs makes their use in this application very fitting: The property states that an NN approximation exists for any smooth function such that the functional approximation error remains bounded. An NN is introduced in each subsystem in order to approximate the unknown part of the virtual control for that subsystem. Taking $h(X)$ to be an unknown function, the approximation is given by

$$h(X) = W^T \varphi\left(V^T X\right) - \varepsilon, \tag{1}$$

where, in this work, the activation function in the hidden layers, φ, is chosen to be the logarithmic sigmoid function and the input layer weights, V^T, is a constant random vector functional link (RVFL), resulting in the generation of a basis [15]. The ideal values of the

tunable weights are denoted by W^T and these weights are bounded such that $\|W\| \leq W_M$; moreover, the NN reconstruction error is also bounded such that, $\|\varepsilon\| < \varepsilon_M$. Finally, note that all NN activation functions are bounded such that $\|\varphi\| \leq \sqrt{N}$, where N is the number of hidden layer neurons in the NN.

What follows is a definition of the strict-feedback system that will be considered in this paper as well as a statement of the control objectives.

2.3 PROBLEM STATEMENT

Consider the strict feedback system given by

$$\dot{x}_i = f_i\left(\overline{x}_i\right) + g_i\left(\overline{x}_i\right) x_{i+1}, \qquad 1 \leq i \leq n-1$$

$$\dot{x}_n = f_n\left(\overline{x}_n\right) + g_n\left(\overline{x}_n\right) u, \qquad n \geq 2 \tag{2}$$

$$y = x_1.$$

In this work, $f_i\left(\overline{x}_i\right)$ and $g_i\left(\overline{x}_i\right)$, $i = 1, \ldots, n$, are unknown, smooth, nonlinear functions. The control objective is to design an event-sampled adaptive NN controller for (2) such that the following criteria are satisfied:

1. All signals in the closed-loop remain locally uniformly ultimately bounded (UUB)

2. The output, y, tracks the desired trajectory, y_d, generated from the given smooth, bounded reference

$$\dot{x}_{di} = f_{di}\left(x_d\right), \qquad 1 \leq i \leq m$$

$$y_d = x_{d1} \qquad m \geq n, \tag{3}$$

where $x_d = [x_{d1}, \ldots, x_{dm}]^T$ are the desired states, y_d is the desired output, and $f_{di}\left(\cdot\right)$, $i = 1, 2, \ldots, m$, are known, smooth, nonlinear functions

The following assumptions will be made in the analysis that will be presented in this paper:

Assumption 1 [1]: The states of the reference model remain bounded, i.e., $x_d \in S_d, \forall t \geq 0$.

Assumption 2 [1]: The signs of $g_i(\cdot)$ are known and there exist constants $0 < g_{mi} \leq g_{Mi}$ such that $g_{mi} \leq |g_i(\cdot)| \leq g_{Mi}, \forall \bar{x}_n \in S \subset \mathbb{R}^n$. This implies that $g_i(\cdot)$ is either strictly positive or strictly negative. Here, the former is assumed.

Assumption 3 [15]: The state vector, $\bar{x}_n$, is not available whereas the system (2) is observable.

Assumption 4 [8]: There are no transmission or computation time delays.

In the following section, the proposed output feedback controller is derived. Next, the state-feedback controller will be considered as a corollary. Since the procedure for the two controllers are nearly identical, details for state-feedback will be largely omitted and only major conclusions will be presented.

3   OUTPUT-FEEDBACK CONTROLLER

Section 2.2 briefly described the implementation of NNs in an uncertain strict feed-back system. In order to demonstrate stability, each subsystem will correspond to a sub-Lyapunov function, V_i, in terms of tracking error, error in the NN weights, and additional bounded terms. Furthermore, each successive sub-Lyapunov function will also be in terms of the previous sub-Lyapunov function. A final Lyapunov function, V_n, will demonstrate the stability of the overall system. For the state-feedback controller, this final Lyapunov expression would be sufficient in guaranteeing boundedness of all signals. However, for the output-feedback controller, a Lyapunov function, V_o, will be first found for the observer and then will be considered with V_n in order to prove stability for the closed-loop; it becomes necessary to consider V_o and V_n together, because the separation principle [15] cannot be applied due to the nonlinear nature of the system.

The NN observer design will be considered first and then the backstepping controller design will be presented. In this work, the event-triggering mechanism is placed at the observer and the state vector is estimated continously whereas the controller is updated only when an event occurs. As a result, the event-sampling measurement errors are explicitly present only in the controller design and not in the observer.

Remark 1. Although the observer NN makes use of continuously estimated values, the NN weights are updated only at events. Since the NN updates are subject to event-sampling, the NN reconstruction errors become functions of measurement errors and, in this way, the observer is implicitly affected by event-sampling. In [14], it is shown that the relationship between reconstruction errors and event-sampling errors is one wherein a greater number of events (which results in smaller measurement errors) corresponds to smaller NN approximation errors.
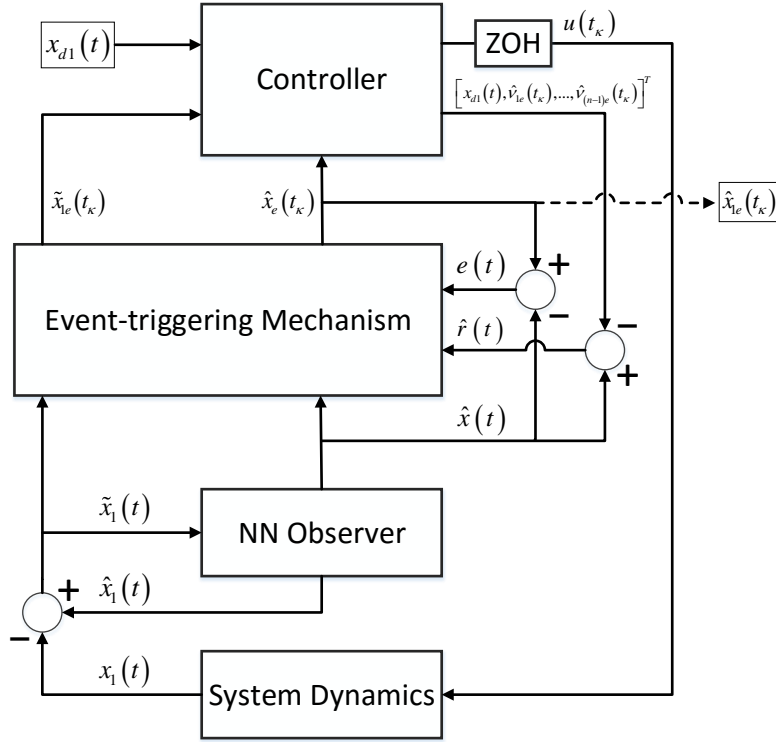
Fig. 3.1   NN Output-Feedback Control Structure

3.1   NN OBSERVER DESIGN

In this section, an NN observer is designed to estimate the unknown state vector. In this work, the observer is located at the sensor. Begin by defining the following terms:

$$c = [1, 0, \ldots, 0] \in \mathbb{R}^{1 \times n}$$

$$L = [l_1, \ldots, l_n]^T \in \mathbb{R}^{n \times 1}$$

$$A = Lc = \begin{bmatrix} l_1 & \cdots & 0 \\ \vdots & \ddots & \vdots \\ l_n & \cdots & 0 \end{bmatrix}$$

where the matrix, A, is used only in analysis and the observer gain vector, L, is used in practice. Next, define the system vector, $F = [f_1 + g_1 x_2, \ldots, f_n + g_n u]^T$, allowing (2) to

be rewritten as

$$\dot{x} = F$$

$$y = cx. \tag{4}$$

Now, introduce an observer NN with ideal weights and denote

$$F = W_o^T \varphi_o (X_o) - \varepsilon_o \tag{5}$$

with $X_o = \left[1, x^T, \tilde{x}_1\right]$, where the observer estimation error is given by, $\tilde{x}_1 = \hat{x}_1 - x_1$. In practice, only estimated weights are available; therefore, introduce estimated weights and use the following observer

$$\hat{F} = \hat{W}_o^T \varphi_o \left(\hat{X}_o\right) - A\tilde{x} \tag{6}$$

with $\hat{X}_o = \left[1, \hat{x}^T, \tilde{x}_1\right]^T$. Note that, in practice, (6) takes the form,

$$\hat{F} = \hat{W}_o^T \varphi_o \left(\hat{X}_o\right) - L\tilde{x}_1. \tag{7}$$

Observing that $\dot{\tilde{x}} = \hat{F} - F$, the observer estimation error dynamics are given by

$$\dot{\tilde{x}} = \hat{W}_o^T \varphi_o \left(\hat{X}_o\right) - A\tilde{x} - W_o^T \varphi_o (X_o) + \varepsilon_o. \tag{8}$$

For brevity, denote $\hat{\varphi} \triangleq \varphi\left(\hat{X}\right)$ and $\varphi \triangleq \varphi(X)$ and define $\tilde{\varphi} = \hat{\varphi} - \varphi$. Next, add and subtract $W_o^T \hat{\varphi}_o$ to (8) and rearrange terms in order to find an expression strictly in terms of observer estimation errors, NN weight estimation errors, and bounded terms. Denote the bounded term by $\xi \triangleq W_o^T \tilde{\varphi}_o + \varepsilon_o$ and note that $\|\xi\| \leq \xi_M$, where $\xi_M = 2W_{Mo}\sqrt{N_o} + \varepsilon_{Mo}$, revealing

$$\dot{\tilde{x}} = -A\tilde{x} + \tilde{W}_o^T \hat{\varphi}_o + \xi. \tag{9}$$

Next, the following theorem is stated in order to show the boundedness of the continuously sampled NN observer. The results of Theorem 1 will be used in demonstrating the local ISS-like behavior of the closed-loop system.

Remark 2. In the following theorem, the control input, u, is assumed to be admissable; the assumption is relaxed in subsequent theorems.

Theorem 1 *(NN Observer Boundedness):* Let the NN observer be defined by (6) with estimation error dynamics given by (9). Furthermore, let the NN observer weights be tuned by

$$\dot{\hat{W}}_o = F_o \left[-\hat{\varphi}_o c \tilde{x}^T - \alpha_o \hat{W}_o \right] \tag{10}$$

where $F_o = F_o^T > 0$ and $\alpha_o > 0$ are design parameters. Then, there exists a constant design parameter A such that the observer estimation errors, $\tilde{x}$, and the NN observer estimation errors, $\tilde{W}_o$, are locally UUB, with the bounds being functions of the NN reconstruction error and other bounded terms.

Proof: Consider the following positive-definite Lyapunov candidate:

$$V_o = \frac{1}{2} c \tilde{x}^T \tilde{x} + \frac{1}{2} \text{tr} \left\{ \tilde{W}_o^T F_o^{-1} \tilde{W}_o \right\} \tag{11}$$

whose first derivative is given by $\dot{V}_o = c \tilde{x}^T \dot{\tilde{x}} + \text{tr} \left\{ \tilde{W}_o^T F_o^{-1} \dot{\tilde{W}}_o \right\}$. Substitution of the error dynamics from (9) and using the NN update law given by (10) shows that

$$\dot{V}_o = -c \tilde{x}^T A \tilde{x} + c \tilde{x}^T \tilde{W}_o^T \hat{\varphi}_o + c \tilde{x}^T \xi + \text{tr} \left\{ -\tilde{W}_o^T \hat{\varphi}_o c \tilde{x}^T - \alpha_o \tilde{W}_o^T \hat{W}_o \right\}. \tag{12}$$

In order to proceed, recall the bounds on the ideal NN weights, the NN activation functions, and the NN reconstruction error. Using properties of the matrix trace operation, note that $c \tilde{x}^T \tilde{W}_o^T \hat{\varphi}_o + \text{tr} \left\{ -\tilde{W}_o^T \hat{\varphi}_o c \tilde{x}^T - \alpha_o \tilde{W}_o^T \hat{W}_o \right\} \leq \text{tr} \left\{ -\alpha_o \tilde{W}_o^T \hat{W}_o \right\}$. Using these results and noting

that $\|c\| = 1$ reveals

$$\dot{V}_o \leq -\|A\|\,\|\tilde{x}\|^2 + \|\tilde{x}\|\,\xi_M - \alpha_o\left\|\tilde{W}_o\right\|^2 + \alpha_o W_{Mo}\left\|\tilde{W}_o\right\|. \tag{13}$$

In order to further simplify (13), group the bounded terms together and denote $\zeta_o \triangleq \frac{1}{2}\left[\alpha_o W_{Mo}^2 + \frac{2\xi_M^2}{\|A\|}\right]$. Invoking Young's inequality gives

$$\dot{V}_o \leq -\frac{3}{4}\|A\|\,\|\tilde{x}\|^2 - \frac{1}{2}\alpha_o\left\|\tilde{W}_o\right\|^2 + \zeta_o. \tag{14}$$

Finally, (14) is less than zero when the gain vector L is selected such that $\|A\| > 0$ and the following inequalities hold:

$$\|\tilde{x}\| > \sqrt{\frac{4\zeta_o}{3\|A\|}} \quad \text{or} \quad \left\|\tilde{W}_o\right\| > \sqrt{\frac{2\zeta_o}{\alpha_o}} \tag{15}$$

It can, therefore, be concluded [15] that $\dot{V}_o$ is less than zero outside a compact set. This implies that, with properly selected gains, the observer estimation and the NN approximation errors are locally UUB.

Remark 3. By observation of (15) and the definition for ζ_o, it can be seen that the bound on $\|\tilde{x}\|$ can be made arbitrarily small by choosing $\|A\|$ to be large and α_o to be small. These conclusions also apply for the bounds on $\left\|\tilde{W}_o\right\|$.

With the derivation for the observer complete, the backstepping controller design is now considered.

3.2   CONTROLLER DESIGN WITH ESTIMATED STATES

In the previous subsection, the derivation of an observer was presented. In this subsection, the estimated state vector from the observer will be used in the backstepping controller design. The standard approach of dividing the design procedure into separate steps corresponding to different subsystems will be assumed here. Details will be provided

for the first step; in order to reduce redundancies, detailed explanations will be omitted for the intermediate i^{th} steps as well as the final n^{th} step.

In the analysis that follows, the derivations will make use of the fact $\hat{x}_i = x_i + \tilde{x}_i$, $i = 1, \ldots, n$. The need for this subtle change arises in finding the tracking error dynamics: Evaluating $\dot{\hat{x}}_i$ would introduce the need to address the problem of evaluating the unknown functions, f_i and g_i, at estimated states; the problem is circumvented by, instead, considering $\dot{x}_i$, from the system dynamics, and $\dot{\tilde{x}}_i$, from the observer dynamics.

Step 1: Define the tracking error, $\hat{r}_1 = \hat{x}_1 - x_{d1}$, whose derivative is

$$\dot{\hat{r}}_1 = f_1 + g_1 x_2 - \dot{x}_{d1} + \dot{\tilde{x}}_1. \tag{16}$$

In this first subsystem, x_2 is taken to be a virtual control input; denote the ideal virtual control by $v_1^* \triangleq x_2^*$. Now, consider the Lyapunov candidate, $V_{\hat{r}1} = \frac{1}{2}\hat{r}_1^2$, whose first derivative is given by

$$\dot{V}_{\hat{r}1} = \hat{r}_1 \dot{\hat{r}}_1 = \hat{r}_1 \left[f_1 + g_1 v_1 - \dot{x}_{d1} + \dot{\tilde{x}}_1 \right]. \tag{17}$$

Choosing the ideal virtual control as $v_1^* = -k_1 \hat{r}_1 - \frac{1}{g_1} \left[f_1 - \dot{x}_{d1} \right]$, with $k_1 > 0$ a constant design parameter, provides

$$\dot{V}_{\hat{r}1} = -k_1 g_1 \hat{r}_1^2 + \hat{r}_1 \dot{\tilde{x}}_1. \tag{18}$$

Given the boundedness of the observer estimation error from Theorem 1, note that (18) is a valid Lyapunov function, provided k_1 is appropriately chosen.

It can be seen that the unknown part of the proposed virtual control is $\frac{1}{g_1} \left[f_1 - \dot{x}_{d1} \right]$. Denote

$$h_1 \left(\hat{X}_1 \right) \triangleq \frac{1}{g_1} \left[f_1 - \dot{x}_{d1} \right], \tag{19}$$

where $\hat{X}_1 = [1, \hat{x}_1, \dot{x}_{d1}, \tilde{x}_1]^T$, and implement an NN to approximate h_1, allowing the desired virtual control to be expressed as

$$v_1^* = -k_1\hat{r}_1 - W_1^T\hat{\varphi}_1 + \varepsilon_1 \tag{20}$$

where it is understood that $\hat{\varphi}_1$ is evaluated at $\hat{X}_1$. Even though the function being approximated is in terms of actual states, $\hat{X}_1$ is taken to be input, because, in practice, only estimated states are available. Recalling that the ideal weights, W_1, are unknown, introduce the NN weight estimates, $\hat{W}_1$, allowing (20) to be rewritten as

$$\hat{v}_1 = -k_1\hat{r}_1 - \hat{W}_1^T\hat{\varphi}_1. \tag{21}$$

It is at this point that the error introduced by event-sampling is incorporated in the analysis. Consider the inter-event time period, $t_\kappa \leq t < t_{\kappa+1}$, where events occur at time instants $t_\kappa, t_{\kappa+1}, \ldots$. In general, the event-sampling measurement error corresponding to the ith subsystem is defined by

$$e_i(t) = x_{ie}(t_\kappa) - x_i(t), \ \forall t \in [t_\kappa, t_{\kappa+1}). \tag{22}$$

Remark 4. By definition (22), $e_i(t_\kappa) = 0$ at each event instant. This fact will be used later in the analysis. Furthermore, in this work, the the event-execution law is designed such that the measurement errors satisfy

$$e_i^2 \leq \sigma_i\mu_i\hat{r}_i^2, \ i = 1, \ldots, n \tag{23}$$

where $0 < \mu_i < 1$ and $0 < \sigma_i < 1$ are design parameters.

Remark 5. In practice, the state vector is continuously sampled; however, until an event occurs, a zero order hold (ZOH) is placed at the controller and the state vector, the

NN weights, and the desired control inputs are held. When an event does occur, the state vector stored in the controller is updated with the most recent measured values and these values are used to update the NN weights and the control input. The errors that result from the intermittent update are what are defined as event-sampling measurement errors. Note that, with event-sampling, the control input is piece-wise continuous; however, in the analysis, a continuously sampled input will be considered with measurement errors written explicitly.

In order to incorporate the effects of event-sampling into the analysis, replace the time-sampled variable, x_i, with the event-sampled variable, x_{ie}; by (22), $x_{ie} = x_i + e_i$. Furthermore, by using the definition for the observer estimation error in tandem with the definition for the measurement error it can be concluded that, in general, $\hat{r}_{ie} = \hat{r}_i + e_i$.

Before incorporating the measurement error, note that x_2 is taken to be the virtual control input to the $\hat{r}_1$-subsystem and not the actual control; for this reason, introduce the error variable $r_2 = x_2 - \hat{v}_{1e}$ and use $x_2 = r_2 + \hat{v}_{1e}$ in the analysis. As a point of clarity, note that x_2 is taken to be virtual control and not $\hat{x}_2$; this is because the dynamics of the strict-feedback system are with regards to actual states and not estimated states. Morever, for this same reason, it is only through the desired virtual control inputs which are injected into the system by the controller that the measurement errors are introduced. With this in consideration, observe that r_2 is introduced in the analysis, however, since the controller relies on estimated states, it is necessary to consider $\hat{r}_2$. This problem is easily addressed by noting that, in general, $r_i = \hat{r}_i - \tilde{x}_i$.

Now, consider the desired event-sampled virtual control

$$\hat{v}_{1e} = -k_1 [\hat{r}_1 + e_1] - \hat{W}_1^T \hat{\varphi}_{1e}, \tag{24}$$

and use these results in the tracking error dynamics, giving

$$
\begin{aligned}
\dot{\hat{r}}_1 &= f_1 + g_1 x_2 - \dot{x}_{d1} + \dot{\tilde{x}}_1 \\
&= g_1 \left[\hat{r}_2 - \tilde{x}_2 + \hat{v}_{1e} + \frac{f_1 - \dot{x}_{d1}}{g_1} \right] + \dot{\tilde{x}}_1 \\
&= g_1 \left[\hat{r}_2 - k_1 \hat{r}_1 - \hat{W}_1^T \hat{\varphi}_{1e} + W_1^T \varphi_1 - \varepsilon_1 \right] + g_1 \left[-k_1 e_1 \right] - g_1 \tilde{x}_2 + \dot{\tilde{x}}_1 .
\end{aligned}
\tag{25}
$$

Now, consider the Lyapunov candidate

$$
V_1 = \frac{\hat{r}_1^2}{2 \, \|A\|^2} + \frac{\mathrm{tr} \left\{ \tilde{W}_1^T F_1^{-1} \tilde{W}_1 \right\}}{2 \, \|A\|^2}
\tag{26}
$$

and the weight update law

$$
\dot{\hat{W}}_1 = F_1 \left[\hat{r}_{1e} \hat{\varphi}_{1e} - \alpha_1 \, |\hat{r}_{1e}| \, \hat{W}_1 \right],
\tag{27}
$$

where $F_1 = F_1^T > 0$ and $\alpha_1 > 0$ are design parameters. Using (27), the first derivative of V_1 is found to be

$$
\begin{aligned}
\dot{V}_1 &= \frac{1}{\|A\|^2} \hat{r}_1 \dot{\hat{r}}_1 + \frac{1}{\|A\|^2} \mathrm{tr} \left\{ \tilde{W}_1^T F_1^{-1} \dot{\hat{W}}_1 \right\} \\
&= \frac{1}{\|A\|^2} \left[g_1 \hat{r}_1 \hat{r}_2 - k_1 g_1 \hat{r}_1^2 - g_1 \hat{r}_1 \hat{W}_1^T \hat{\varphi}_{1e} + g_1 \hat{r}_1 W_1^T \varphi_1 - g_1 \hat{r}_1 \varepsilon_1 \right. \\
&\quad \left. + g_1 \hat{r}_1 \left[-k_1 e_1 \right] - g_1 \hat{r}_1 \tilde{x}_2 + \hat{r}_1 \dot{\tilde{x}}_1 \right] + \frac{1}{\|A\|^2} \mathrm{tr} \left\{ \hat{r}_{1e} \tilde{W}_1^T \hat{\varphi}_{1e} - \alpha_1 \, |\hat{r}_{1e}| \, \tilde{W}_1^T \hat{W}_1 \right\}
\end{aligned}
\tag{28}
$$

In order to further simplify the expression for $\dot{V}_1$, introduce the temporary variables

$$
\begin{aligned}
A_1 &= -k_1 g_1 \hat{r}_1^2 - g_1 \hat{r}_1 \varepsilon_1 \\
B_1 &= -g_1 \hat{r}_1 \hat{W}_1^T \hat{\varphi}_{1e} + g_1 \hat{r}_1 W_1^T \varphi_1 + \mathrm{tr} \left\{ \hat{r}_{1e} \tilde{W}_1^T \hat{\varphi}_{1e} - \alpha_1 \, |\hat{r}_{1e}| \, \tilde{W}_1^T \hat{W}_1 \right\}
\end{aligned}
\tag{29}
$$

and consider them separately. Using completion of squares with respect to $\hat{r}_1$ reveals

$$
\begin{aligned}
A_1 &\leq -\frac{1}{2}k_1 g_1 \hat{r}_1^2 - \frac{1}{2}k_1 g_1 \left[\hat{r}_1^2 - 2\hat{r}_1 \frac{\varepsilon_1}{k_1} + \frac{\varepsilon_1^2}{k_1^2}\right] + \frac{g_1 \varepsilon_1^2}{2k_1} \\
&= -\frac{1}{2}k_1 g_1 \hat{r}_1^2 - \frac{1}{2}k_1 g_1 \left[\hat{r}_1 - \frac{\varepsilon_1}{k_1}\right]^2 + \frac{g_1 \varepsilon_1^2}{2k_1} \\
&\leq -\frac{1}{2}k_1 g_{1m} \hat{r}_1^2 + \frac{g_{1M} \varepsilon_{1M}^2}{2k_1}
\end{aligned}
$$

The simplification process for B_1 makes use of the bounding condition on the activation functions with respect to the number of hidden layer neurons. With that, as well as properties of the matrix trace and norm operators and the conditions imposed by (23), the following conclusion can be made:

$$
\begin{aligned}
B_1 &\leq \frac{1}{2}\hat{r}_1^2 - \alpha_1 \left[2 - \chi_1\right] |\hat{r}_1| \left\|\tilde{W}_1\right\|^2 + 2g_{1M}^2 W_{1M}^2 N_1 \\
&\qquad\qquad + |\hat{r}_1| \left[\sqrt{N_1} \left[g_{1M} + \chi_1\right] + \chi_1 \alpha_1 W_{1M}\right] \left\|\tilde{W}_1\right\|
\end{aligned}
$$

where, in general, $\chi_i = \sqrt{\sigma_i \mu_i} + 1$. The expressions for A_1 and B_1 can be used to rewrite (28). Denoting the bounded term, $\zeta_1 \triangleq \frac{g_{1M} \varepsilon_{1M}^2}{2\|A\|^2 k_1} + \frac{2g_{1M}^2 W_{1M}^2 N_1}{\|A\|^2}$, and rearranging terms gives

$$
\begin{aligned}
\dot{V}_1 &\leq \frac{g_1 \hat{r}_1 \hat{r}_2}{\|A\|^2} - \frac{|\hat{r}_1|}{\|A\|^2}\left[\frac{1}{2}\left[k_1 g_{1m} - 1\right] |\hat{r}_1| + \alpha_1 \left[2 - \chi_1\right] \left\|\tilde{W}_1\right\|^2 \right. \\
&\qquad\qquad \left. - \left[\sqrt{N_1}\left[g_{1M} + \chi_1\right] + \chi_1 \alpha_1 W_{1M}\right] \left\|\tilde{W}_1\right\|\right] \\
&\qquad\qquad + \zeta_1 + \frac{1}{\|A\|^2}\left[g_1 \hat{r}_1 \left[-k_1 e_1\right] - g_1 \hat{r}_1 \tilde{x}_2 + \hat{r}_1 \dot{\tilde{x}}_1\right] \quad (30)
\end{aligned}
$$

Step 2: Begin by defining the tracking error $\hat{r}_2 = \hat{x}_2 - \hat{v}_{1e}$, whose derivative is given by $\dot{\hat{r}}_2 = f_2 + g_2 x_3 - \dot{\hat{v}}_{1e} + \dot{\tilde{x}}_2$. Here, x_3 is taken to be the virtual control input to the

$\hat{r}_2$-subsystem and the ideal feedback control is given by

$$v_2^* = -r_1 - k_2 r_2 - \frac{1}{g_2} \left[f_2 - \dot{\hat{v}}_{1e} \right] \tag{31}$$

where $k_2 > 0$ is a design constant. Denote the unknown part with

$$h_2 \left(\hat{X}_{2e} \right) \triangleq \frac{1}{g_2} \left[f_2 - \dot{\hat{v}}_{1e} \right]. \tag{32}$$

Note that the unknown part of v_2^* is a function of $\bar{\hat{x}}_{2e}$ and $\dot{\hat{v}}_{1e}$; in turn, $\dot{\hat{v}}_{1e}$ is a function of $\hat{x}_{1e}$, $\dot{x}_{d1}$, and $\hat{W}_1$. In order to minimize the number of inputs to the NN, introduce the computable intermediate variable

$$\hat{\psi}_{1e} = \frac{\partial \hat{v}_{1e}}{\partial x_d} \dot{x}_d + \frac{\partial \hat{v}_{1e}}{\partial \hat{W}_1} \left[F_1 \left[\hat{r}_{1e} \hat{\varphi}_{1e} - \alpha_1 \left| \hat{r}_{1e} \right| \hat{W}_1 \right] \right] \tag{33}$$

and use it in the input, $\hat{X}_{2e} = \left[1, \bar{\hat{x}}_{2e}, \partial \hat{v}_{1e}/\partial x_{1e}, \hat{\psi}_{1e}, \tilde{x}_{1e} \right]^T$, for the NN approximating h_2, allowing (31) to be rewritten as

$$v_2^* = -\hat{r}_1 - k_2 \hat{r}_2 - W_2^T \hat{\varphi}_2 + \varepsilon_2. \tag{34}$$

With estimated weights and event-sampling, the desired virtual control becomes

$$\hat{v}_{2e} = - \left[\hat{r}_1 + e_1 \right] - k_2 \left[\hat{r}_2 + e_2 \right] - \hat{W}_2^T \hat{\varphi}_{2e}. \tag{35}$$

Using these results, tracking error dynamics are given by

$$\dot{\hat{r}}_2 = g_2 \left[\hat{r}_3 - k_2 \hat{r}_2 - \hat{r}_1 - \hat{W}_2^T \hat{\varphi}_{2e} + W_2^T \varphi_2 - \varepsilon_2 \right] + g_2 \left[-k_2 e_2 - e_1 \right] - g_2 \tilde{x}_3 + \dot{\tilde{x}}_2. \tag{36}$$

Consider the Lyapunov candidate

$$V_2 = V_1 + \frac{\hat{r}_2^2}{2\,\|A\|^2} + \frac{\text{tr}\left\{\tilde{W}_2^T F_2^{-1} \tilde{W}_2\right\}}{2\,\|A\|^2} \tag{37}$$

and the weight update law

$$\dot{\hat{W}}_2 = F_2 \left[\hat{r}_{2e}\hat{\varphi}_{2e} - \alpha_2 \left|\hat{r}_{2e}\right| \hat{W}_2\right], \tag{38}$$

where $F_2 = F_2^T > 0$ and $\alpha_2 > 0$ are design parameters.

Remark 6. The general i^{th} desired virtual control is given by

$$\hat{v}_{ie} = -\left[\hat{r}_{i-1} + e_{i-1}\right] - k_i\left[\hat{r}_i + e_i\right] - \hat{W}_i^T \hat{\varphi}_{ie}, \tag{39}$$

the tracking error dynamics become

$$\dot{\hat{r}}_i = g_i \left[\hat{r}_{i+1} - k_i\hat{r}_i - \hat{r}_{i-1} - \hat{W}_i^T \hat{\varphi}_{ie} + W_i^T \varphi_i - \varepsilon_i\right] + g_i\left[-k_i e_i - e_{i-1}\right] - g_i\tilde{x}_{i+1} + \dot{\tilde{x}}_i, \tag{40}$$

the Lyapunov candidate is provided by

$$V_i = V_{i-1} + \frac{\hat{r}_i^2}{2\,\|A\|^2} + \frac{\text{tr}\left\{\tilde{W}_i^T F_i^{-1} \tilde{W}_i\right\}}{2\,\|A\|^2}, \tag{41}$$

and the weight update law is given by

$$\dot{\hat{W}}_i = F_i \left[\hat{r}_{ie}\hat{\varphi}_{ie} - \alpha_i \left|\hat{r}_{ie}\right| \hat{W}_i\right], \tag{42}$$

where $F_i = F_i^T > 0$ and $\alpha_i > 0$ are design parameters.

Then, by introducing temporary variables and using procedures identical to what was used in Step 1, the expression for $\dot{V}_2$ becomes

$$\dot{V}_2 \leq \frac{1}{\|A\|^2} \left[\hat{r}_1\hat{r}_2 \left[g_1 - g_2\right] + g_2\hat{r}_2\hat{r}_3\right] - \frac{1}{\|A\|^2} \sum_{j=1}^{2} |\hat{r}_j| \left[\frac{1}{2} \left[k_j g_{jm} - 1\right] |\hat{r}_j|\right]$$

$$+ \alpha_j \left[2 - \chi_j\right] \left\|\tilde{W}_j\right\|^2 - \left[\sqrt{N_j} \left[g_{jM} + \chi_j\right] + \chi_j\alpha_j W_{jM}\right] \left\|\tilde{W}_j\right\| + \sum_{j=1}^{2} \zeta_j$$

$$+ \frac{1}{\|A\|^2} \sum_{j=1}^{2} \hat{r}_j\dot{\tilde{x}}_j - \frac{1}{\|A\|^2} \sum_{j=1}^{2} g_j\hat{r}_j\tilde{x}_j + \frac{1}{\|A\|^2} \left[g_1\hat{r}_1 \left[-k_1 e_1\right] + g_2\hat{r}_2 \left[-k_2 e_2 - e_1\right]\right] \quad (43)$$

where $\zeta_j = \frac{g_{jM}\varepsilon_{jM}^2}{2\|A\|^2 k_j} + \frac{2g_{jM}^2 W_{jM}^2 N_j}{\|A\|^2}$ is bounded.

Step n: Define the tracking error $\hat{r}_n = \hat{x}_n - \hat{v}_{(n-1)e}$, whose derivative is given by $\dot{\hat{r}}_n = f_n + g_n u - \dot{\hat{v}}_{(n-1)e} + \dot{\tilde{x}}_n$. Here, u is the actual control input to the overall system and the ideal feedback control is given by

$$u^* = -r_{n-1} - k_n r_n - \frac{1}{g_n} \left[f_n - \dot{\hat{v}}_{(n-1)e}\right] \quad (44)$$

where $k_n > 0$ is a design constant. Denote the unknown part with

$$h_n\left(\hat{X}_{ne}\right) \triangleq \frac{1}{g_n} \left[f_n - \dot{\hat{v}}_{(n-1)e}\right] . \quad (45)$$

In order to minimize the number of inputs to the NN, introduce the computable intermediate variable

$$\hat{\psi}_{(n-1)e} = \sum_{j=1}^{n-1} \frac{\partial \hat{v}_{(n-1)e}}{\partial x_d} \dot{x}_d + \sum_{j=1}^{n-1} \frac{\partial \hat{v}_{(n-1)e}}{\partial \hat{W}_j} \left[F_j \left[\hat{r}_{je}\hat{\varphi}_{je} - \alpha_j |\hat{r}_{je}| \hat{W}_j\right]\right] . \quad (46)$$

Use a NN with input $\hat{X}_{ne} = \left[1, \bar{\tilde{x}}_{ne}, \partial \hat{v}_{(n-1)e}/\partial x_{1e}, \ldots, \partial \hat{v}_{(n-1)e}/\partial x_{(n-1)e}, \hat{\psi}_{(n-1)e}, \tilde{x}_{1e}\right]^T$ to approximate h_n, allowing (44) to be rewritten as

$$u^* = -\hat{r}_{n-1} - k_n \hat{r}_n - W_n^T \hat{\varphi}_n + \varepsilon_n. \tag{47}$$

With estimated weights and event-sampling, the desired control input is given by

$$u_e = -[\hat{r}_{n-1} + e_{n-1}] - k_n [\hat{r}_n + e_n] - \hat{W}_n^T \hat{\varphi}_{ne} \tag{48}$$

and the tracking error dynamics become

$$\dot{\hat{r}}_n = g_n \left[-k_n \hat{r}_n - \hat{r}_{n-1} - \hat{W}_n^T \hat{\varphi}_{ne} + W_n^T \varphi_n - \varepsilon_n\right] + g_n \left[-k_n e_n - e_{n-1}\right] + \dot{\tilde{x}}_n. \tag{49}$$

Note that, since u_e is the actual control input to the system, there is no need to introduce an additional error term and, therefore, the $\tilde{x}_i$ term that exists in previous subsystems is absent here.

Now, consider the final Lyapunov candidate

$$V_n = V_{n-1} + \frac{\hat{r}_n^2}{2\,\|A\|^2} + \frac{\mathrm{tr}\left\{\tilde{W}_n^T F_n^{-1} \tilde{W}_n\right\}}{2\,\|A\|^2} \tag{50}$$

and the weight update law

$$\dot{\hat{W}}_n = F_n \left[\hat{r}_{ne} \hat{\varphi}_{ne} - \alpha_n |\hat{r}_{ne}| \hat{W}_n\right], \tag{51}$$

where $F_n = F_n^T > 0$ and $\alpha_n > 0$ are design parameters. Then, introducing temporary variables and using a procedure identical to what was used in previous steps reveals

$$\dot{V}_n \leq \frac{1}{\|A\|^2} \sum_{j=2}^{n} \hat{r}_{j-1}\hat{r}_j \left[g_{j-1} - g_j\right] - \frac{1}{\|A\|^2} \sum_{j=1}^{n} |\hat{r}_j| \left[\frac{1}{2} \left[k_j g_{jm} - 1\right] |\hat{r}_j| + \alpha_j \left[2 - \chi_j\right] \|\tilde{W}_j\|^2\right.$$
$$- \left[\sqrt{N_j} \left[g_{jM} + \chi_j\right] + \chi_j \alpha_j W_{jM}\right] \|\tilde{W}_j\|\right] + \sum_{j=1}^{n} \zeta_j + \frac{1}{\|A\|^2} \sum_{j=1}^{n} \hat{r}_j \dot{\tilde{x}}_j$$
$$- \frac{1}{\|A\|^2} \sum_{j=1}^{n-1} g_j \hat{r}_j \tilde{x}_{j+1} + \frac{1}{\|A\|^2} \left[g_1 \hat{r}_1 \left[-k_1 e_1\right] + \sum_{j=2}^{n} g_j \hat{r}_j \left[-k_j e_j - e_{j-1}\right]\right] \quad (52)$$

Now, in order to simplify (52), introduce the following temporary variables:

$$T_1 = \frac{1}{\|A\|^2} \sum_{j=2}^{n} \hat{r}_{j-1}\hat{r}_j \left[g_{j-1} - g_j\right]$$

$$T_2 = \frac{1}{\|A\|^2} \sum_{j=2}^{n} g_j \hat{r}_j \left[-k_j e_j - e_{j-1}\right] + g_1 \hat{r}_1 \left[-k_1 e_1\right]$$

$$T_3 = \frac{1}{\|A\|^2} \sum_{j=1}^{n} \hat{r}_j \dot{\tilde{x}}_j$$

$$T_4 = -\frac{1}{\|A\|^2} \sum_{j=1}^{n-1} g_j \hat{r}_j \tilde{x}_{j+1}$$

First, consider T_1 and T_2. In order to simplify these terms, begin by defining $g_M = \max\{g_{1M}, \ldots, g_{nM}\}$ and $g_m = \min\{g_{1m}, \ldots, g_{nm}\}$. Expanding and rearranging terms and invoking Young's inequality reveals $T_1 \leq \frac{1}{2\|A\|^2} \sum_{j=1}^{n} \left[1 + g_M^2\right] \hat{r}_j^2$ and $T_2 \leq \frac{1}{\|A\|^2} \sum_{j=1}^{n} \left[g_M^2\right] \hat{r}_j^2 + \frac{1}{2\|A\|^2} \sum_{j=1}^{n} \left[k_j^2 + 1\right] e_j^2$. Using these results in (52) reveals

$$\dot{V}_n \leq -\frac{1}{\|A\|^2} \sum_{j=1}^{n} |\hat{r}_j| \left[\frac{1}{2} \left[k_j g_m - 3g_M^2 - 2\right] |\hat{r}_j| + \alpha_j \left[2 - \chi_j\right] \|\tilde{W}_j\|^2 - \left[\sqrt{N_j} \left[g_M + \chi_j\right]\right.\right.$$
$$\left.+ \chi_j \alpha_j W_{jM}\right] \|\tilde{W}_j\|\right] + \sum_{j=1}^{n} \zeta_j + \frac{1}{2\|A\|^2} \sum_{j=1}^{n} \left[k_j^2 + 1\right] e_j^2 + \frac{1}{\|A\|^2} \sum_{j=1}^{n} \hat{r}_j \dot{\tilde{x}}_j - \frac{1}{\|A\|^2} \sum_{j=1}^{n-1} g_j \hat{r}_j \tilde{x}_{j+1}$$

$$(53)$$

Now, considering T_3, recall the observer estimation error dynamics from (9). Using Young's inequality with these dynamics gives

$$T_3 \leq \frac{1}{2\|A\|^2} \sum_{j=1}^{n} \left[\frac{N_o}{\|A\|^2} + 2\right] \hat{r}_j^2 + \frac{1}{2} \|\tilde{x}\|^2 + \frac{1}{2} \left\|\tilde{W}_o\right\|^2 + \frac{1}{2}\xi_M^2$$

Finally, for T_4, use a similar procedure to discover

$$T_4 \leq \frac{g_M^2}{2\|A\|^4} \|\hat{r}\|^2 + \frac{1}{2} \|\tilde{x}\|^2 .$$

The expressions for T_3 and T_4 are only useful in the presence of the closed-loop. Therefore, proceed by focusing on the closed-loop dynamics.

3.3   CLOSED-LOOP OUTPUT FEEDBACK DYNAMICS

Consider the closed-loop Lyapunov candidate, $V = V_o + V_n$ and define the following bounded terms:

$$\zeta = \zeta_o + \sum_{j=1}^{n} \zeta_j + \frac{1}{2\|A\|^2}\xi_M^2$$

$$\eta_j = \frac{\left[g_M + \chi_j\right]\sqrt{N_j} + \chi_j\alpha_j W_{jM}}{\alpha_j\left[2 - \chi_j\right]}$$

$$\delta_j = k_j g_m - 3g_M^2 - \frac{g_M^2}{\|A\|^2} - \frac{N_o}{\|A\|^2} - 4$$

$$\beta_j = k_j^2 + 1$$

Furthermore, recall the bounding term on the event-sampling errors, $\left|e_j\right| \leq B_{ej}$. Finally, with completion of squares with respect to $\left\|\tilde{W}_j\right\|$, the final Lyapunov candidate for the

closed-loop system is given by

$$
\dot{V} \leq -\frac{1}{4} \left[3 \, \|A\| - 4\right] \|\tilde{x}\|^2 - \frac{1}{2} \left[\alpha_o - 1\right] \left\|\tilde{W}_o\right\|^2 + \zeta + \frac{1}{2 \, \|A\|^2} \sum_{j=1}^{n} \beta_j B_{ej}^2
$$

$$
- \sum_{j=1}^{n} \left|\hat{r}_j\right| \left[\frac{1}{2} \delta_j \left|\hat{r}_j\right| + \alpha_j \left[2 - \chi_j\right] \left[\left\|\tilde{W}_j\right\| - \frac{\eta_j}{2}\right]^2 - \frac{\eta_j^2 \alpha_j \left[2 - \chi_j\right]}{4}\right]. \quad (54)
$$

Now the following theorem is presented in order to show that the continuously sampled closed loop dynamics are ISS-like in the presence of bounded measurement errors.

Theorem 2 *(Output Feedback Input-to-State Stability):* Let the NN observer be defined by (6) with estimation error dynamics given by (9). Consider the NN observer weight tuning given by (10). Given *Assumptions 1-4,* consider the tracking error dynamics given by (25), (36), (40), and (49). Let the desired virtual control inputs and the actual control input be given by (24), (35), and (39) and (48), respectively. Select the NN weight tuning given by (27), (38), (42), and (51). Finally, let the measurement error in the ith subsystem be bounded such that $|e_i| \leq B_{ei}, \, i = 1, 2, \ldots, n$. Then, there exists design parameters, A and k_i such that the observer estimation error, $\tilde{x}$, the tracking errors, $\hat{r}_i$, and the NN weight estimation errors, $\tilde{W}_o$ and $\tilde{W}_i$, are locally UUB, with bounds as functions of measurement errors and NN reconstruction errors.

Proof: Consider the following positive-definite Lyapunov candidate describing the closed loop:

$$
V = V_o + V_n \quad (55)
$$

where V_o was defined in (11) and V_n was defined in (50). The first derivative of V is given by $\dot{V} = \dot{V}_o + \dot{V}_n$. In Theorem 1, $\dot{V}_o$ was found to be bounded above by (14); in further derivations, $\dot{V}_n$ was found to be bounded above by (53). Making use of the observer estimation error dynamics given by (9), the results from (14) and (53) are able to be connected. Based

on the results given by (54), select controller gains satisfying the following conditions:

$$\|A\| > \frac{4}{3} \quad \text{and} \quad k_i > \Gamma_i \tag{56}$$

where $\Gamma_i = \frac{1}{g_m}\left[3g_M^2 + \frac{g_M^2}{\|A\|^2} + \frac{N_o}{\|A\|^2} + 4\right]$ for all $i = 1, \ldots, n$. It can be concluded that $\dot{V}$ is less than zero when the controller gains are selected according to (56) and the following inequalities hold:

$$\|\tilde{x}\| > \sqrt{\frac{4\zeta + 2B_E}{3\|A\| - 4}} \qquad \text{or} \qquad \left\|\tilde{W}_o\right\| > \sqrt{\frac{2\zeta + B_E}{[\alpha_o - 1]}}$$

or

$$\left|\hat{r}_j\right| > \frac{\eta_j^2 \alpha_j \left[2 - \chi_j\right]}{2\delta_j} \qquad \text{or} \qquad \left\|\tilde{W}_j\right\| > \eta_j \tag{57}$$

where $B_E = \frac{1}{\|A\|^2} \sum_{j=1}^{n} \beta_j B_{ej}^2$. It can, therefore, be concluded [15] that $\dot{V}$ is less than zero outside a compact set. This implies that the observer estimation error, the tracking errors, and the NN estimation errors are locally UUB.

Remark 7. The conclusions made in *Remark 3* with regards to the bounds on $\|\tilde{x}\|$ and $\left\|\tilde{W}_o\right\|$ are valid here. Similarly, by choosing α_j such that η_j is minimized and choosing k_j such that δ_j is maximized, the bounds on $\left|\hat{r}_j\right|$ and $\left\|\tilde{W}_j\right\|$ can be made arbitrarily small.

Remark 8. The result in Theorem 2 shows that the system exhibits local ISS-like behavior with respect to bounded measurement errors and bounded NN reconstruction errors. This can be seen by introducing an augmented vector, $z = \left[\hat{r}_1, \ldots, \hat{r}_n, \left\|\tilde{W}_1\right\|, \ldots, \left\|\tilde{W}_n\right\|\right]^T$, and observing that (54) can be written in the form $\dot{V}(z) \leq -\Lambda(\|z\|) + \gamma(\|E\|)$, where the positive part, γ, is viewed as an input to the closed-loop system and is a function of bounded measurement and NN reconstruction errors. It can, therefore, be concluded that

the continuously sampled, closed-loop system generates a local ISS-like Lyapunov function [8]. However, in order to implement the event-sampled controller, the boundedness of the measurement errors must also be demonstrated.

Next, the following theorem is presented in order to demonstrate the boundedness of the measurement error as well as to show the derivation of an event-execution law.

Theorem 3 *(Overall Stability and Boundedness of Measurement Error):* Let the NN observer be defined by (6) with estimation error dynamics given by (9). Select the NN observer weight tuning given by (10). Given *Assumptions 1-4,* consider the tracking error dynamics given by (25), (36), (40), and (49). Let the desired virtual control inputs and the actual control input be given by (24), (35), and (39) and (48), respectively. Moreover, select the NN weight tuning at the event-sampling instants to be (27), (38), (42), and (51). Finally, let the event-sampling error satisfy the condition given by (23). Then, there exists design parameters, A and k_i, such that the observer estimation error, $\tilde{x}$, the tracking errors, $\hat{r}_i$, and the NN weight estimation errors, $\tilde{W}_o$ and $\tilde{W}_i$, are locally UUB, both at event-sampling instants as well as during inter-event periods. Furthermore, the bounds on these errors can be expressed as functions of bounded terms and NN reconstruction errors. Finally, the errors introduced by event-sampling remain bounded during inter-event periods.

Proof: Two cases are considered. The first case will analyze the system when measurement errors are zero and the second case will analyze the system during the inter-event periods.

Case 1. Recall that, from definition (22), at the event-sampling instants, the event-sampling error is zero, $e_i(t_\kappa) = 0$. Furthermore, it is at the event-sampling instants that the NNs are updated with (10), (27), (38), (42), and (51); however, in this case, the tracking error terms and the activation function terms in the weight update laws are not under the influence of measurement errors.

Begin by observing that the expression for $\dot{V}_o$ remains identical to (14) and the definition for the bounded term, ζ_o, also remains unchanged. Continue by rewriting the

tracking error dynamics as

$$
\begin{aligned}
\dot{\hat{r}}_1 &= g_1 \left[\hat{r}_2 - k_1 \hat{r}_1 - \tilde{W}_1^T \hat{\varphi}_1 + W_1^T \tilde{\varphi}_1 - \varepsilon_1 \right] - g_1 \tilde{x}_2 + \dot{\tilde{x}}_1 \\
\dot{\hat{r}}_i &= g_i \left[\hat{r}_{i+1} - k_i \hat{r}_i - \hat{r}_{i-1} - \tilde{W}_i^T \hat{\varphi}_i + W_i^T \tilde{\varphi}_i - \varepsilon_i \right] - g_i \tilde{x}_{i+1} + \dot{\tilde{x}}_i \\
\dot{\hat{r}}_n &= g_n \left[-k_n \hat{r}_n - \hat{r}_{n-1} - \tilde{W}_n^T \hat{\varphi}_n + W_n^T \tilde{\varphi}_n - \varepsilon_n \right] + \dot{\tilde{x}}_n
\end{aligned}
\tag{58}
$$

with $i = 2, \ldots, n - 1$. Using these error dynamics with the Lyapunov candidates (26), (37), (41), and (50) and implementing a simplification procedure similar to what was presented in Section 3.2 gives

$$
\begin{aligned}
\dot{V}_n &\leq \frac{1}{\|A\|^2} \sum_{j=2}^{n} \hat{r}_{j-1} \hat{r}_j \left[g_{j-1} - g_j \right] - \frac{1}{\|A\|^2} \sum_{j=1}^{n} \left[k_j g_{jm} \left| \hat{r}_j \right| + \alpha_j \left\| \tilde{W}_j \right\|^2 \right. \\
&\quad \left. - \left[\sqrt{N_j} \left[g_{jM} + 1 \right] + \alpha_j W_{jM} \right] \left\| \tilde{W}_j \right\| - \zeta_{j1} \right] \left| \hat{r}_j \right| + \frac{1}{\|A\|^2} \sum_{j=1}^{n} \hat{r}_j \dot{\tilde{x}}_j - \frac{1}{\|A\|^2} \sum_{j=1}^{n-1} g_j \hat{r}_j \tilde{x}_{j+1}
\end{aligned}
\tag{59}
$$

where $\zeta_{j1} = g_{jM} \varepsilon_{jM} + 2 g_{jM} W_{jM} \sqrt{N_j}$ is bounded. Note that simplification procedure here was different in that the constant bounded terms were not separated from the tracking error - this was done in order to be able to include the ζ_{j1} terms in the same summation as the other terms.

In order to further simplify, the first term and the last two terms of (59) are considered separately. Simplifying the first terms allows the expression for $\dot{V}_n$ to be simplified, but the results for the simplification of the last two terms only make sense in the presence of the closed loop. Therefore, consider the Lyapunov candidate (55). First, define the following

bounded terms:

$$\zeta_{B1} = \sum_{j=1}^{n} \zeta_{j1} + \xi_M$$

$$\eta_{j1} = \frac{\sqrt{N_j}}{\alpha_j} [g_M + 1] + W_{jM}$$

$$\delta_{j1} = 2k_j g_m - g_M^2 - \frac{g_M^2}{\|A\|^2} - \frac{N_o}{\|A\|^2} - 2$$

Simplifying and rearranging terms gives

$$\dot{V} \le -\frac{1}{4} [3\|A\| - 4] \|\tilde{x}\|^2 - \frac{1}{2} [\alpha_o - 1] \|\tilde{W}_o\|^2$$
$$- \frac{1}{\|A\|^2} \sum_{j=1}^{n} \left[\frac{1}{2} \delta_{j1} |\hat{r}_j| + \alpha_j \left[\left[\|\tilde{W}_j\| - \frac{\eta_{j1}}{2} \right]^2 - \left[\zeta_{B1} + \frac{\eta_{j1}^2 \alpha_j}{4} \right] \right] \right] + \zeta_o. \quad (60)$$

Select controller gains satisfying the following conditions:

$$\|A\| > \frac{4}{3} \quad \text{and} \quad k_i > \Gamma_{i1} \tag{61}$$

where $\Gamma_{i1} = \frac{1}{2g_m} \left[g_M^2 + \frac{g_M^2}{\|A\|^2} + \frac{N_o}{\|A\|^2} + 2 \right]$ for all $i = 1, \ldots, n$. Then, (60) is less than zero when the following inequalities hold:

$$\|\tilde{x}\| > \sqrt{\frac{4\zeta_o}{3\|A\| - 4}} \qquad \text{or} \qquad \|\tilde{W}_o\| > \sqrt{\frac{2\zeta_o}{[\alpha_o - 1]}}$$

or

$$|\hat{r}_j| > \frac{4\zeta_{B1} + \eta_{j1}^2 \alpha_j}{2\delta_{j1}} \qquad \text{or} \qquad \|\tilde{W}_j\| > \frac{\eta_{j1}}{2} + \sqrt{\frac{4\zeta_{B1} + \alpha_j \eta_{j1}^2}{4\alpha_j}}. \tag{62}$$

The bounds given by (62) are different than those given by (57) from Theorem 2 in that they do not account for the effects of intermittent sampling; as a result, the χ_j term, which is an artifact from the event-triggering mechanism, is altogether absent here.

Case 2. Now, consider the inter-event period, $t \in [t_\kappa, t_{\kappa+1})$, during which time there is a nonzero event-sampling error, but with constant NN weights; in other words, in this case, $e_i(t) \neq 0$ and $\dot{\hat{W}} = 0$ for all NN weights.

As before, begin by considering the observer estimation error dynamics and notice that they remain identical to (9). The primary difference in this analysis arises in the Lyapunov candidate, (11), noting that its first derivative simplifies to

$$\dot{V}_o = \tilde{x}^T \dot{\tilde{x}} + \mathrm{tr}\left\{ \tilde{W}_o^T F_o^{-1} \dot{\tilde{W}}_o \right\}^{\;\;0}$$
$$= \tilde{x}^T \dot{\tilde{x}}. \tag{63}$$

Use (9) in (63) and implement a similar simplification procedure as before to arrive at

$$\dot{V}_o \leq -\frac{1}{4}\left[3\|A\| - 2N_o\right]\|\tilde{x}\|^2 + \frac{1}{2}\left\|\tilde{W}_o\right\|^2 + \zeta_{o2} \tag{64}$$

where $\zeta_{o2} = \frac{\xi_M^2}{\|A\|}$.

Similar to the observer estimation error dynamics, the tracking error dynamics remain unchanged from (25), (36), (40), and (49). However, it is discovered that the derivatives of the Lyapunov candidates are simplified to include only the first terms, $\hat{r}_i \dot{\hat{r}}_i$ for all $i = 1, \ldots, n$. With these facts and using a similar simplification procedure as before reveals

$$\dot{V}_n \leq -\frac{1}{2\|A\|^2}\sum_{j=1}^{n}\left[k_j g_{jm} - 4g_{jM}^2 - 1\right]\hat{r}_j^2 + \frac{1}{2\|A\|^2}\sum_{j=1}^{n}\left[k_j^2 + 1\right]e_j^2$$
$$+ \frac{1}{2\|A\|^2}\sum_{j=1}^{n}N_j\left[W_{jM} + \left\|\hat{W}_j\right\|\right]^2 + \sum_{j=1}^{n}\zeta_{j2} + \frac{1}{\|A\|^2}\sum_{j=1}^{n}\hat{r}_j\dot{\tilde{x}}_j - \frac{1}{\|A\|^2}\sum_{j=1}^{n-1}g_j\hat{r}_j\tilde{x}_{j+1} \tag{65}$$

where $\zeta_{j2} = \frac{g_M \varepsilon_{jM}^2}{2\|A\|^2 k_j}$ is bounded. Furthermore, note that, because the NN weights are not being updated during the inter-event period, the term $\frac{1}{2}\sum_{j=1}^{n}N_j\left[W_{jM} + \left\|\hat{W}_j\right\|\right]^2$ remains

bounded, subject to the NN weight estimates from the previous event-sampling instant, $\hat{W}_j = \hat{W}_j\,(t_\kappa)$.

As before, the final terms in (65) can be simplified and incorporated in the closed-loop dynamics, revealing

$$\dot{V} \leq -\frac{1}{4}\left[3\,\|A\| - 2N_o - 4\right]\|\tilde{x}\|^2 - \frac{1}{2\,\|A\|^2}\sum_{j=1}^{n}\left[k_j g_m - 4g_M^2 - \frac{g_M^2}{\|A\|^2} - \frac{N_o}{\|A\|^2} - 3\right]\hat{r}_j^2$$
$$+ \frac{1}{2\,\|A\|^2}\sum_{j=1}^{n}\left[k_j^2 + 1\right]e_j^2 + \zeta_{B2} \quad (66)$$

where $\zeta_{B2} = \left\|\tilde{W}_o\right\|^2 + \frac{1}{2}\sum_{j=1}^{n}N_j\left[W_{jM} + \left\|\hat{W}_j\right\|\right]^2 + \sum_{j=1}^{n}\zeta_{j2} + \zeta_{o2}$ is bounded (recall that the observer NN weight estimation errors also remain bounded as a result of the weights remaining constant during the inter-event period).

It is at this point that an event execution law is selected. Recall the form of the execution law given by (23), where μ_j is to be selected such that the number of terms in (66) is reduced. Therefore, consider

$$\mu_j = \frac{1}{k_j^2 + 1}, \quad (67)$$

a constant, computable value. After using (67) in (23) and substituting into (66), combine like terms and arrive at the final expression for $\dot{V}$:

$$\dot{V} \leq -\frac{1}{4}\left[3\,\|A\| - 2N_o - 4\right]\|\tilde{x}\|^2 - \frac{1}{2\,\|A\|^2}\sum_{j=1}^{n}\delta_{j2}\hat{r}_j^2 + \zeta_{B2} \quad (68)$$

where $\delta_{j2} = k_j g_m - 4g_M^2 - \frac{g_M^2}{\|A\|^2} - \frac{N_o}{\|A\|^2} - \sigma_j - 3$. Observe that the first two terms in (68) are less than zero when controller gains are selected such that

$$\|A\| > \frac{2N_o + 4}{3} \quad \text{and} \quad k_i > \Gamma_{i2} \quad (69)$$

where $\Gamma_{i2} = \frac{1}{g_m} \left[4g_M^2 + \frac{g_M^2}{\|A\|^2} + \frac{N_o}{\|A\|^2} + \sigma_i + 3 \right]$ for all $i = 1, \ldots, n$. Therefore, it can be concluded that $\dot{V}$ is less than zero given that gains are selected according to (69) and the following inequalities hold:

$$\|\tilde{x}\| > \sqrt{\frac{4\zeta_{B2}}{3\|A\| - 2N_o - 4}} \quad \text{or} \quad \left| \hat{r}_j \right| > \|A\| \sqrt{\frac{2\zeta_{B2}}{\delta_{j2}}}. \tag{70}$$

In this case, the selection of an event-execution law resulted in the elimination of an explicit presence of measurement errors while adding an additional term, σ_j, in the δ_{j2} term of (70). In this way, (70) is different from the bounds obtained in Theorem 2 in that the measurement errors are not explicitly present.

In Case 1, the stability of the system was demonstrated at moments when the measurement errors are zero and when the NN's are updated and it was shown that all signals remain bounded. Then, in Case 2, it was shown how all signals in the system remain bounded during periods of time when there are nonzero measurement errors and when the NN weight estimates are held. In connecting these two cases, one may consider the dynamics that exist at the moments of transition. In other words, the results from Case 1 only show that the dynamics that exist at a single event-sampling instant are bounded; however, by considering "jump dynamics" that may exist in the transitions in the dynamics described by Cases 1 and 2, it may also be shown that these bounded effects do not accumulate over time and, ultimately, result in instability.

This can be accomplished by extending the results for Case 2 and by considering, not only the estimation error and tracking error dynamics, but also the dynamics of the NN weight estimation errors at event-sampling instants. Since the observer estimation errors and tracking errors have already been shown to be stable for Case 2, it is sufficient to show

that a bound exists for the expression

$$\Delta V_W = \frac{1}{2}\text{tr}\left\{\tilde{W}_o^T\left(t_{\kappa+1}\right)\tilde{W}_o\left(t_{\kappa+1}\right)\right\} - \frac{1}{2}\text{tr}\left\{\tilde{W}_o^T\left(t_\kappa\right)\tilde{W}_o\left(t_\kappa\right)\right\}$$
$$+ \sum_{j=1}^{n}\left[\frac{1}{2}\text{tr}\left\{\tilde{W}_j^T\left(t_{\kappa+1}\right)\tilde{W}_j\left(t_{\kappa+1}\right)\right\} - \frac{1}{2}\text{tr}\left\{\tilde{W}_j^T\left(t_\kappa\right)\tilde{W}_j\left(t_\kappa\right)\right\}\right] \tag{71}$$

where the discretized observer and controller NN weight updates are given by

$$\hat{W}_o\left(t_{\kappa+1}\right) = \hat{W}_o\left(t_\kappa\right) + \left[F_o\left[-\hat{\varphi}_o\left(t_\kappa\right)c\tilde{x}^T\left(t_\kappa\right) - \alpha_o\hat{W}_o\left(t_\kappa\right)\right]\right] \tag{72}$$

and

$$\hat{W}_i\left(t_{\kappa+1}\right) = \hat{W}_i\left(t_\kappa\right) + \left[F_i\left[\hat{r}_{ie}\left(t_\kappa\right)\hat{\varphi}_{ie}\left(t_\kappa\right) - \alpha_i\left|\hat{r}_{ie}\left(t_\kappa\right)\right|\hat{W}_i\left(t_\kappa\right)\right]\right], \tag{73}$$

respectively. Using (72) and (73), it is not difficult to show that (71) is bounded and, therefore, the jump dynamics that exist in the transitions remain bounded for all time [15]. As an additional remark, note that, in Case 2, the results were given in terms of the ideal and estimated NN weights; however, with the results presented here, it is easy to show that the bounds on the NN weight estimation errors are decreasing. Hence, the bounds that exist for the observer estimation errors, the tracking errors, and the NN weight estimation errors are decreasing during the inter-event periods as well as in the jump dynamics.

From Case 1 and Case 2, it can be concluded that the tracking errors and the NN weight estimation errors remain bounded for all time. Define the bounding terms

$$r_{jB} = \max\left\{\frac{4\zeta_{j1} + \alpha_j\eta_{j1}^2}{2\delta_{j1}}, \sqrt{\frac{2\zeta_{B2}}{\delta_{j2}}}\right\} \quad \text{and} \quad W_{jB} = \frac{1}{2}\left[\sqrt{\frac{4\zeta_{j1} + \alpha_j\eta_{j1}^2}{\alpha_j}} + \eta_{j1}\right]. \tag{74}$$

Next, by selecting controller gains satisfying (69), it can be concluded that $\dot{V}$ is less than zero when following inequalities hold

$$\left|r_j\right| > r_{jB} \quad \text{or} \quad \left\|\tilde{W}_j\right\| > W_{jB}. \tag{75}$$

Finally, with bounded tracking errors and an event-execution law defined by (23) and (67), it can be concluded that the measurement errors are bounded for all time.

Remark 9. By Theorems 2 and 3, the tracking errors in terms of estimated states, $\hat{r}_i$, $i = 1, \ldots, n$, are shown to be bounded. From Theorem 1, the observer estimation errors, $\|\tilde{x}\|$, are also bounded. Together, these results imply that the actual tracking errors, r_i, are also bounded.

Corollary 1. The result for the output-feedback controller (Theorems 2 and 3) can be easily realized for a state-feedback controller. As a matter of fact, the derivations for the state-feedback case become simpler due to the fact that an observer becomes unnecessary and the dynamics that result from one's incorporation vanish from the analysis. A detailed presentation for the derivation of the state-feedback controller would be highly redundant and, therefore, only major conclusions will be provided.

For clarity, the desired event-sampled control inputs that result when all states are measurable are provided; note that they are identical in form to (24), (39), and (48):

$$
\hat{v}_{1e} = -k_1 \left[r_1 + e_1 \right] - \hat{W}_1^T \varphi_{1e}
$$

$$
\hat{v}_{ie} = - \left[r_{i-1} + e_{i-1} \right] - k_i \left[r_i + e_i \right] - \hat{W}_i^T \varphi_{ie}
$$

$$
u_e = - \left[r_{n-1} + e_{n-1} \right] - k_n \left[r_n + e_n \right] - \hat{W}_n^T \varphi_{ne}. \tag{76}
$$

The inputs to the NNs are identical to those specified in the output-feedback controller with the differences being the absence of an observer estimation error term and the use of actual states instead of estimated states. Using these control inputs (76), the tracking error dynamics with measured states become

$$
\dot{r}_1 = g_1 \left[r_2 - k_1 r_1 - \hat{W}_1^T \varphi_{1e} + W_1^T \varphi_1 - \varepsilon_1 \right] + g_1 \left[-k_1 e_1 \right]
$$

$$
\dot{r}_i = g_i \left[r_{i+1} - k_i r_i - r_{i-1} - \hat{W}_i^T \varphi_{ie} + W_i^T \varphi_i - \varepsilon_i \right] + g_i \left[-k_i e_i - e_{i-1} \right]
$$

$$
\dot{r}_n = g_n \left[-k_n r_n - r_{n-1} - \hat{W}_n^T \varphi_{ne} + W_n^T \varphi_n - \varepsilon_n \right] + g_n \left[-k_n e_n - e_{n-1} \right]. \tag{77}
$$

Again, these results are similar to the error dynamics that were found in the presence of an observer and estimated states. The primary difference in (77) is the absence of $\dot{\hat{x}}$ terms, which are generated from the observer, and the absence of $\tilde{x}$ terms which are generated by the distinction between the system dynamics and the estimated states. Similar to before, these tracking error dynamics can be considered in the context of Lyapunov candidates that have identical forms as (26), (41), and (50); however, with the absence of an observer, it is not necessary to include the scaling term, $\frac{1}{\|A\|^2}$, that was incorporated in the output-feedback derivation in order to avoid controller gain bounds that are directly proportional to $\|A\|$. Choosing the weight update laws

$$\dot{\hat{W}}_i = F_i \left[r_{ie} \varphi_{ie} - \alpha_i \left| r_{ie} \right| \hat{W}_i \right] \ i = 1, \ldots, n \tag{78}$$

where $F_i = F_i^T > 0$ and $\alpha_i > 0$ are design parameters, and using a procedure similar to what was presented in the output feedback controller reveals

$$\dot{V}_n \leq -\sum_{j=1}^{n} \left| r_j \right| \left[\frac{1}{2} \delta_{j3} \left| r_j \right| + \alpha_j \left[2 - \chi_j \right] \left[\left\| \tilde{W}_j \right\| - \frac{\eta_{j3}}{2} \right]^2 - \frac{\eta_{j3}^2 \alpha_j \left[2 - \chi_j \right]}{4} \right]$$
$$+ \frac{1}{2} \sum_{j=1}^{n} \beta_j B_{ej}^2 + \zeta_{FS1} \tag{79}$$

where B_{ei} is the bound on the measurement error in the ith subsystem and

$$\zeta_{FS1} = \sum_{j=1}^{n} \zeta_{j3}, \quad \eta_{j3} = \frac{\left[g_M + \chi_j \right] \sqrt{N_j} + \chi_j \alpha_j W_{jM}}{\alpha_j \left[2 - \chi_j \right]}$$

$$\beta_j = k_j^2 + 1, \quad \delta_{j3} = k_j g_m - 3g_M^2 - 2.$$

with $\zeta_{j3} = \frac{g_{jM} \varepsilon_{jM}^2}{2k_j} + 2g_{jM}^2 W_{jM}^2 N_j$.

With (79) and an approach similar to what was presented in Theorem 2, it is easy to demonstrate that the system is ISS-like with respect to the measurement error, provided

that controller gains are selected satisfying the following condition:

$$k_i > \Gamma_{i3} \tag{80}$$

where $\Gamma_{i3} = \frac{1}{g_m}\left[3g_M^2 + 2\right]$ for all $i = 1, \ldots, n$. Bounds on the tracking errors and the NN weight estimation errors can be found in terms of bounded terms and measurement errors introduced by event-sampling. However, in order to implement the event-sampled controller, it must also be shown that the event-sampling errors are also bounded.

Using the line of reasoning that was presented in Theorem 3, it is not difficult to prove that the measurement errors in the state-feedback controller remain bounded at events as well as during inter-event periods. Letting the event-sampling error satisfy the condition

$$e_i^2 \le \sigma_i \mu_i r_i^2, \ i = 1, \ldots, n \tag{81}$$

and choosing

$$\mu_j = \frac{1}{k_j^2 + 1}, \tag{82}$$

reveals

$$\dot{V}_n \le -\frac{1}{2} \sum_{j=1}^{n} \delta_{j4} r_j^2 + \zeta_{FS2} \tag{83}$$

where $\delta_{j4} = k_j g_m - 4g_M^2 - \sigma_j - 1$ and $\zeta_{FS2} = \frac{1}{2}\sum_{j=1}^{n} N_j \left[W_{jM} + \left\|\hat{W}_j\right\|\right]^2 + \sum_{j=1}^{n} \frac{g_M \varepsilon_{jM}^2}{2k_j}$ is bounded. The bound on the tracking error can, hence, be expressed as functions of bounded terms.

Remark 10. From Theorem 3, Case 2, an event-execution law was derived in terms of values that are known. An alternate derivation makes use of a Lipschitz condition on the NN activation functions, generating an execution law in terms of the NN weight estimates [14]. An immediate drawback with such execution law is that it requires the computation of NN weight estimates during inter-event periods. Though more computationally expensive,

this approach is not without benefit: It can be shown that the bounds on the tracking errors resulting from this derivation are smaller than the bounds resulting from the derivation presented in Theorem 3. The engineering decision thus becomes a compromise between computational efficiency and tracking performance.

Remark 11. In Theorem 2, the system was shown to be ISS-like with respect to bounded measurement errors and, in Theorem 3, the measurement errors were shown to be bounded in the presence of an appropriately selected event-execution law. Given that the dynamics of the system are Lipschitz, all necessary conditions are satisfied in order to demonstrate the existence of inter-event time periods that are bounded away from zero [8][13].

Remark 12. In the derivations presented, a measurement error and an event-execution law is considered at each subsystem. Moreover, the event-sampling errors are upper-bounded by triggering mechanisms that are in terms of their respective tracking errors. In other words, the magnitude of the error between the event-sampled state vector and the continuously-sampled state vector is contained by a threshold that is determined by the errors between the continuously-sampled state vector and their desired values:

$$[x_{ie} - x_i]^2 \leq \sigma_i \mu_i [x_i - x_{di}]^2$$

In practice, during an inter-event period, only the desired value in the first subsystem is dynamic and the desired values in each subsequent subsystem - the desired virtual controls that are approximated with NNs - remain static; in other words, it is not necessary to continuously compute the desired virtual control inputs and the only information that is necessary to implement the event-triggering mechanisms is knowledge of the continuously sampled state vector, the state vector from the previous event, and the continuously sampled desired value for the first subsystem.

Remark 13. In the expressions for the bounds on the tracking errors and the NN weight estimation errors, note the frequent appearance of terms stemming from the unknown functions, $g_i(\cdot)$; in other words, many of the bounds are in terms of g_M and/or g_m. The presence of these terms can be largely avoided by invoking an assumption on the boundedness of $|\dot{g}_i(\cdot)|$, as was done in [1]. With an assumption on $|\dot{g}_i(\cdot)|$ being bounded, and using Barbalat's lemma, it would not be difficult to show that the tracking errors converge to zero in the ideal case when all states are available and when errors from NN approximations are zero and all sigma-modification terms, α_i, $i = 1, \ldots n$, are zero.

Remark 14. Once the signals reach their bounds, additional events may become redundant - in other words, after a certain point, the occurrence of an event may not reduce any of the errors and it becomes superfluous to spend any computational energy. In order to avoid this, a deadzone operator may be implemented.

With the derivations complete, simulation results may now be presented.

4 SIMULATION RESULTS

Given that the primary contribution of this work is the introduction of event-sampling in the backstepping design for a strict-feedback system, the goal of the simulations will be to compare the results of the proposed controllers when event-sampling is used to when traditional time-sampling is used. Results for the output-feedback controller will be shown first and then for the state-feedback controller.

Event-sampling in a strict-feedback system presents an interesting design decision in that there are a number of ways in which the event-triggering mechanism can be implemented in the system. As an example, separate triggering mechanisms can be placed in each subsystem and, when an event occurs in one subsystem, the state vector is updated with the state-variable corresponding to that subsystem; additionally, the controller in that subsystem is also updated. Alternatively, the measurement errors and the dynamic thresholds in each subsystem can be combined and a single event-triggering mechanism can be used for the whole system. The results of Theorem 2 and Theorem 3 remain valid regardless of which approach is implemented. In the simulation results that follow, the latter approach was used and the sum of the square of the measurement errors in each subsystem was compared to the sum of the dynamic thresholds generated for each subsystem.

Prior to giving results, details common to both simulations will be specified. The proposed controllers will be applied to the following strict-feedback system:

$$
\begin{aligned}
\dot{x}_1 &= x_1^2 - x_1^3 + x_2 \\
\dot{x}_2 &= x_1 + x_2 + u \\
y &= x_1.
\end{aligned}
\tag{84}
$$

The desired trajectory, y_d, is generated from the following van der Pol oscillator system:

$$\dot{x}_{1d} = x_{d2}$$

$$\dot{x}_{2d} = -x_{d1} + 0.4 \left[1 - x_{d1}^2\right] x_{d2} \tag{85}$$

$$y_d = x_{d1}.$$

In both simulations, the controller NNs each contain 25 nodes and, for the results shown in the figures, event-execution parameters of $\sigma_1 = \sigma_2 = 0.0008$ were selected. Initial conditions of $[x_1(0), x_2(0)]^T = [1.1, 0.9]^T$ and $[x_{d1}(0), x_{d2}(0)]^T = [1.6, 0.8]^T$ were used.

4.1 OUTPUT FEEDBACK SIMULATION RESULTS

An observer NN with 10 nodes was implemented. Control gains of $k_1 = k_2 = 6.5$ and $l_1 = l_2 = 60$ and NN parameters of $F_1 = F_2 = 0.01$, $\alpha_1 = 140$, $\alpha_2 = 40$, $F_o = 0.2$, and $\alpha_o = 0.1$ were selected.

The output results are shown in Fig. 4.1 and the observer estimation errors are shown in Fig. 4.2. It can be seen that the event-sampled controller performs nearly identically to that of the time-sampled controller, in both outputs as well as observer convergence. When considering the control input (Fig. 4.3), it is found that the control effort is nearly identical. This demonstrates that, with respect to tracking performance and control effort, it is unnecessary to execute updates and control laws at every available instant, allowing for fewer computations. When the NN weights are considered (Fig. 4.4) it can be seen that event-sampled controller results in smaller magnitudes, a result from the fact that NN weights are not updated as frequently and do not have the opportunity to grow before repeating their growth/decay cycles. Fig. 4.5 compares the dynamic event-sampling thresholds with the evolving event-sampling errors. Finally, the primary benefit of event-sampling can be seen in Fig. 5.8: It is discovered that, out of an available 2500 samples, the event-sampled controller is able to achieve exceptional tracking performance making

use of fewer than 1200 samples. Moreover, observe the linear nature of Fig. 5.8, indicating that the occurence of events is fairly evenly distributed.

4.2   STATE FEEDBACK SIMULATION RESULTS

Control gains of $k_1 = k_2 = 6.5$ and NN parameters of $F_1 = F_2 = 0.01$, $\alpha_1 = 140$, and $\alpha_2 = 40$ were selected.

The output results are shown in Fig. 4.7. It can be seen that the event-sampled controller performs nearly identically to that of the time-sampled controller. This is also true when the control input to the system is considered (Fig. 4.8). This demonstrates that, with respect to tracking performance and control effort, it is unnecessary to execute updates and control laws at every available instant, allowing for fewer computations. When the NN weights are considered (Fig. 4.9) it can be seen that event-sampled controller results in smaller magnitudes, a result from the fact that NN weights are not updated as frequently and do not have the opportunity to grow before repeating their growth/decay cycles. Fig. 4.10 compares the dynamic event-sampling thresholds with the evolving event-sampling errors. Finally, the primary benefit of event-sampling can be seen in Fig. 4.11: It is discovered that, out of an available 2500 samples, the event-sampled controller is able to achieve exceptional tracking performance making use of fewer than 1300 samples.

4.3   EFFECTS OF EVENT-EXECUTION PARAMETER

Table 4.1 shows how the event-execution parameters, σ_1 and σ_2, effect the number of events that occur. Observe that, by increasing the execution-parameter, the number of events decreases; practically, the number of computations is reduced with larger σ_1 and σ_2. However, if the execution parameters are taken to be too large and, as a result, the state vector and the control laws are not updated frequently enough, either the tracking performance begins to suffer or the control effort begins to increase. The design challenge thus becomes selecting parameters that result in a reduction in computations while maintaining acceptable controller performance.

Table 4.1　Number of Events out of Total Available Samples

$\sigma_{1,2}$	Total Samples	Number of Events	
		Output-Feedback	State-Feedback
0.0008	2500	1110	1235
0.008	2500	919	1188
0.08	2500	370	899
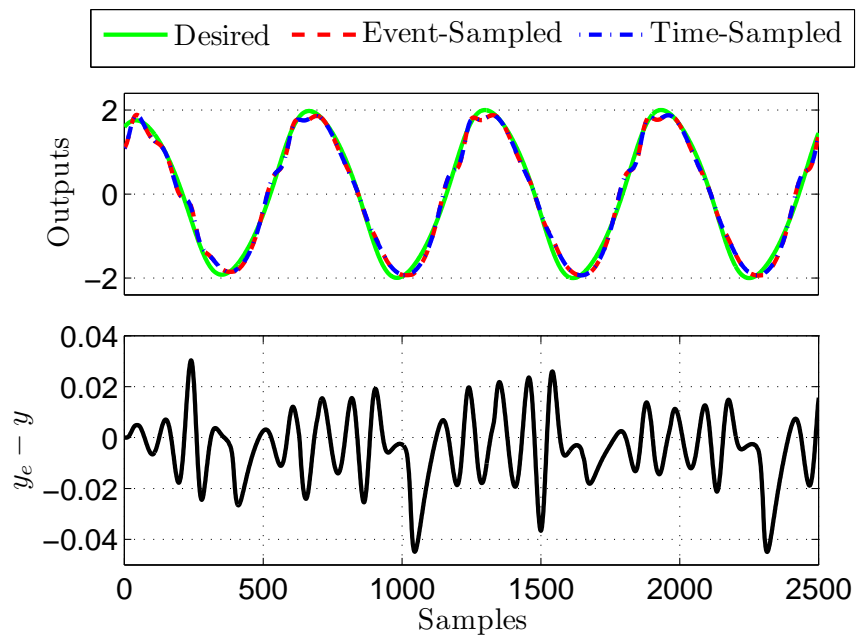
Fig. 4.1　Controller Outputs - Output Feedback
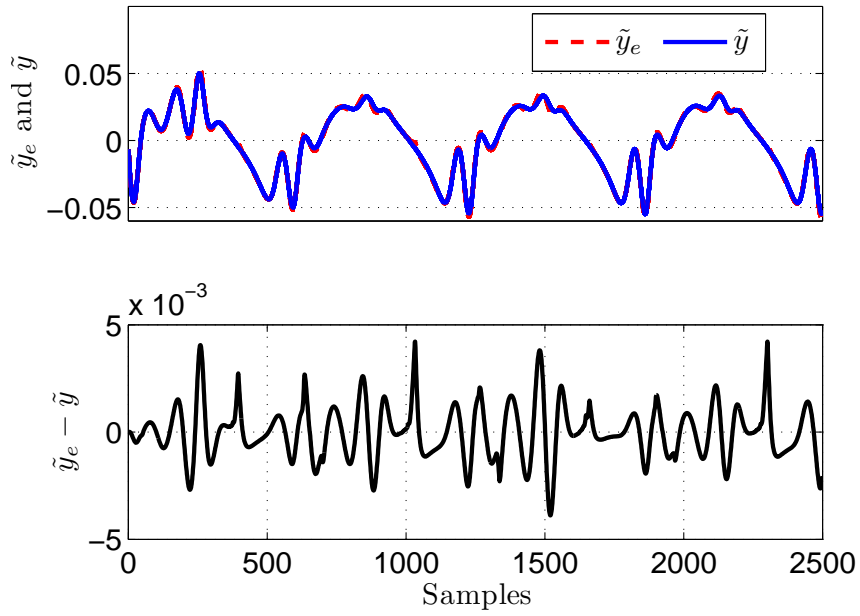
Fig. 4.2   Observer Estimation Errors

Fig. 4.3   Time-Sampled (Solid), Event-Sampled (Dashed) - Output Feedback

Fig. 4.4   Time-Sampled (Solid), Event-Sampled (Dashed) - Output Feedback
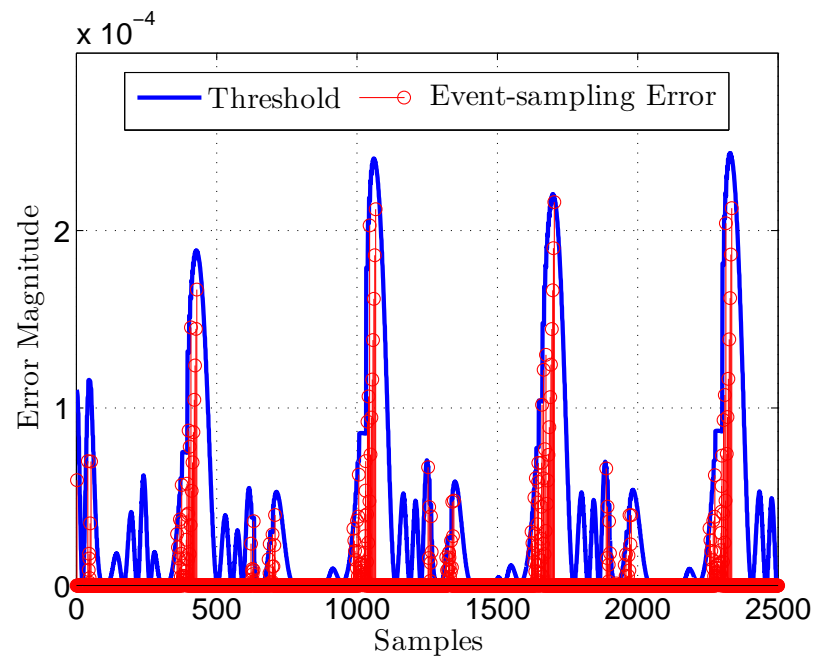
Fig. 4.5   Event-threshold vs. Measurement Error - Output Feedback
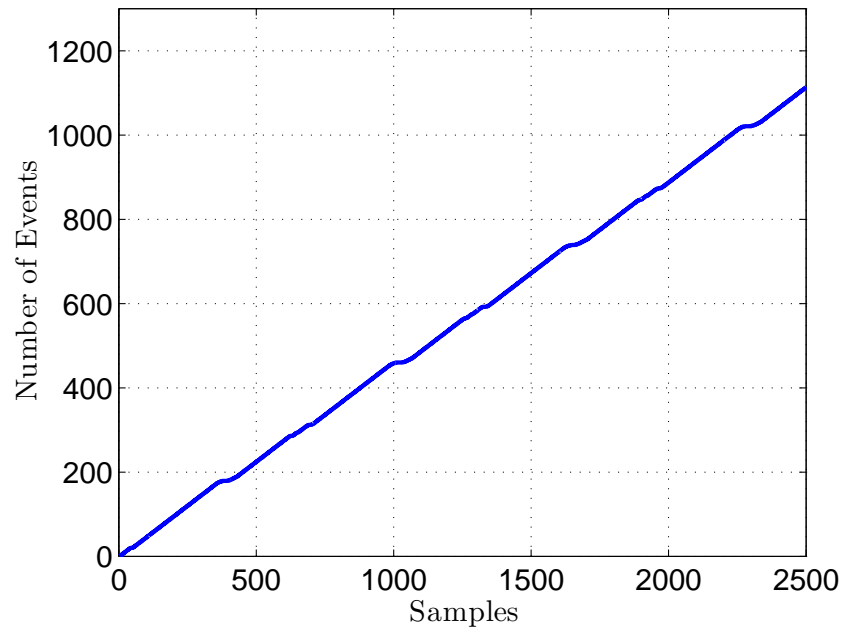
Fig. 4.6   Number of Events - Output Feedback
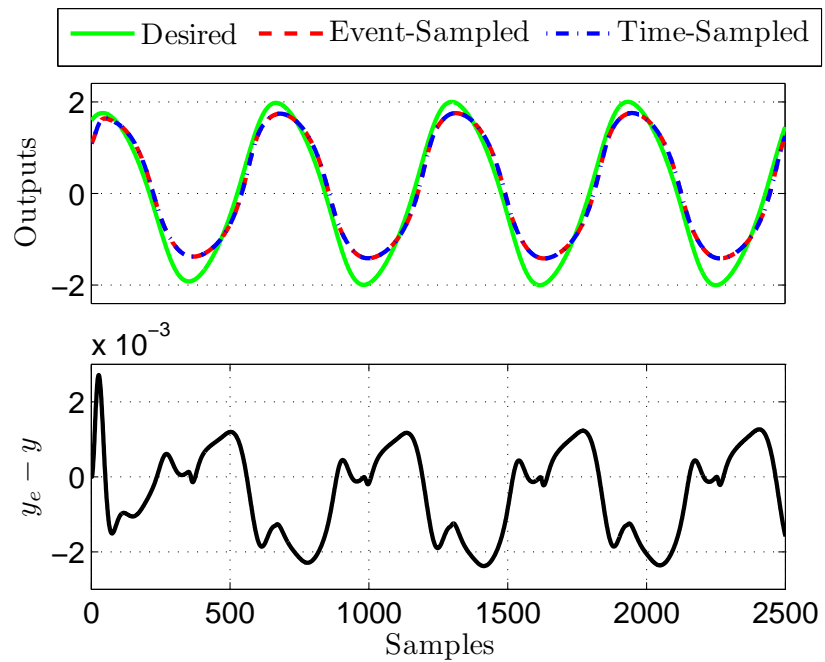
Fig. 4.7   Controller Outputs - State Feedback
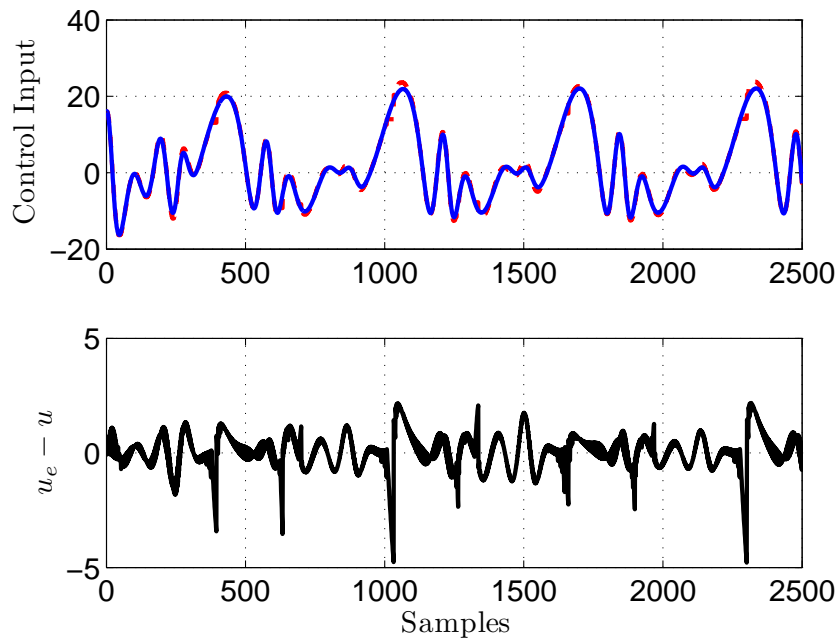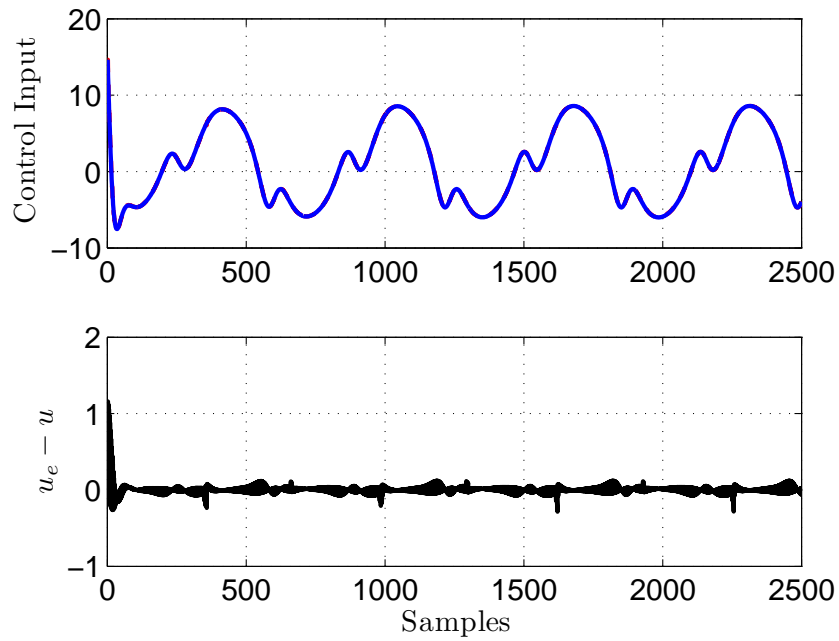
Fig. 4.8   Time-Sampled (Solid), Event-Sampled (Dashed) - State Feedback
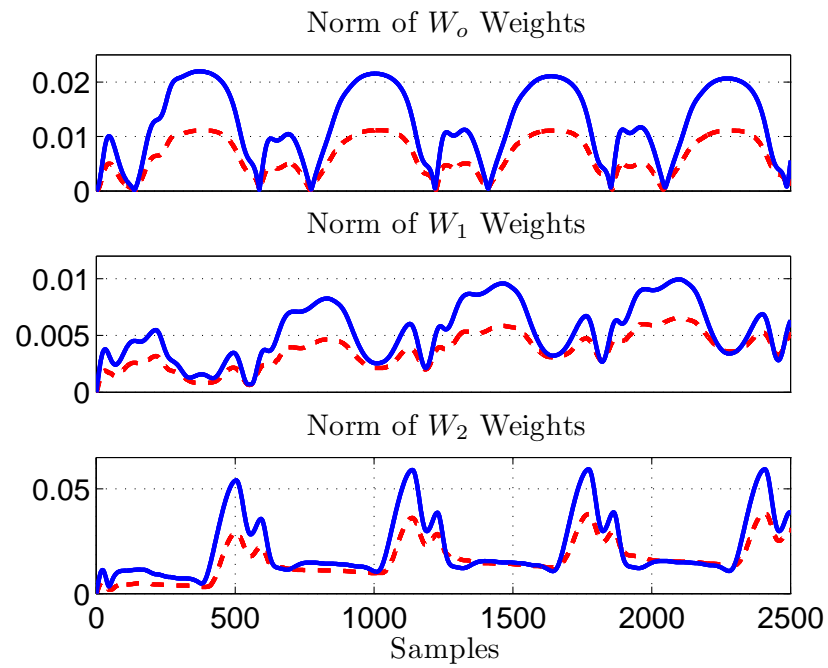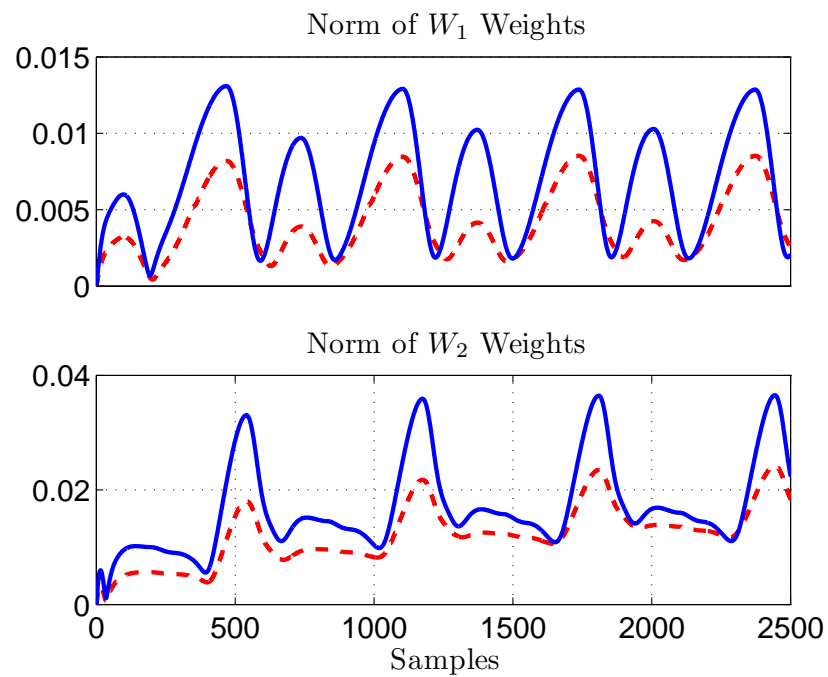

Fig. 4.9   Time-Sampled (Solid), Event-Sampled (Dashed) - State Feedback
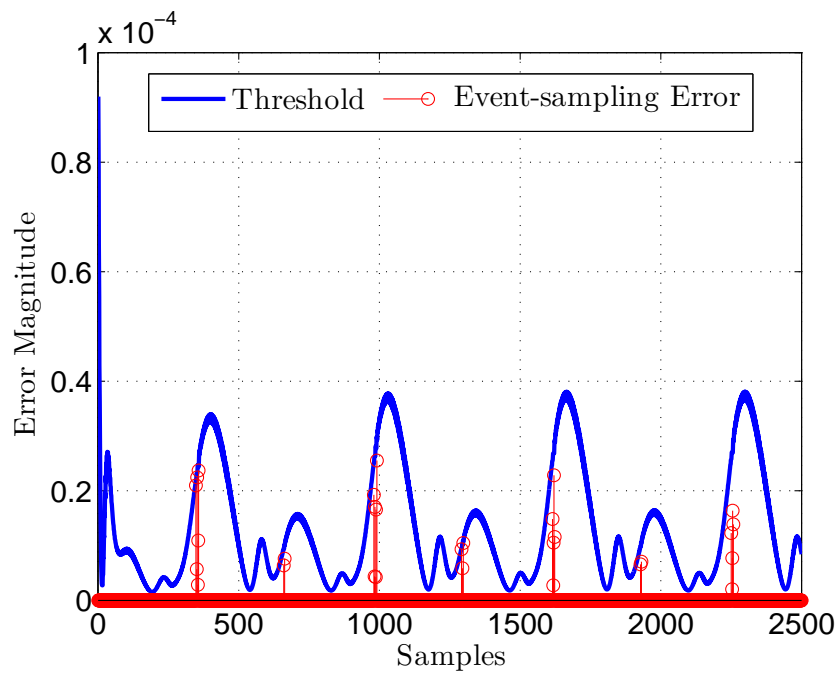
Fig. 4.10   Event-threshold vs. Measurement Error - State Feedback
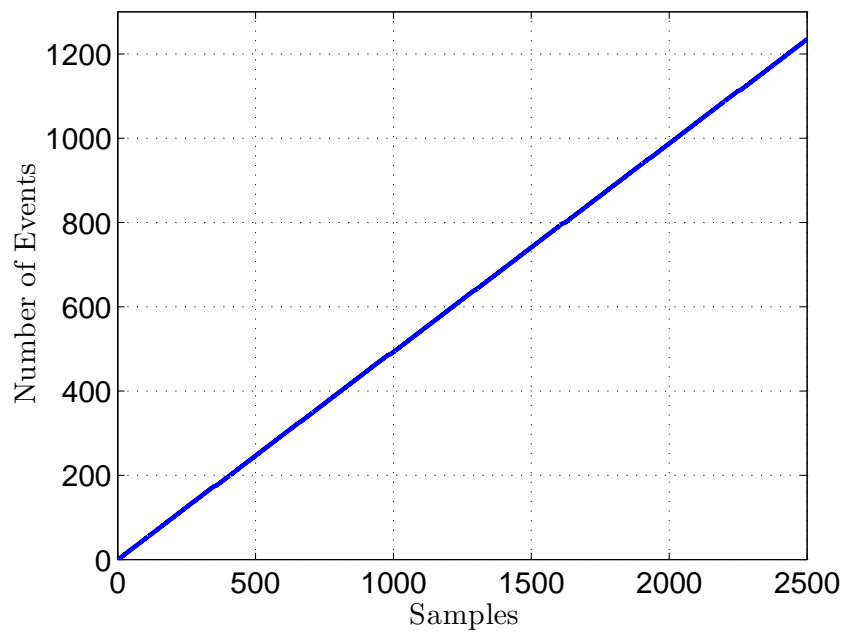
Fig. 4.11   Number of Events - State Feedback

5 CONCLUSIONS

This work presented the derivation for two NN-based controllers that assume an event-sampling paradigm: The first was an output-feedback controller that required an observer to estimate an unknown state vector and the second was a state-feedback controller which, in practice, would require the use of additional sensors in order to obtain full knowledge of the state vector. In both cases, Lyapunov analysis was used to demonstrate the input-to-state stability of the controllers as well as to show the boundedness of the errors introduced by event-sampling; moreover, it was also shown how the Lyapunov method could be used to derive an event-execution law. With these, simulations were conducted and the performances of the controllers were compared to results given by their time-sampled counter-parts. It was found that the number of samples could be substantially reduced without having to sacrifice tracking fidelity or control effort.

BIBLIOGRAPHY

[1] S. Ge and Cong Wang, "Direct adaptive NN control of a class of nonlinear systems," *IEEE Trans. Neural Netw.*, vol. 13, no. 1, pp. 214-221, 2002.

[2] B. Xu, C. Yang and Y. Pan, "Global neural dynamic surface tracking control of strict-feedback systems with application to hypersonic flight vehicle," *IEEE Trans. Neural Netw. Learning Syst.*, vol. 26, no. 10, pp. 2563-2575, 2015.

[3] T. Dierks and S. Jagannathan, "Output feedback control of a quadrotor UAV using neural networks," *IEEE Trans. Neural Netw.*, vol. 21, no. 1, pp. 50-66, 2010.

[4] Zhi Liu, Fang Wang, Yun Zhang, Xin Chen and C. Chen, "Adaptive fuzzy output-feedback controller design for nonlinear systems via backstepping and small-gain approach," *IEEE Trans. Cybern.*, vol. 44, no. 10, pp. 1714-1725, 2014.

[5] S. Tong and Y. Li, "Adaptive fuzzy output feedback tracking backstepping control of strict-feedback nonlinear systems with unknown dead zones," *IEEE Trans. Fuzzy Syst.*, vol. 20, no. 1, pp. 168-180, 2012.

[6] S. Tong, Y. Li and P. Shi, "Observer-based adaptive fuzzy backstepping output feedback control of uncertain MIMO pure-feedback nonlinear systems," *IEEE Trans. Fuzzy Syst.*, vol. 20, no. 4, pp. 771-785, 2012.

[7] S. Shanwei, "Output-feedback tracking control for a class of nonlinear non-minimum phase systems via backstepping method," *in 34th Chinese Control Conference*, 2015, pp. 475-480.

[8] P. Tabuada, "Event-triggered real-time scheduling of stabilizing control tasks," *IEEE Transactions on Automatic Control*, vol. 52, no. 9, pp. 1680-1685, 2007.

[9] M. Mazo Jr. and P. Tabuada, "Input-to-state stability of self-triggered control systems," in *Joint 48th IEEE Conference on Decision and Control*, Shanghai, P.R. China, 2009, pp. 928-933.

[10] M. Mazo and P. Tabuada, "Decentralized event-triggered control over wireless sensor/actuator networks," *IEEE Transactions on Automatic Control*, vol. 56, no. 10, pp. 2456-2461, 2011.

[11] D. Lehmann and J. Lunze, "A state-feedback approach to event-based control," *Automatica*, vol. 46, no. 1, pp. 211-215, 2010.

[12] D. Lehmann and J. Lunze, "Event-based output-feedback control," *in 19th Mediterranean Conference on Control and Automation*, Corfu, Greece, 2011, pp. 982-987.

[13] P. Tallapragada and N. Chopra, "On event triggered tracking for nonlinear systems," *IEEE Transactions on Automatic Control*, vol. 58, no. 9, pp. 2343-2348, 2013.

[14] A. Sahoo, H. Xu and S. Jagannathan, "Neural network-based event-triggered state feedback control of nonlinear continuous-time systems," *IEEE Trans. Neural Netw. Learning Syst.*, pp. 1-1, 2015.

[15] F. Lewis, S. Jagannathan and A. Yeşildirek, *Neural Network Control of Robot Manipulators and Nonlinear Systems*. London: Taylor & Francis, 1999.

[16] X. Zhong and H. He,"An Event-Triggered ADP Control Approach for Continuous-Time System With Unknown Internal States," *IEEE Trans. Cybern.*, pp. 1-12, 2016.

II. EVENT-SAMPLED CONTROL OF QUADROTOR
UNMANNED AERIAL VEHICLE

Abstract

In this paper, an event-sampled output-feedback neural network (NN) controller for a quadrotor Unmanned Aerial Vehicle (UAV) is considered. First an observer design is presented, allowing the need for a full knowledge of the state-vector to be avoided. Next, a kinematic controller is designed in order to find a desired translational velocity; the information provided by the kinematic controller will be used in the design of a virtual controller wherein a desired rotational velocity will be determined such that the UAV' s orientation converges to its desired value. Finally, the information from the observer, the kinematic controller, and the virtual controller are used in the design of a dynamic controller where NNs will be implemented to approximate uncertainties in the UAV's dynamics; the signals generated by the dynamic controller will ensure that the desired lift velocity and the desired rotational velocities are tracked. In all these designs, the effects of sampling errors are highlighted. Using these results, the continuously sampled closed-loop controller is considered in the presence of bounded measurement errors and it is shown that the system generates a local ISS-like Lyapunov function. Next, by designing an appropriate event-execution law, the measurement errors are shown to be bounded for all time. Finally, the effectiveness of the proposed event-sampled controller will be demonstrated with simulation results.

1 INTRODUCTION

The emergence of quadrotors as unmanned aerial vehicles (UAVs) has resulted in a significant amount of research in efforts to develop effective means by which they can be controlled [1]-[5]. In particular, the work in [1] presented a novel output-feedback controller with the use of neural networks (NNs). The objectives of the proposed controller in [1] were to alleviate the need for unnecessary sensors by introducing an observer and to compensate for unknown nonlinear dynamics by making use of the universal approximation property of NNs. The effectiveness and robustness of the controller was demonstrated with simulation results.

The use of NNs has proven to be a very powerful asset in the control for a quadrotor UAV. By implementing a NN observer, thereby relaxing the need for full-knowledge of the state-vector, and by using NNs to compensate for uncertainties, a greater degree of flexibility is made available for engineers. Certainly, the works [1]-[5] have provided thorough approaches to the problem of controlling the underactuated quadrotor system. However, one aspect of the problem that they did not address was the sampling scheme; since the focus of the papers was not in exploring different sampling approaches, they simply assumed the traditional time-based sampling whereby the control law is updated at a fixed frequency. An alternative to this approach, event-based sampling, was introduced in [6] and explored at great lengths in following effort [7]-[12] wherein the derivation of an event-execution law that ensures the boundedness of the measurement errors introduced by the intermittent sampling is shown. Additionally, the benefit of event-sampling is also demonstrated where for an appropriately designed event-execution law, a reduction in computations can be achieved without having to significantly compromise the controller's performance. In other words, a successful implementation of event-sampling will yield computational efficiency. By and large, however, the literature [6]-[12] makes developments in event-sampling in the context of generalized systems.

In addition to its theoretical aspects, the notion of event-sampling has also been considered in the context of real-world applications [13] and [14]. In [13], event-sampling is implemented in a vibration analysis application for pneumatic tires and, in [14], an event-sampled observer-based design is applied in a networked visual control system. Even still, the types of applications that are considered in the works [13]-[14] do not take complex dynamics into account. To our knowledge, the incorporation of event-sampling in complex robotics applications is not one that has been substantially explored. Specifically, the union of event-sampling with the control of an underactuated quadrotor UAV is a topic which has not been given attention.

In this paper, first an observer design is briefly presented, allowing the need for a full knowledge of the state-vector to be avoided. Next, a kinematic controller is designed in order to find a desired translational velocity such that the UAV' s position converges to a desired trajectory which is selected as an external input; additionally, it is in the kinematic controller that the quadrotor' s desired orientation is found. Then, the information provided by the kinematic controller will be used in the design of a virtual controller wherein a desired rotational velocity will be determined such that the UAV' s orientation converges to its desired value. In these developments, it will be discussed how the effects of event-sampling can be injected either implicitly through NN approximation errors or explicitly through an intermittently updated state-vector.

After these, details will be given showing how it is through the kinematic controller that event-sampling measurement errors are explicitly injected into the system. Finally, the information from the observer, the kinematic controller, and the virtual controller are used in the design of a dynamic controller where NNs will be implemented to approximate uncertainties in the UAV's dynamics; the signals generated by the dynamic controller will ensure that the desired lift velocity and the desired rotational velocities are tracked. Here, too, it will be illustrated how the dynamic controller injects explicit measurement errors into the system.

Therefore, the main contribution of this paper is to add an additional degree of flexibility to the adaptive NN control of a quadrotor UAV by incorporating notions of event-sampling. For a complex quadrotor UAV system, the benefits of event-sampling are two-fold: first, computational costs would be reduced due to aperiodic tuning of NN weights. With fewer computations being performed, battery life and, subsequently, flight time, could be extended. Secondly, event-sampling may also save in communications costs. In a quadrotor UAV system, the regular transmission of data from external sensors, such as GPS and gyro readings, is essential for stable flight and, in these transmissions, packet-losses are inevitable. A reduction in the number of samples being used would minimize the effects of these losses and save in communication costs.

In order to accomplish the incorporation of event-sampling in the control of a quadrotor UAV, first, it will be shown how the system exhibits ISS-like behavior with respect to bounded measurement errors; this result is a necessary requirement in order to implement the event-sampled controller because it ensures the existence of nonzero inter-event times. Next, it will be necessary to demonstrate that the measurement errors remain bounded for all time. This will be demonstrated by considering the dynamics of the system at event-sampling instants as well as during inter-event periods. The boundedness of the measurement errors during inter-event periods will be guaranteed by the implementation of an event-execution law, which will also be derived in this work. Finally, simulation results will be given to demonstrate the effectiveness of the event-sampled controller as well as to illustrate how its performance compares to its time-sampled counterpart.

The rest of this paper will be organized as follows: Section 2 will provide background information and a statement of the problem; Section 3 will present the derivation for an observer and section 4 will present the derivation of the event-sampled controller as well as for the design of an event-execution law; Section 5 will present simulation results showing the effectiveness of the proposed controller as well as preliminary hardware results for an event-based PID controller; and, finally, conclusions will be given in Section 6.

2   BACKGROUND AND PROBLEM STATEMENT

In this section, an introduction on the notations used in this paper will be given and a brief background on the control of a quadrotor UAV will be provided. Then, the control objectives which will be considered in this paper will be specified.

2.1   NOTATIONS

The measurement errors that result from event-sampling will be denoted by Ξ. In order to distinguish event-sampled variables with their time-sampled counterparts, this symbol will appear as a subscript; for example, the event-sampled position of the quadrotor will be denoted by ρ_Ξ. A formal definition for Ξ will be presented in the background section. In the analysis that will be presented, $\|\cdot\|$ and $\|\cdot\|_F$ will be used as the Euclidean norm for vectors and the Frobenius norm for matrices, respectively [15].

2.2   BACKGROUND

The states of the quadrotor UAV are given by its measured coordinate position, $\rho = [x,y,z]^T$; its orientation $\Theta = [\phi,\theta,\psi]^T$ (roll, pitch, yaw), which are measured with respect to the inertial fixed frame; its translational velocity in the body fixed frame, $v = [v_{xb},v_{yb},v_{zb}]^T$; and its rotational velocity in the body fixed frame, $\omega = [\omega_{xb},\omega_{yb},\omega_{zb}]^T$. With these, the kinematics of the quadrotor can be written as [1]

$$\dot{\rho} = Rv \tag{1}$$

and

$$\dot{\Theta} = T\omega. \tag{2}$$

The translational rotation matrix relating a vector in the body fixed frame to the inertial coordinate frame will be defined by

$$R\left(\Theta\right) = R = \begin{bmatrix} c_\theta c_\psi & s_\phi s_\theta c_\psi - c_\phi s_\psi & c_\phi s_\theta c_\psi + s_\phi s_\psi \\ c_\theta s_\psi & s_\phi s_\theta s_\psi - c_\phi c_\psi & c_\phi s_\theta s_\psi - s_\phi c_\psi \\ -s_\theta & s_\phi c_\theta & c_\phi c_\theta \end{bmatrix}$$

where $s_{(\bullet)}$ and $c_{(\bullet)}$ are used as abbreviations for $\sin\left(\bullet\right)$ and $\cos\left(\bullet\right)$, respectively. Moreover, the rotational transformation matrix from the fixed body to the inertial coordinate frame is defined with its inverse as

$$T\left(\Theta\right) = T = \begin{bmatrix} 1 & s_\phi t_\theta & c_\phi t_\theta \\ 0 & c_\phi & -s_\phi \\ 0 & \frac{s_\phi}{c_\theta} & \frac{c_\phi}{c_\theta} \end{bmatrix} \qquad T^{-1} = \begin{bmatrix} 1 & 0 & -s_\theta \\ 0 & c_\phi & s_\phi c_\theta \\ 0 & -s_\phi & c_\phi c_\theta \end{bmatrix}$$

where $t_{(\bullet)}$ is used as an abbreviation for $\tan\left(\bullet\right)$. Lastly, define the augmented transformation matrix $A = \text{diag}\left\{R, T\right\}$. Next, the UAV dynamics will be presented and the control objective will be given.

2.3 PROBLEM STATEMENT

The dynamics of the quadrotor UAV in the body fixed frame are given by [1]

$$M\begin{bmatrix} \dot{v} \\ \dot{\omega} \end{bmatrix} = \bar{S}\left(\omega\right)\begin{bmatrix} v \\ \omega \end{bmatrix} + \begin{bmatrix} N_1\left(v\right) \\ N_2\left(\omega\right) \end{bmatrix} + \begin{bmatrix} G\left(R\right) \\ 0_{3\times 1} \end{bmatrix} + U + \tau_d \tag{3}$$

where $M = \text{diag}\left\{mI_{3\times 3}, J\right\}$, with m being a positive scalar representing the total mass of the UAV and J being a positive definite inertia matrix; $\bar{S}\left(\omega\right) = diag\left\{-mS\left(\omega\right), S\left(J\omega\right)\right\}$, where $S\left(\bullet\right)$ is a skew symmetric matrix satisfying $h^T Sh = 0$ for any appropriately dimensioned vector h; $N_1\left(v\right)$ and $N_2\left(\omega\right)$ are nonlinear aerodynamic effects; $G\left(R\right) = mgR^T\left(\Theta\right)E_z$

is the gravity vector, with $g = 9.8 \, m/s^2$ and $E_z = [0, 0, 1]^T$; $U = [0, 0, u_1, u_2]^T$ is an augmented vector containing the control inputs corresponding to the total thrust, u_1, and to the rotational torques, $u_2 = [u_{21}, u_{22}, u_{23}]^T$, corresponding to roll, pitch, and yaw, respectively; and $\tau_d = \left[\tau_{d1}^T, \tau_{d2}^T \right]^T$ represents unknown, bounded disturbances such that $\|\tau_d\| \leq \tau_M$ for a known positive constant, τ_M.

Before giving the control objective, a definition of the measurement errors that result from event-sampling will be introduced. Define the measurement errors to be

$$\Xi_\chi (t) = \chi_\Xi (t_l) - \chi (t), \, \forall t \in [t_l, t_{l+1}) \tag{4}$$

where, in general, $\chi (t)$, represents a time-sampled state variable. Moreover, $\chi_\Xi (t_l)$ denotes the event-sampled state variable that was measured at the previous event-sampling instant at time t_l; it is this event-sampled variable that is stored in the controller during the inter-event period. Finally, $\Xi_\chi (t)$ is the measurement error that results from intermittent sampling. The introduction of this error will present an additional challenge in the control objective in that it necessitates additional considerations that will guarantee the controller's stable performance. In particular, it will be necessary to design an event-triggering mechanism that will ensure that the values that are stored are being updated frequently enough for the controller to be able to achieve acceptable performance while reducing the number of computations. With these considerations in mind, the control objective may be stated.

The control objective is to design an event-sampled output-feedback controller for (3) such that the UAV follows a desired trajectory given by $\rho_d = [x_d, y_d, z_d]^T$ and a desired yaw, ψ_d, while maintaining stable flight. This requires knowledge of the quadrotor's dynamics as well as knowledge of the UAV's translational and rotational velocities. However, these requirements will be relaxed by utilizing the universal approximation property of NNs [15] in order to estimate the uncertainties.

In order to avoid the measurement of the UAV's state-vector, a NN observer will be implemented to estimate the translational and rotational velocity vector, which will be assumed to be immeasurable. The estimated values will be used in the kinematic controller, the NN virtual controller, and the NN dynamic controller. With these, it will be possible to design an event-sampled control law that will achieve the control objective. In order to ensure that the control law is being updated frequently enough for the UAV to achieve its tracking objective, an event-execution law will be derived such that the measurement errors remain bounded for all time.

In the analyses that will be presented, the following assumptions will be made.

Assumptions: The states of the reference trajectory, ρ_d and ψ_d, remain bounded [1]. The state-vector corresponding to the UAV's velocity is not available whereas the system (3) is observable [1]. There are no transmission or computation time delays [6]. The dynamics of the system (3) are locally Lipschitz.

With these considerations in mind, the derivation of the event-sampled quadrotor UAV controller may be presented. The derivation of the event-sampled controller will be presented as two sections: In the first section, the observer design will be considered and, in the following section, the controller design will be demonstrated.

3 OBSERVER DESIGN

In order to relax the need for state-vector measurability, an observer will be designed to estimate unknown values. Subsequently, the estimated values will be used in the controller. Since the stability of the controller relies on accurate sensor readings, the observer's quick convergence is imperative. The introduction of event-sampling only adds to the challenge of designing an observer that performs well enough for the control objectives to be accomplished. Additionally, the implementation of the event-triggering mechanism must also be taken into consideration; since the mechanism that will be designed in this paper relies on continuous sensor data, the observer's placement must allow for continuous estimation. For these reasons, the placement of the observer is taken to be at the sensor (see Fig. 3.1); practically, this means that, even with event-sampling, the observer will estimate the state-vector continuously, allowing for quicker convergence as well as for sufficient information for the implementation of the proposed event-execution law.
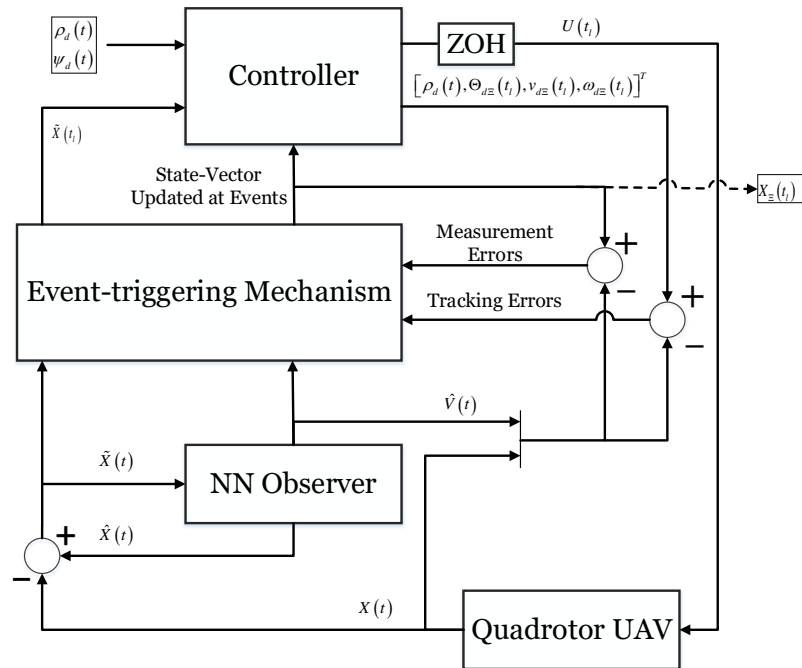

Figure 3.1   Event-triggered Output Feedback Structure

Although the NN observer estimates the state-vector continuously, the NN itself is only updated at event sampled instants. This decision was made in order to further reduce the computational effort. With a continuously updated state-vector, it would not be correct to directly assign measurement errors to the estimated states. However, since the NN is only being updated intermittently, there will be an approximation error due to the event-sampling. Using the fact that the inputs of the NN will only be updated at events, the ideal NN approximation can be manipulated in a manner that allows event-sampling measurement errors to be extracted from the approximation error that results from intermittent updates. The measurement errors that will be introduced in this section include Ξ_{SX}, $\hat{\Xi}_{SX}$, and $\check{\Xi}_{SV}$, corresponding to the quadrotor's measured position and orientation, estimated position and orientation, and measured and estimated velocity, respectively. It will be discussed why the uncertainess of the UAV's measured velocity requires the velocity measurement error to be written in terms of the derivative of the UAV's measured position and orientation. Once the measurement errors are extracted, it is not difficult to account for their effects when the event-execution law is designed.

Begin by defining the augmented vectors $X = \left[\rho^T, \Theta^T\right]^T$ and $V = \left[v^T, \omega^T\right]^T$. Using these augmented vectors, the dynamics (1), (2), and (3) can be rewritten with

$$\dot{X} = AV + \xi_1$$

$$\dot{V} = f_o(x_o) + \bar{G} + M^{-1}U + \bar{\tau}_d. \tag{5}$$

where ξ_1 represents bounded sensor measurement noise such that $\|\xi_1\| \leq \xi_{1M}$; $\bar{\tau}_d = \left[\tau_{d1}/m, \left[J^{-1}\tau_{d1}\right]^T\right]$ satisfies $\bar{\tau}_d \leq M_M \tau_M$ with $M_M = \left\|M^{-1}\right\|_F$; $\bar{G} = M^{-1}G(R)$; and $U_\Xi = [0, 0, u_{1\Xi}, u_{2\Xi}]^T$ is the event-sampled control input which will be addressed in later derivations. Note that there is an explicit measurement error present in U_Ξ, however, since this term is canceled out in the observer analysis, it is not considered. Furthermore, by observation of (3), $f_o(x_o) = M^{-1}\left[\bar{S}(\omega)V + [N_1(v), N_2(\omega)]^T\right]$ are unknown dynamics.

Next, introduce the change of variable, $Z = V$ and denote the observer estimates for X and V with hats, specifically $\hat{X}$ and $\hat{V}$, respectively. Finally, the observer estimation error is denoted with a tilde, $\tilde{X} = X - \hat{X}$. With these, the proposed observer takes the form [1]

$$\dot{\hat{X}} = A\hat{Z} + K_{o1}\tilde{X}$$

$$\dot{\hat{Z}} = \hat{f}_{o1\Xi} + \bar{G} + K_{o2}A^{-1}\tilde{X} + M^{-1}U_\Xi$$

$$\hat{V} = \hat{Z} + K_{o3}A^{-1}\tilde{X} \tag{6}$$

where K_{o1}, K_{o2}, and K_{o3} are positive design constants and A^{-1} is bounded by $\left\|A^{-1}\right\|_F \leq A_M^I$ where A_M^I is a positive constant. Additionally, $\hat{f}_{o1\Xi}$ is the event-sampled NN estimate of the unknown function, $f_{o1}(x_o) = f_o(x_o) + \left[A^T - K_{o3}\dot{A}^{-1}\right]\tilde{X}$; the second term of the unknown function, $\left[A^T - K_{o3}\dot{A}^{-1}\right]\tilde{X}$, will arise in the derivation for the observer estimation error dynamics. This work will make use of the *universal approximation property of NNs* [15]: For an unknown, smooth function, $f_N(x_N)$, its NN approximation will be denoted by $f_N(x_N) = W_N^T\sigma\left(V_N^T x_N\right) + \varepsilon_N$, where W_N are ideal NN weights which are bounded such that $\|W_N\|_F \leq W_M$; $\sigma(\bullet)$ is the activation function in the hidden layers which, in this work, is chosen to be the logarithmic sigmoid function and has the property $\|\sigma\| \leq \sqrt{N}$, with N being the number of hidden layer neurons in the NN; V_N consists of randomly selected constant weights; and ε_N is the NN reconstruction error which is bounded such that $\|\varepsilon_N\| \leq \varepsilon_M$. Since the ideal NN weights are not available, it becomes necessary to introduce NN weight estimates, $\hat{W}_N$, for which an acceptable tuning law will be derived. Specifically, the ideal, continuously updated approximation for the unknown function corresponding to the observer is given by $f_{o1}(x_o) = W_o^T\sigma\left(V_o^T x_o\right) + \varepsilon_o = W_o^T\sigma_o + \varepsilon_o$ where the target NN weights are bounded by $\|W_o\|_F \leq W_{Mo}$ and the approximation error is bounded by $\|\varepsilon_o\| \leq \varepsilon_{Mo}$. Moreover, using estimated weights, the approximation for the unknown

function in (6) is given by $\hat{f}_{o1\Xi} = \hat{W}_{o\Xi}\sigma_o\left(V_o^T\hat{x}_o\right) = \hat{W}_{o\Xi}\hat{\sigma}_o$ and its input is given with $\hat{x}_o = \left[1, \hat{X}^T, \hat{V}^T, \tilde{X}^T\right]^T$.

In order to account for the effects of intermittent NN updates, begin by adding and subtracting $W_o^T\sigma\left(x_{o\Xi}\right) = W_o^T\sigma_{o\Xi}$ to the ideal approximation

$$f_{o1}\left(x_o\right) = W_o^T\sigma_{o\Xi} - W_o^T\sigma_{o\Xi} + W_o^T\sigma_o + \varepsilon_o$$

$$= W_o^T\sigma_{o\Xi} + W_o^T\left[\sigma_o - \sigma_{o\Xi}\right] + \varepsilon_o. \tag{7}$$

The expression given by (7) can be interpretted as the ideal approximation given by an intermittently updated NN and $W_o^T\left[\sigma_o - \sigma_{o\Xi}\right]$ can be viewed as the approximation error that results from the intermittent updating. As the frequency of events increases, the values of the event-sampled variables approach those of their continuously sampled counterparts. As a result, with a very large number of events, the approximation error caused by event-sampling begins to vanish and the ideal NN approximation is eventually reverted back to its original form. With this, the engineering tradeoff is clear: Fewer events will yield more computational efficiency, however, the efficiency comes at the expense of accuracy. With regards to its effects on stability, the approximation error that results from intermittent NN updates will be addressed by designing an event-execution law that will ensure acceptable behavior in the closed-loop dynamics; the details for this will be shown in Theorem 3, Case 2.

Next, by adding and subtracting $\left[A^T - K_{o3}\dot{A}^{-1}\right]\tilde{X}$ and using the information in (5) and (6), the estimation error dynamics are found to be

$$\dot{\tilde{X}} = A\tilde{V} - \left[K_{o1} - K_{o3}\right]\tilde{X} + \xi_1$$

$$\dot{\tilde{Z}} = \left[f_o + \left[A^T - K_{o3}\dot{A}^{-1}\right]\tilde{X}\right] - \hat{f}_{o1\Xi} - K_{o2}A^{-1}\tilde{X} - \left[A^T - K_{o3}\dot{A}^{-1}\right]\tilde{X} - \varepsilon_{o\Xi} + \bar{\tau}_d. \tag{8}$$

Next, observe that, from (6), $\tilde{V} = V - \hat{V} = \tilde{Z} - K_{o3}A^{-1}\tilde{X}$. The derivative of this expression can be taken and, by adding and subtracting $W_o^T\sigma(\hat{x}_{o\Xi}) = W_o^T\hat{\sigma}_{o\Xi}$ as well as using (7) and (8), the estimation error dynamics corresponding to V are found to be

$$
\begin{aligned}
\dot{\tilde{V}} &= \left[f_o + \left[A^T - K_{o3}\dot{A}^{-1} \right]\tilde{X} \right] - W_o^T\sigma\left(V_o^T\hat{x}_{o\Xi} \right) + W_o^T\sigma\left(V_o^T\hat{x}_{o\Xi} \right) - \hat{f}_{o1\Xi} - K_{o2}A^{-1}\tilde{X} \\
&\quad - \left[A^T - K_{o3}\dot{A}^{-1} \right]\tilde{X} + \bar{\tau}_d - K_{o3}\dot{A}^{-1}\tilde{X} - K_{o3}A^{-1}\left[A\tilde{V} - [K_{o1} - K_{o3}]\tilde{X} + \xi_1 \right] \\
&= -K_{o3}\tilde{V} + \tilde{f}_{o\Xi} - A^{-1}[K_{o2} - K_{o3}[K_{o1} - K_{o3}]]\tilde{X} - A^T\tilde{X} + \varepsilon_{o\Xi} + \xi_2
\end{aligned}
\tag{9}
$$

where $\tilde{f}_{o\Xi} = \left[W_o^T - \hat{W}_{o\Xi}^T \right]\hat{\sigma}_{o\Xi}$, $\varepsilon_{o\Xi} = W_o^T[\sigma_o - \sigma_{o\Xi}] + W_o^T[\sigma_{o\Xi} - \hat{\sigma}_{o\Xi}] = W_o^T[\sigma_o - \hat{\sigma}_{o\Xi}]$ contains the approximation error due to event-sampling, and $\xi_2 = \varepsilon_o + \bar{\tau}_d - K_{o3}A^{-1}\xi_1$ is bounded such that $\|\xi_2\| \le \xi_{2M}$ where $\xi_{2M} = \varepsilon_{Mo} + M_M\tau_M + K_{o3}A_M^I\xi_{1M}$. These dynamics given by 8 and (9) are used in demonstrating the boundedness of the observer subsystem when the NN is updated intermittently.

Next, the following theorem is given in order to demonstrate that the proposed observer generates an ISS-like Lyapunov function with respect to bounded measurement errors. The results for Theorem 1 are needed in order to make conclusions on the inter-event periods being bounded away from zero.

Theorem 1. *(NN Observer Boundedness):* Consider the observer given by (6) with estimation error dynamics described by 8 and (9). Furthermore, let the NN weights be updated with

$$
\dot{\hat{W}}_{o\Xi} = F_o\hat{\sigma}_o\tilde{X}^T - \kappa_{o1}F_o\hat{W}_{o\Xi}
\tag{10}
$$

where $F_o = F_o^T > 0$ and $\kappa_{o1} > 0$ are constant design parameters, and let the initial weights be in a compact set. Moreover, let the activation function for the NN be Lipschitz. Finally, let the event-sampling measurement errors corresponding to X, $\hat{X}$, and $\dot{X}$ be assumed to be bounded such that $\Xi_{SX} \le \Xi_{X\max}$, $\hat{\Xi}_{SX} \le \hat{\Xi}_{X\max}$, and $\check{\Xi}_{SV} \le \check{\Xi}_{V\max}$, respectively. Then, there exist design constants, K_{o1}, K_{o2}, and K_{o3}, such that the observer estimation errors, $\tilde{X}$

and $\tilde{V}$, as well as the observer NN weight estimation errors, $\tilde{W}_{o\Xi}$, are locally universally ultimately bounded (UUB).

Proof. Consider the positive-definite Lyapunov candidate

$$V_{o\Xi} = \frac{1}{2}\tilde{X}^T\tilde{X} + \frac{1}{2}\tilde{V}^T\tilde{V} + \frac{1}{2}\text{tr}\left\{\tilde{W}_{o\Xi}^T F_o^{-1}\tilde{W}_{o\Xi}\right\} \tag{11}$$

whose derivative is given by $\dot{V}_{o\Xi} = \tilde{X}^T\dot{\tilde{X}} + \tilde{V}^T\dot{\tilde{V}} + \text{tr}\left\{\tilde{W}_{o\Xi}^T F_o^{-1}\dot{\tilde{W}}_{o\Xi}\right\}$. The estimation error dynamics given by (8) and (9), along with the NN weight update law given by (10), can be substituted to find

$$\dot{V}_{o\Xi} = -\tilde{X}^T\left[K_{o1} - K_{o3}\right]\tilde{X} + \tilde{X}^T\xi_1 - \tilde{V}^T K_{o3}\tilde{V} + \tilde{V}^T\xi_2 + \tilde{V}^T\varepsilon_{o\Xi}$$

$$- \text{tr}\left\{\tilde{W}_{o\Xi}^T\left[\hat{\sigma}_o\tilde{X}^T - \hat{\sigma}_{o\Xi}\tilde{V} - \kappa_{o1}\left[W_o - \tilde{W}_{o\Xi}\right]\right]\right\}. \tag{12}$$

Then, by invoking known bounding conditions, and by using properties of the matrix trace operation, it is discovered that

$$\dot{V}_{o\Xi} \leq -\left[\frac{[K_{o1} - K_{o3}]}{2} - \frac{N_o}{\kappa_{o1}}\right]\left\|\tilde{X}\right\|^2 - \left[\frac{K_{o3}}{2} - \frac{N_o}{\kappa_{o1}} - \frac{1}{2}\right]\left\|\tilde{V}\right\|^2 - \frac{\kappa_{o1}}{4}\left\|\tilde{W}_{o\Xi}\right\|_F^2$$

$$+ \kappa_{o1}W_{Mo}^2 + \frac{\xi_{1M}^2}{2[K_{o1} - K_{o3}]} + \frac{\xi_{2M}^2}{2K_{o3}} + \frac{1}{2}\varepsilon_{o\Xi}^2 \tag{13}$$

after completion of squares with respect to $\left\|\tilde{X}\right\|$, $\left\|\tilde{V}\right\|$, and $\left\|\tilde{W}_{o\Xi}\right\|_F$.

It is at this point that the measurement errors are extracted from the approximation error caused by intermittent NN updates. In order to do this, the Lipschitz condition on the NN activation function will need to be invoked. Additionally, observe that the unknown function that is approximated by the NN is defined in terms of V and $\tilde{X}$. With these in

consideration, it is discovered

$$
\begin{aligned}
\varepsilon_{o\Xi}^2 &\leq W_{Mo}^2 \left[\sigma_o - \hat{\sigma}_{o\Xi}\right]^2 \\
&\leq \frac{1}{2} W_{Mo}^4 + \frac{1}{2} \left[\sigma_o - \hat{\sigma}_{o\Xi}\right]^4 \\
&\leq \frac{1}{2} W_{Mo}^4 + \frac{1}{2} L_\sigma \left\|\left[V - \hat{V}_\Xi\right] + \left[\tilde{X} - \tilde{X}_\Xi\right]\right\|^4 \\
&= \frac{1}{2} W_{Mo}^4 + \frac{1}{2} L_\sigma \left\|\left[V - \hat{V}_\Xi\right] + \left[\left[X - \hat{X}\right] - \left[X_\Xi - \hat{X}_\Xi\right]\right]\right\|^4 \\
&= \frac{1}{2} W_{Mo}^4 + \frac{1}{2} L_\sigma \left\|[X - X_\Xi] - \left[\hat{X} - \hat{X}_\Xi\right] + \left[\dot{X} - \hat{V}_\Xi\right]\right\|^4 \\
&= \frac{1}{2} W_{Mo}^4 + \frac{1}{2} L_\sigma \left\|\Xi_{SX} - \hat{\Xi}_{SX} + \check{\Xi}_{SV}\right\|^4 \\
&\leq \frac{1}{2} W_{Mo}^4 + \frac{1}{2} L_\sigma \left\|\Xi_{SX}\right\|^4 + \frac{1}{2} L_\sigma \left\|\hat{\Xi}_{SX}\right\|^4 + \frac{1}{2} L_\sigma \left\|\check{\Xi}_{SV}\right\|^4
\end{aligned}
\tag{14}
$$

where L_σ is the Lipschitz constant and $\check{\Xi}_{SV}$, Ξ_{SX}, and $\hat{\Xi}_{SX}$ are the event-sampling measurement errors corresponding to V and $\hat{V}$, X, and $\hat{X}$, respectively. Note that the measurement error corresponding to V is rewritten in terms of $\dot{X}$; this is done because, in practice, the measured velocity is not available and, therefore, it would not be possible to implement an execution law directly for V. This problem can be circumvented by placing a differentiator at the sensor and considering a measurement error in terms of $\dot{X}$. Finally, (13) and (14) are combined to give

$$
\dot{V}_{o\Xi} \leq -K_{\tilde{X}} \left\|\tilde{X}\right\|^2 - K_{\tilde{V}} \left\|\tilde{V}\right\|^2 - K_{Wo} \left\|\tilde{W}_{o\Xi}\right\|_F^2 + B_o
\tag{15}
$$

where $B_o = \eta_o + \frac{1}{4} L_\sigma \Xi_{X\max}^4 + \frac{1}{4} L_\sigma \hat{\Xi}_{X\max}^4 + \frac{1}{4} L_\sigma \check{\Xi}_{V\max}$ with $\eta_o = \kappa_{o1} W_{Mo}^2 + \frac{1}{4} W_{Mo}^4 + \xi_{1M}^2 / \left[2\left[K_{o1} - K_{o3}\right]\right] + \xi_{2M}^2 / \left[2K_{o3}\right]$; $K_{\tilde{X}} = \left[K_{o1} - K_{o3}\right]/2 - N_o/\kappa_{o1}$; $K_{\tilde{V}} = \left[K_{o1} - 1\right]/2 - N_o/\kappa_{o1}$; and $K_{Wo} = \kappa_{o1}/4$. Finally, (15) is less than zero provided that $K_{o1} > K_{o3} + \left[2N_o\right]/\kappa_{o1}$ and $K_{o3} > \left[2N_o\right]/\kappa_{o1} + 1$ and the following inequalities hold:

$$
\left\|\tilde{X}\right\| > \sqrt{\frac{B_o}{K_{\tilde{X}}}} \qquad \text{or} \qquad \left\|\tilde{V}\right\| > \sqrt{\frac{B_o}{K_{\tilde{V}}}} \qquad \text{or} \qquad \left\|\tilde{W}_{o\Xi}\right\|_F > \sqrt{\frac{B_o}{K_{S\max}^2}}.
\tag{16}
$$

Therefore, it can be concluded [15] that all signals in the observer are locally UUB.

Remark 1. The results from Theorem 1 can be easily used to demonstrate how the observer generates an ISS-like Lyapunov function with respect to bounded measurement errors. This result, along with the assumption that the dynamics (3) are Lipschitz, fulfills the necessary requirements needed to show the existence of nonzero inter-event periods [6]. However, rather than showing how the observer generates an ISS-like Lyapunov function by itself, (15) will be used later when the closed-loop dynamics are considered and it will be demonstrated how the whole system exhibits ISS-like behavior.

In Theorem 1, the measurement errors were assumed to be bounded. However, in order to implement the event-sampled controller, it must be demonstrated that the measurement errors are, in fact, bounded for all time. This can be done by, first, considering the system dynamics when event-sampling measurement errors are zero and, second, considering the system dynamics with nonzero measurement errors. With nonzero measurement errors, an event-execution law can be designed in order to ensure that the system dynamics remain stable. In this paper, a single event-execution law will be designed when the closed-loop dynamics are considered in Theorem 3. However, before proceeding, the following lemma will be given in order to show that the proposed observer with an intermittently updated NN is eligible for implementation in the event-sampled controller.

Lemma 1. Consider the observer given by (6) with estimation error dynamics described by 8 and (9). Furthermore, let the NN weights be updated with (10) with initial weights in a compact set. Then, there exist design constants, K_{o1}, K_{o2}, and K_{o3}, such that the observer estimation errors, $\tilde{X}$ and $\tilde{V}$, as well as the observer NN weight estimation errors, $\tilde{W}_{o\Xi}$, are locally UUB for all time.

Proof. Case 1. In this case, the NN weights are updated using (10) and, furthermore, all approximation and measurement errors that are caused by event-sampling are taken to be zero. As a result, $\varepsilon_{o\Xi}$ is absent from the observer estimation error dynamics for $\dot{\tilde{V}}$. Because of this, the coefficient defined in Theorem 1 corresponding to $\left\|\tilde{V}\right\|^2$ needs

to be changed to $K_{\tilde{V}} = [K_{o1}]/2 - N_o/\kappa_{o1}$ and the bounded term needs to be revised to

$B_o = \kappa_{o1} W_{Mo}^2 + \xi_{1M}^2/[2[K_{o1} - K_{o3}]] + \xi_{2M}^2/[2K_{o3}]$. Additionally, the event-sampled term

that was previously combined with the approximation error due to intermittent updates no

longer needs to be considered in the presence of measurement errors and, therefore, the

expression for ξ_2 becomes $\xi_2 = \varepsilon_o + \bar{\tau}_d - K_{o3}A^{-1}\xi_1 + W_o^T[\sigma_o - \hat{\sigma}_o]$ with $\|\xi_2\| \leq \xi_{2M}$

where $\xi_{2M} = \varepsilon_{Mo} + M_M\tau_M + K_{o3}A_M^I\xi_{1M} + 2W_{Mo}\sqrt{N_o}$. With these changes in mind, and by

selecting gains satisfying $K_{o1} > K_{o3} + [2N_o]/\kappa_{o1}$ and $K_{o3} > [2N_o]/\kappa_{o1}$, it can be concluded

[15] that (15) is less than zero and that all signals in the observer are locally UUB.

Case 2. In this case, the NN weights are held and, therefore, the effects of the

third term in (11) vanish when the derivative is taken. However, since the approximation

error caused by event-sampling is injected through the estimation error dynamics, $\dot{\tilde{V}}$, it

becomes necessary to account for the nonzero measurement errors. Using an approach

similar to what was done for *Case 1*, the coefficients are updated with $B_o = W_{Mo}^4/4 +$

$\xi_{1M}^2/[2[K_{o1} - K_{o3}]] + \xi_{2M}^2/[2K_{o3}]$; $K_{\tilde{X}} = [K_{o1} - K_{o3}]/2$; $K_{\tilde{V}} = [K_{o1} - 2]/2$; and $K_{Wo} = -N_o/2$. With these changes in mind, the expression for $\dot{V}_{o\Xi}$ is rewritten with

$$\dot{V}_{o\Xi} \leq -K_{\tilde{X}}\left\|\tilde{X}\right\|^2 - K_{\tilde{V}}\left\|\tilde{V}\right\|^2 - K_{Wo}\left\|\tilde{W}_{o\Xi}\right\|_F^2 + B_o + \frac{1}{4}L_\sigma\|\Xi_{SX}\|^4 + \frac{1}{4}L_\sigma\left\|\hat{\Xi}_{SX}\right\|^4 + \frac{1}{4}L_\sigma\left\|\check{\Xi}_{SV}\right\|^4.$$

(17)

In this case, the measurement errors cannot be assumed to be bounded and it becomes

necessary to address their effects. This could be accomplished by designing an event-

execution law that takes the form

$$\left\|\Xi_\chi\right\|^4 \leq \gamma_\chi\mu_\chi\left\|e_\chi\right\|^2$$

(18)

where, in general, $0 < \gamma_\chi, \mu_\chi < 1$ are design constants and $e_\chi = \chi_d - \chi$ is the tracking error

corresponding to the measurement error. An execution-law bearing strong resemblance to

(18) is what will be designed in this paper, however, the benefits of this design cannot be

easily seen by considering the observer dynamics alone and (18) is given here only for illustration purposes. When the tracking errors are addressed in the closed-loop dynamics, it will be demonstrated how an execution law in the form of (18) can be used to eliminate the measurement errors from the observer subsystem. Hence, the effects of event-sampling will be addressed for inter-event periods as well.

The results for *Case 1* and *Case 2* can be combined in order to make conclusions which apply for all time. However, since the dynamics in *Case 2* can only be fully assessed in the closed-loop, this final combination will not be done here, but, instead, will be shown for the entire UAV system. From the results that are presented, however, it can be concluded that, with an appropriately designed event-execution law, the proposed observer with an intermittently updated NN qualifies as a candidate for an event-sampled output feedback controller.

Remark 2. In this paper, a single event-execution law will be designed for the whole system. In other words, the measurement errors that originate in the observer are combined with the measurement errors in the controller and a single condition is used as the basis by which events occur. Moreover, when an event does occur, both the observer NN as well as the controller are updated with the most recent position and orientation sensor measurements and velocity observer estimates.

Next, the event-sampled controller design will be presented. First, the virtual controller will be briefly addressed, then the kinematic and dynamic controllers will be designed under the influence of event-sampling, and, lastly, the closed-loop dynamics will be considered.

4 EVENT-SAMPLED CONTROL OF QUADROTOR UAV

A natural progression for the derivation of the controller would be to begin with the design of the kinematic controller, to proceed with the virtual controller, and to conclude with an analysis for the dynamic controller. This progression is followed in [1]. However, in order to incorporate the effects of event-sampling, it is, perhaps, easier to first address the stability of the virtual controller and then consider the kinematic and dynamic controllers. The reason for this is that the assessment of the virtual controller' s stability does not involve any explicit presence of event-sampling measurement errors and its analysis can be quickly summarized. An important consideration that needs to be made in the development of event-sampled controllers is in determining how and where the controller injects measurement errors into the system. In the development for the virtual controller, only the stability of the virtual control estimates is considered and the injection of any term into the system is altogether absent. Instead, it is only through the analysis for the kinematic and dynamic controllers where there is an injection of errors caused by event-sampling. For this reason, the stability of the virtual control estimates will be considered first and then the kinematic and dynamic controllers will be considered under the influence of event-sampling.

4.1 VIRTUAL CONTROLLER DESIGN

In the developments made in this subsection, the stability of the desired virtual control estimates, $\hat{\Theta}_d$ and $\hat{\omega}_d$, as well as the boundedness of the virtual control NN weight estimates, $\hat{W}_\Omega$, will be considered. Since the desired virtual controls are written in terms of the UAV's measured position and orientation, there is an explicit presence of event-sampling measurement errors. However, the derivations made for the virtual controller here will only assess the stability of the estimates and not how they are injected into the system.

Begin by defining the proposed virtual controller [1]

$$\dot{\hat{\Theta}}_{d\Xi} = T\hat{\Omega}_{d\Xi} + K_{\Omega 1}\tilde{\Theta}_{d\Xi}$$

$$\dot{\hat{\Omega}}_{d\Xi} = \hat{f}_{\Omega 1\Xi} + K_{\Omega 2}T^{-1}\tilde{\Theta}_{d\Xi}$$

$$\hat{\omega}_{d\Xi} = \hat{\Omega}_{d\Xi} + T^{-1}K_{\Theta}e_{\Theta\Xi} + K_{\Omega 3}T^{-1}\tilde{\Theta}_{d\Xi} \tag{19}$$

where $\hat{f}_{\Omega 1\Xi}$ is the event-sampled NN estimation of the unknown function, $f_{\Omega 1\Xi}(x_\Omega) = f_{\Omega\Xi} + T^T\tilde{\Theta}_{d\Xi} - K_{\Omega 3}\dot{T}^{-1}\tilde{\Theta}_{d\Xi}$, where $f_{\Omega\Xi} = \dot{T}^{-1}\dot{\Theta}_{d\Xi} + T^{-1}\ddot{\Theta}_{d\Xi}$; specifically, its estimation is given by $\hat{f}_{\Omega 1\Xi} = \hat{W}_{\Omega\Xi}^T\sigma\left(V_\Omega^T\hat{x}_{\Omega\Xi}\right) = \hat{W}_{\Omega\Xi}^T\hat{\sigma}_{\Omega\Xi}$, where its input is $\hat{x}_{\Omega\Xi} = \left[1,\ \rho_d,\ \dot{\rho}_d^T,\ \ddot{\rho}_d^T,\ \dddot{\rho}_d^T,\ \Theta_{d\Xi}^T,\ \hat{\Omega}_{d\Xi},\ \hat{V}^T,\ \tilde{\Theta}_{d\Xi}\right]^T$. Here, the subscript Ξ is used to reinforce the idea that the virtual control NN weight estimates are updated only at event-sampling instants. Additionally, $e_{\Theta\Xi}$ is the UAV's event-sampled orientation tracking error which will be addressed later, and $K_{\Omega 1}$, $K_{\Omega 2}$, $K_{\Omega 3}$, and K_Θ are positive design constants.

Next, choose the NN weight update law

$$\dot{\hat{W}}_{\Omega\Xi} = F_\Omega\hat{\sigma}_{\Omega\Xi}\tilde{\Theta}_{d\Xi}^T - \kappa_{\Omega 1}F_\Omega\hat{W}_{\Omega\Xi} \tag{20}$$

where $F_\Omega = F_\Omega^T > 0$ and $\kappa_{\Omega 1} > 0$ are constant design parameters. Then, using (19) and (20), the virtual control estimation error dynamics can be determined and the first derivative of the Lyapunov candidate describing the virtual control system, $V_{\Omega\Xi} = \frac{1}{2}\tilde{\Theta}_{d\Xi}^T\tilde{\Theta}_{d\Xi} + \frac{1}{2}\tilde{\omega}_{d\Xi}^T\tilde{\omega}_{d\Xi} + \frac{1}{2}\text{tr}\left\{\tilde{W}_{\Omega\Xi}^TF_\Omega^{-1}\tilde{W}_{\Omega\Xi}\right\}$, can be found to satisfy [1]

$$\dot{V}_{\Omega\Xi} \leq -\left[K_{\Omega 1} - K_{\Omega 3} - \frac{N_\Omega}{\kappa_{\Omega 1}}\right]\left\|\tilde{\Theta}_{d\Xi}\right\|^2 - \left[\frac{K_{\Omega 3}}{2} - \frac{N_\Omega}{\kappa_{\Omega 1}}\right]\|\tilde{\omega}_{d\Xi}\|^2 - \frac{\kappa_{\Omega 1}}{4}\left\|\tilde{W}_{\Omega\Xi}\right\|_F^2 + \eta_\Omega \tag{21}$$

where $\eta_\Omega = \kappa_{\Omega 1}W_{M\Omega}^2 + \xi_{\Omega M}^2/[2K_{\Omega 3}]$ and N_Ω is the number of hidden layer neurons in the virtual control NN. By observation of (21), it can be seen that, with appropriate selection of design parameters, all signals in the virtual controller remain bounded [1]. Next, the

kinematic control and dynamic control will be considered under the influence of event-sampling.

4.2   INJECTION OF EVENT-SAMPLED VIRTUAL CONTROL

The tracking errors that correspond to the desired virtual control inputs are with respect to position and orientation. Begin by defining the position tracking error

$$e_\rho = \rho_d - \rho. \tag{22}$$

The dynamics of (22) are found to be

$$\dot{e}_\rho = \dot{\rho}_d - Rv. \tag{23}$$

In order to stabilize (23), the desired velocity is selected to be

$$v_d = R^T \left[\dot{\rho}_d + K_\rho e_\rho \right] \tag{24}$$

where $K_\rho = \text{diag} \left\{ k_{\rho x}, k_{\rho y}, k_{\rho z} \right\}$ is a design matrix with all positive constants.

Since the desired velocity is a term that will be injected into the system by the event-sampled controller, it becomes necessary to consider (24) in the presence of measurement errors. Observe that the measurement error that is injected into the system can be introduced into the analysis by noting that, from (4), the event-sampled position measurement is given by $\rho_\Xi = \rho + \Xi_\rho$, which allows (22) to be rewritten as

$$e_{\rho\Xi} = \rho_d - \left[\rho + \Xi_\rho \right] = e_\rho - \Xi_\rho \tag{25}$$

where $\Xi_\rho = \left[\Xi_x, \Xi_y, \Xi_z\right]^T$ is the vector of measurement errors corresponding to the quadrotor's measured position. Using (25) in (24) reveals

$$
\begin{aligned}
v_{d\Xi} &= R^T \left[\dot{\rho}_d + K_\rho \left[e_\rho - \Xi_\rho\right]\right] \\
&= R^T \left[\dot{\rho}_d + K_\rho e_\rho\right] - R^T K_\rho \Xi_\rho.
\end{aligned}
\tag{26}
$$

Next, define $e_v = v_{d\Xi} - v$ and note that, from this, $v = v_{d\Xi} - e_v$. Then, using $v_{d\Xi}$ as a virtual control input in the tracking error dynamics and substituting (26) into (23) gives

$$
\dot{e}_{\rho\Xi} = -K_\rho e_\rho + Re_v + K_\rho \Xi_\rho.
\tag{27}
$$

Next, the desired virtual control input corresponding to the quadrotor's orientation is considered. Begin by defining the orientation tracking error

$$
e_\Theta = \Theta_d - \Theta
\tag{28}
$$

where $\Theta_d = \left[\phi_d, \theta_d, \psi_d\right]^T$ is the desired orientation. Recall that ψ_d is an external input to be selected by the designer. Furthermore, it is shown in [1] how ϕ_d and θ_d can be calculated in terms of $\dot{\rho}_d$, $\ddot{\rho}_d$, ψ_d, K_ρ, and the unknown function $f_{c1}(x_{c1})$. The NN approximation for f_{c1} is given by

$$
\hat{f}_{c1} = \hat{W}_{c1}^T \sigma \left(V_{c1}^T \hat{x}_{c1}\right) = \hat{W}_{c1}^T \hat{\sigma}_{c1} = \left[\hat{f}_{c11}, \hat{f}_{c12}, \hat{f}_{c13}\right]^T
$$

where the input is $\hat{x}_{c1} = \left[1, \dot{\rho}_d^T, \ddot{\rho}_d^T, \hat{V}, \Theta^T, \tilde{X}^T\right]^T$. These estimates will be used in the derivation for the actual dynamic control.

Moving on, the dynamics of (28) are found to be

$$
\dot{e}_\Theta = \dot{\Theta}_d - T\omega.
\tag{29}
$$

In order to stabilize (29), the desired angular velocity is selected to be

$$\omega_d = T^{-1} \left[\dot{\Theta}_d + K_\Theta e_\Theta \right] \tag{30}$$

where $K_\Theta = \text{diag}\,\{k_{\Theta 1}, k_{\Theta 2}, k_{\Theta 3}\}$ is a design matrix with all positive constants.

Since the desired angular velocity is a term that will be injected into the system by the event-sampled controller, it becomes necessary to consider (30) in the presence of measurement errors. This is accomplished by observing that the event-sampled tracking error can be expressed as

$$e_{\Theta\Xi} = \Theta_d - [\Theta + \Xi_\Theta] = e_\Theta - \Xi_\Theta \tag{31}$$

where $\Xi_\Theta = \left[\Xi_\phi, \Xi_\theta, \Xi_\psi \right]^T$ is the vector of measurement errors corresponding to the quadrotor's measured orientation. Using (31) in (30) reveals

$$
\begin{aligned}
\omega_{d\Xi} &= T^{-1} \left[\dot{\Theta}_d + K_\Theta \left[e_\Theta - \Xi_\Theta \right] \right] \\
&= T^{-1} \left[\dot{\Theta}_d + K_\Theta e_\Theta - K_\Theta \Xi_\Theta \right]
\end{aligned}
\tag{32}
$$

Next, define $e_\omega = \omega_{d\Xi} - \omega$ and note that, from this, $\omega = \omega_{d\Xi} - e_\omega$. Then, using $\omega_{d\Xi}$ as a virtual control input in the tracking error dynamics and substituting (32) into (29) gives

$$\dot{e}_{\Theta\Xi} = -K_\Theta e_\Theta + T e_\omega + K_\Theta \Xi_\Theta. \tag{33}$$

It is the tracking error dynamics given by (27) and (33) that will be used when the closed-loop dynamics are considered.

Remark 3. In contrast to the results in [1], the tracking error dynamics, (27) and (33), contain additional terms, $K_\rho \Xi_\rho$ and $K_\Theta \Xi_\Theta$, respectively. These terms are the artifacts that result from event-sampling.

4.3 EVENT-SAMPLED OUTPUT FEEDBACK DYNAMIC CONTROL

The actual control input consists of two parts: u_1 is a scalar corresponding to the total thrust and $u_2 = [u_{21}, u_{22}, u_{23}]^T$ gives the rotational torques corresponding to roll, pitch, and yaw directions, respectively. These two parts will be considered separately.

TOTAL THRUST. The time-sampled total thrust control input is given by [1]

$$
\begin{aligned}
u_1 = {} & mk_{v3}\hat{e}_{vz} \\
& + m\left[c_{\phi d}s_{\theta d}c_{\psi d} + s_{\phi d}s_{\psi d}\right]\left[\ddot{x}_d + k_{\rho x}\dot{x}_d - \hat{v}_{R1} + \hat{f}_{c11}\right] \\
& + m\left[c_{\phi d}s_{\theta d}s_{\psi d} - s_{\phi d}c_{\psi d}\right]\left[\ddot{y}_d + k_{\rho y}\dot{y}_d - \hat{v}_{R2} + \hat{f}_{c12}\right] \\
& + mc_{\phi d}c_{\theta d}\left[\ddot{z}_d + k_{\rho z}\dot{z}_d - \hat{v}_{R3} + \hat{f}_{c13} - g\right]
\end{aligned}
\tag{34}
$$

where the gain, k_{v3}, is an element in the design matrix, $K_v = \text{diag}\{k_{v1}, k_{v2}, k_{v3}\}$, with all positive elements; $\hat{e}_v = \left[\hat{e}_{vx}, \hat{e}_{vy}, \hat{e}_{vz}\right]^T = v_d - \hat{v}$ with $\hat{v}$ being the translational velocity observer estimate; $\hat{v}_R = [\hat{v}_{R1}, \hat{v}_{R2}, \hat{v}_{R3}]^T = K_\rho R\hat{v}$; and $\hat{f}_{c1} = \left[\hat{f}_{c11}, \hat{f}_{c12}, \hat{f}_{c13}\right]$ is the NN estimate introduced in the previous subsection. Since the estimates from the observer are being stored in the controller and only being updated intermittently, it becomes necessary here to consider explicit measurement errors corresponding to the estimated state-vector. As a result, the terms $\hat{e}_v$ and $\hat{v}_R$ both have an explicit presence of measurement errors.

In order to incorporate the measurement errors in the analysis, it becomes necessary to expand certain computations so that the terms $\hat{e}_{vz}$, $\hat{v}_{R1}$, $\hat{v}_{R2}$, and $\hat{v}_{R3}$ can be extracted. First, in order to be able to consider $\hat{e}_{vz} = v_{dz} - \hat{v}_z$, it is necessary to consider the desired velocity (26) under the influence of event-sampling. By expanding the matrix multiplications, the expression for $v_{dz\Xi}$ is obtained as

$$
v_{dz\Xi} = v_{dz} + \bar{R}_{3R}K_\rho\Xi_\rho
\tag{35}
$$

where $\bar{R}_{3R}$ is the third row of R^T. Next, a similar procedure is used to find $\hat{v}_{R1}$, $\hat{v}_{R2}$, and $\hat{v}_{R3}$ under the influence of event-sampling. Using $\hat{v}_{x\Xi} = \hat{v}_x + \hat{\Xi}_{vx}$, $\hat{v}_{y\Xi} = \hat{v}_y + \hat{\Xi}_{vy}$, and $\hat{v}_{z\Xi} = \hat{v}_z + \hat{\Xi}_{vz}$, it is discovered that

$$\hat{v}_{R1\Xi} = \hat{v}_{R1} + k_{\rho x} R_{1R} \hat{\Xi}_v \qquad \hat{v}_{R2\Xi} = \hat{v}_{R2} + k_{\rho y} R_{2R} \hat{\Xi}_v \qquad \hat{v}_{R3\Xi} = \hat{v}_{R3} + k_{\rho z} R_{3R} \hat{\Xi}_v \qquad (36)$$

where R_{1R}, R_{2R}, and R_{3R} are the first, second, and third rows of R, respectively, and $\hat{\Xi}_v = \left[\hat{\Xi}_{vx}, \hat{\Xi}_{vy}, \hat{\Xi}_{vz}\right]^T$ is the vector of measurement errors corresponding to the translational velocity estimates. Finally, using (35) and (36) in (34) reveals

$$u_{1\Xi} = u_1^{f\Xi} + m k_{v3} \left[R_{3R}^T K_\rho\right] \Xi_\rho - m \left[k_{\rho x} R_{1R} + k_{\rho y} R_{2R} + k_{\rho z} R_{3R} + \begin{bmatrix} 0 & 0 & k_{v3} \end{bmatrix}\right] \hat{\Xi}_v. \tag{37}$$

where $u_1^{f\Xi}$ is identical to u_1 34, but assumes the event-sampled NN estimates, $\hat{f}_{c1\Xi}$; the implicitly affected NN estimation has no effect on further analyses. The control input, $u_{1\Xi}$, is designed in order to stabilize the translational velocity tracking error dynamics, which are given by

$$\dot{e}_{v\Xi} = -S(\omega) e_v - \frac{1}{m} G(R_d) - \bar{\tau}_{d1} + R_d^T \left[\ddot{\rho}_d + K_\rho \dot{\rho}_d - K_\rho R \hat{v} + f_{c1}(x_{c1})\right] - \frac{1}{m} u_{1\Xi} E_z. \tag{38}$$

Since the event-sampled control input is the sum of the time-sampled control input and the measurement error terms, the results of substituting the expression for $u_{1\Xi}$ into the tracking error dynamics (38) can be used to easily find that [1]

$$\dot{e}_{v\Xi} = -[S(\omega) + K_v] e_v - K_v \tilde{v} + R_d^T \tilde{W}_{c1\Xi} \hat{\sigma}_{c1\Xi}^T + \xi_{c1}$$
$$+ \left[k_{v3} \left[R_{3R}^T K_\rho\right] \Xi_\rho - \left[k_{\rho x} R_{1R} + k_{\rho y} R_{2R} + k_{\rho z} R_{3R} + \begin{bmatrix} 0 & 0 & k_{v3} \end{bmatrix}\right] \hat{\Xi}_v\right] E_z \tag{39}$$

where $\xi_{c1} = R_d^T W_{c1\Xi}^T \tilde{\sigma}_{c1\Xi}^T + R_d^T \varepsilon_{c1} - \bar{\tau}_{d1}$, $\tilde{W}_{c1\Xi} = W_{c1} - \hat{W}_{c1\Xi}$, and $\tilde{\sigma}_{c1\Xi} = \sigma_{c1\Xi} - \hat{\sigma}_{c1\Xi}$. In contrast to [1], the dynamics (39) have the additional measurement error terms that result from event-sampling.

Later, the tracking error dynamics given by (39) will be combined in an augmented vector along with the angular velocity tracking error dynamics, where they will both considered together. Before doing that, however, the event-sampled control inputs corresponding to the rotational torques and the angular velocity tracking errors must be considered.

ROTATIONAL TORQUES. First, consider the angular velocity tracking error dynamics given by

$$J\dot{e}_\omega = f_{c2}(x_{c2}) - u_2 - \tau_{d2} - T^T e_\Theta \tag{40}$$

where $f_{c2}(x_{c2})$ is an unknown function whose NN approximation is given by $\hat{f}_{c2} = \hat{W}_{c2}^T \sigma_{c2}(V_{c2}^T \hat{x}_{c2}) = \hat{W}_{c2}^T \hat{\sigma}_{c2}$ with an input $\hat{x}_{c2} = \left[1, \hat{\omega}^T, \dot{\hat{\Omega}}_d^T, \tilde{\Theta}_d^T, e_\Theta^T \right]$. Next, the rotational torque control input is given by [1]

$$u_2 = \hat{f}_{c2} + K_\omega \hat{e}_\omega$$

where $K_\omega = \text{diag}\{k_{\omega 1}, k_{\omega 2}, k_{\omega 3}\}$ is a design matrix with all positive constants, and $\hat{e}_\omega = \hat{\omega}_d - \hat{\omega}$. The event-sampled control input $u_{2\Xi}$ injects explicit measurement errors into the system through the $\hat{e}_\omega$ term. Observing that

$$\hat{\omega}_d = \hat{\Omega}_d + T^{-1} K_\Theta e_\Theta + K_{\Omega 3} T^{-1} \tilde{\Theta}_d$$

it can be seen that, here, a measurement error corresponding to the measured orientation will be injected into the system. Using (31) it is found that

$$\hat{\omega}_{d\Xi} = \hat{\omega}_d - T^{-1} K_\Theta \Xi_\Theta.$$

Now, noting that $\hat{\omega}_\Xi = \hat{\omega} + \hat{\Xi}_\omega$, it is revealed

$$u_{2\Xi} = \hat{f}_{c2\Xi} + K_\omega \hat{e}_\omega - K_\omega \left[T^{-1} K_\Theta \Xi_\Theta - \hat{\Xi}_\omega \right] \tag{41}$$

where $\hat{f}_{c2\Xi}$ is the event-sampled NN estimate given earlier and $\hat{\Xi}_\omega = \left[\hat{\Xi}_{\omega x}, \hat{\Xi}_{\omega y}, \hat{\Xi}_{\omega z} \right]^T$ is the vector of measurement errors corresponding to the rotational velocity estimates. Next, making use of the fact that $\hat{e}_\omega = e_\omega - \tilde{\omega}_d + \tilde{\omega}$, as well as adding and subtracting $W_{c2}^T \hat{\sigma}_{c\Xi}$, the event sampled tracking error dynamics (40) can be rewritten as

$$J \dot{e}_{\omega\Xi} = \tilde{W}_{c2\Xi}^T \hat{\sigma}_{c2\Xi} - K_\omega e_\omega + K_\omega \tilde{\omega}_d - K_\omega \tilde{\omega} - T^T e_\Theta + \xi_{c2} - K_\omega \left[T^{-1} K_\Theta \Xi_\Theta - \hat{\Xi}_\omega \right] \tag{42}$$

where $\tilde{W}_{c2\Xi}^T = W_{c2}^T - \hat{W}_{c2\Xi}^T$, $\xi_{c2} = \varepsilon_{c2} + W_{c2}^T \tilde{\sigma}_{c\Xi} - \tau_{d2}$, and $\tilde{\sigma}_{c2\Xi} = \sigma_{c2} - \hat{\sigma}_{c2\Xi}$.

Next, define the augmented vector, $e_{S\Xi} = \left[e_{v\Xi}^T, e_{\omega\Xi}^T \right]^T$, with which the translation and angular velocities can be considered together. With this, it becomes necessary to also define $\bar{J} = [I_{3\times3}, 0_{3\times3}; 0_{3\times3}, J]$, a constant matrix; $K_S = [K_v, 0_{3\times3}; 0_{3\times3}, K_\omega] > 0$, a positive definite design matrix; $S_S(\omega) = [S(\omega), 0_{3\times3}; 0_{3\times3}, 0_{3\times3}]$, where $e_{S\Xi}^T S_S(\omega) e_{S\Xi} = 0$; $\bar{T} = [0_{3\times6}; 0_{3\times3}, T]$; $\bar{e}_\Theta = \left[0_{1\times3}, e_\Theta^T \right]^T$; $\tilde{\omega}_d = \left[0_{1\times3}, \tilde{\omega}_d^T \right]^T$; $\xi_c = \left[\xi_{c1}^T, \xi_{c2}^T \right]^T$; and $A_d = \text{diag}\{R_d, I_{3\times3}\}$, with $R_d = R(\Theta_d)$. Additionally, $\tilde{f}_{c\Xi} = \tilde{W}_{c\Xi}^T \hat{\sigma}_{c\Xi}$ with $\tilde{W}_{c\Xi} = \text{diag}\left\{ \tilde{W}_{c1\Xi}, \tilde{W}_{c2\Xi} \right\}$ and $\hat{\sigma}_{c\Xi} = \left[\hat{\sigma}_{c1\Xi}^T, \hat{\sigma}_{c2\Xi}^T \right]^T$ and $\tilde{V}$ is the velocity tracking error vector defined in the observer development. Finally, in order to make provisions for the effects of event-sampling, define the augmented measurement error vector, $\hat{\Xi}_{SV} = \left[\hat{\Xi}_v^T, \hat{\Xi}_\omega^T \right]^T$. The augmented coefficient matrix, $K_{V\Xi}$, corresponding to Ξ_{SV} can be found in terms of the gain matrices K_ρ and K_ω as well as the elements of R and the gain k_{v3}. With these, the tracking error dynamics described by (39) and (42) can be rewritten with the single expression

$$\bar{J} \dot{e}_{S\Xi} = A_d^T \tilde{f}_{c\Xi} - [K_S + S_S(\omega)] e_S - K_S \tilde{V} - \bar{T}^T \bar{e}_\Theta + K_S \tilde{\omega}_d + \xi_c + K_{V\Xi} \hat{\Xi}_{SV} + K_{X\Xi}^V \Xi_{SX} \tag{43}$$

where $\Xi_{SX} = \begin{bmatrix} \Xi_\rho^T, & \Xi_\Theta^T \end{bmatrix}^T$ is the augmented measurement error vector corresponding to the position and orientation measurements and the coefficient matrix $K_{X\Xi}^V$ accounts for the Ξ_ρ and Ξ_Θ from (39) and (42); the augmented cofficient matrix $K_{X\Xi}^V$ can be found in terms of gain matrices K_ρ, K_Θ, and K_ω as well as the elements of T^{-1}.

With these results, the final two theorems of this paper may be presented. In Theorem 2, for the purposes of analysis, the time-sampled controller will be considered and the explicit measurement errors that would be injected into the system by event-sampling will be viewed as bounded inputs. In this way, the ISS-like behavior of the system will be demonstrated. In Theorem 3, the assumption on the boundedness of the measurement errors will be relaxed and it will be shown that the measurement errors are, in fact, bounded with the implementation of an appropriately selected event-execution law.

4.4 EVENT-SAMPLED QUADROTOR UAV STABILITY

Theorem 2. *(ISS-like Behavior of Quadrotor System):* Consider the dynamics described by (3). Let the NN observer be defined by (6) and let the observer NN weights be updated at event-sampling instants with (10) with initial weights in a compact set; additionally, let the event-sampled virtual controller be defined by (19) and let the virtual control NN weights be updated at event-sampling instants with (20) with initial weights in a compact set. Moreover, consider the event-sampled desired virtual control inputs and actual control inputs, (26), (32), (37), and (41), respectively, that are designed to stabilize the event-sampled tracking error dynamics given by (27), (33), and(43). Additionally, let the NN weights corresponding to the actual control be updated at event-sampling instants with

$$\dot{\hat{W}}_{c\Xi} = F_c \hat{\sigma}_{c\Xi} \left[A_d \hat{e}_S \right]^T - \kappa_{c1} F_c \hat{W}_{c\Xi}, \tag{44}$$

with initial weights in a compact set and where $\kappa_{c1} > 0$ and $F_c = F_c^T > 0$ are constant design parameter. Finally, let the measurement errors that would be injected into the system as a result of intermittent sampling be bounded such that $\|\Xi_{SX}\| \leq \Xi_{X\ max}$, $\left\|\hat{\Xi}_{SX}\right\| \leq \hat{\Xi}_{X\ max}$,

$\left\|\dot{\Xi}_{SX}\right\| \leq \dot{\Xi}_{X\,\max}$, and $\left\|\dot{\hat{\Xi}}_{SV}\right\| \leq \dot{\hat{\Xi}}_{V\,\max}$. Then, there exist positive design constants K_{o1}, K_{o2}, K_{o3}, $K_{\Omega1}$, $K_{\Omega2}$, and $K_{\Omega3}$, and positive-definite design matrices K_{ρ}, K_{Θ}, K_v, and K_{ω}, such that the observer estimation errors, $\tilde{X}$ and $\tilde{V}$, the NN weight estimation errors, $\tilde{W}_{o\Xi}$, the desired virtual control estimation errors, $\tilde{\Theta}_{d\Xi}$ and $\tilde{\omega}_{d\Xi}$, the virtual control NN estimation errors, $\tilde{W}_{\Omega\Xi}$, the actual control NN weight estimation errors, $\tilde{W}_{c\Xi}$, and the position, orientation, and translational and rotational velocity tracking errors, e_{ρ}, e_{Θ}, and e_S, respectively, are all locally UUB.

Proof. The positive-definite Lyapunov candidate that describes the complete system is given by

$$V_{UAV\,\Xi} = K_{S\,\max}^2 V_{o\Xi} + K_{S\,\max}^2 V_{\Omega\Xi} + V_{c\Xi}$$

where $K_{S\,\max}$ is the maximum singular value of K_S and

$$V_c = \frac{1}{2}e_{\rho}^T e_{\rho} + \frac{1}{2}e_{\Theta}^T e_{\Theta} + \frac{1}{2}e_S^T \bar{J} e_S + \frac{1}{2}\mathrm{tr}\left\{\tilde{W}_c^T F_c^{-1}\tilde{W}_c\right\} \tag{45}$$

The first derivative of $V_{UAV\,\Xi}$ is given by $\dot{V}_{UAV\,\Xi} = K_{S\,\max}^2 \dot{V}_{o\Xi} + K_{S\,\max}^2 \dot{V}_{\Omega\Xi} + \dot{V}_{c\Xi}$. Recall that $\dot{V}_{\Omega\Xi}$ has no explicit measurement errors and were found to be upper bounded by (21). Hence, the effects of event-sampling are considered by evaluating the derivative of (45), which is given by $\dot{V}_{c\Xi} = e_{\rho\Xi}^T \dot{e}_{\rho\Xi} + e_{\Theta\Xi}^T \dot{e}_{\Theta\Xi} + e_{S\Xi}^T \bar{J} \dot{e}_{S\Xi} + \mathrm{tr}\left\{\tilde{W}_{c\Xi}^T F_c^{-1}\dot{\tilde{W}}_{c\Xi}\right\}$ and by combining it with the results found for the observer in Theorem 1. Using the event-sampled tracking error dynamics (27), (33), and (43), it is discovered that

$$\dot{V}_{c\Xi} = -e_{\rho}^T K_{\rho} e_{\rho} + e_{\rho}^T R e_v - e_{\Theta}^T K_{\Theta} e_{\Theta} - e_S^T K_S e_S - e_S^T K_S \tilde{V} + e_S^T K_S \tilde{\omega}_d + e_S^T \xi_c + e_{\rho}^T K_{\rho}\Xi_{\rho}$$
$$+ \mathrm{tr}\left\{\tilde{W}_{c\Xi}^T\left[F_c^{-1}\dot{\tilde{W}}_{c\Xi} + \hat{\sigma}_{c\Xi}\left[A_d e_S\right]^T\right]\right\} + e_{\Theta}^T K_{\Theta}\Xi_{\Theta} + e_S^T K_{X\Xi}^V\Xi_{SX} + e_S^T K_{V\Xi}\dot{\hat{\Xi}}_{SV} \tag{46}$$

after simplification. Additionally, define $e_K = \left[e_{\rho}^T, e_{\Theta}^T\right]^T$, $\Pi = [R, 0_{3\times3}; 0_{3\times6}]$, and $K_K = \left[K_{\rho}, 0_{3\times3}; 0_{3\times3}, K_{\Theta}\right]$. With these, along with the NN weight update law (44), $\dot{V}_{c\Xi}$ can be

rewritten

$$\dot{V}_{c\Xi} = - e_K^T K_K e_K - e_S^T K_S e_S + e_K^T \Pi e_S - e_S^T K_S \tilde{V} + e_S^T K_S \tilde{\omega}_d + e_S^T \xi_c + e_K^T K_K \Xi_{SX}$$

$$+ \operatorname{tr}\left\{ \tilde{W}_{c\Xi}^T \left[\hat{\sigma}_{c\Xi} \left[\tilde{\omega}_d - \tilde{V} \right] A_d^T + \kappa_{c1} \hat{W}_{c1\Xi} \right] \right\} + e_S^T K_{X\Xi}^V \Xi_{SX} + e_S^T K_{V\Xi} \hat{\Xi}_{SV}. \qquad (47)$$

Next, note that $\|\Pi\|_F < \Pi_{\max}$ and $\|W_c\|_F \leq W_{Mc}$ for known constants $\Pi_{\max}$ and W_{Mc}, $\|\tilde{\tilde{\omega}}_d\| = \|\tilde{\omega}_d\|$, and $\operatorname{tr}\left\{ \tilde{W}_{c\Xi}^T \left[W_c - \tilde{W}_{c\Xi} \right] \right\} \leq \left\| \tilde{W}_{c\Xi} \right\|_F W_{c\Omega} - \left\| \tilde{W}_{c\Xi} \right\|_F^2$. Then, introduce the minimum singular values corresponding to K_K and K_S, $K_{K\min}$ and $K_{S\min}$, respectively. Next, observe that $\|A_d\|_F \leq A_{dM}$ for a known constant A_{dM}. Additionally, the computable maximum singular values corresponding to $K_{X\Xi}^V$ and $K_{V\Xi}$ are denoted by $K_{X\Xi\max}^V$ and $K_{V\Xi\max}$, respectively. With these provisions in mind, by completion of squares with respect to $\|e_K\|$, $\left\| \tilde{W}_{c\Xi} \right\|_F$, and $\|e_S\|$, it is discovered that

$$\dot{V}_{c\Xi} \leq - \frac{1}{2} \left[K_{K\min} - 1 \right] \|e_K\|^2 - \frac{1}{2} \left[K_{S\min} - \frac{\Pi_{\max}^2}{K_{K\min}} - 4 \right] \|e_S\|^2 - \frac{\kappa_{c1}}{6} \left\| \tilde{W}_{c\Xi} \right\|_F^2$$

$$+ \frac{1}{2} \left[K_{S\max}^2 + 3 \frac{\left[A_{dM}\sqrt{N_c} \right]^2}{\kappa_{c1}} \right] \left\| \tilde{V} \right\|^2 + \frac{1}{2} \left[K_{S\max}^2 + 3 \frac{\left[A_{dM}\sqrt{N_c} \right]^2}{\kappa_{c1}} \right] \|\tilde{\omega}_{d\Xi}\|^2$$

$$+ \frac{1}{2} \left[K_{K\max}^2 + \left[K_{X\Xi\max}^V \right]^2 \right] \|\Xi_{SX}\|^2 + \frac{1}{2} K_{V\Xi\max}^2 \|\Xi_{SV}\|^2 + \eta_c \qquad (48)$$

where $\eta_c = \kappa_{c1} W_{Mc}^2/2 + \xi_{cM}^2/[2K_{S\min}]$. Now, the results from (48) can be combined with the results found for the observer and virtual controller, (15) and (21), respectively. Recalling the bounds on the measurement errors, it is revealed

$$\dot{V}_{UAV\Xi} \leq -K_{S\max}^2 K_{\tilde{X}} \left\| \tilde{X} \right\|^2 - \frac{K_{S\max}^2}{2} K_{\tilde{V}} \left\| \tilde{V} \right\|^2 - K_{S\max}^2 K_{\tilde{\Theta}d} \left\| \tilde{\Theta}_{d\Xi} \right\|^2 - \frac{K_{S\max}^2}{2} K_{\tilde{\omega}d} \|\tilde{\omega}_{d\Xi}\|^2$$

$$- \frac{1}{2} K_{ek} \|e_K\|^2 - \frac{1}{2} K_{es} \|e_S\|^2 - K_{Wc} \left\| \tilde{W}_{c\Xi} \right\|_F^2 - K_{S\max}^2 K_{Wo} \left\| \tilde{W}_{o\Xi} \right\|_F^2$$

$$- K_{S\max}^2 K_{W\Omega} \left\| \tilde{W}_{\Omega\Xi} \right\|_F^2 + \eta_{UAV} + \Xi_{UAV} \qquad (49)$$

where

$$K_{\tilde{\Theta}d} = K_{\Omega 1} - K_{\Omega 3} - \frac{N_\Omega}{\kappa_{\Omega 1}}, \qquad K_{\tilde{X}} = \frac{[K_{o1} - K_{o3}]}{2} - \frac{N_o}{\kappa_{o1}}, \qquad K_{ek} = K_{K\min} - 1,$$

$$K_{\tilde{V}} = K_{o3} - \frac{2N_o}{\kappa_{o1}} - 2 - \frac{3\left[A_{dM}\sqrt{N_c}\right]^2}{\kappa_{c1}K_{S\max}^2}, \qquad K_{\tilde{\omega}d} = K_{\Omega 3} - \frac{2N_\Omega}{\kappa_{\Omega 1}} - 1 - \frac{3\left[A_{dM}\sqrt{N_c}\right]^2}{\kappa_{c1}K_{S\max}^2},$$

$$K_{Wo} = \frac{\kappa_{o1}}{4}, \qquad K_{W\Omega} = \frac{\kappa_{\Omega 1}}{4}, \qquad K_{Wc} = \frac{\kappa_{c1}}{6},$$

$$\eta_{UAV} = K_{S\max}^2 \eta_o + K_{S\max}^2 \eta_\Omega + \eta_c, \qquad K_{es} = K_{S\min} - \frac{\Pi_{\max}^2}{K_{K\min}} - 4,$$

$$\Xi_{UAV} = \frac{1}{2}\left[K_{K\max}^2 + \left[K_{X\Xi\max}^V\right]^2\right]\Xi_{X\,\max}^2 + \frac{1}{2}K_{V\Xi\max}^2 \hat{\Xi}_{V\,\max}^2$$
$$+ \frac{1}{4}K_{S\max}^2 L_\sigma \Xi_{X\,\max}^4 + \frac{1}{4}K_{S\max}^2 L_\sigma \hat{\Xi}_{X\,\max}^4 + \frac{1}{4}K_{S\max}^2 L_\sigma \dot{\Xi}_{X\,\max}^4. \quad (50)$$

where the bounded term from the observer dynamics, η_o, is defined in Theorem 1. Then, by choosing controller gains satisfying

$$K_{o1} > K_{o3} + \frac{2N_o}{\kappa_{o1}} \qquad K_{o3} > \frac{2N_o}{\kappa_{o1}} + 2 + \frac{3\left[A_{dM}\sqrt{N_c}\right]^2}{\kappa_{c1}K_{S\max}^2}$$

$$K_{\Omega 1} > K_{\Omega 3} + \frac{N_\Omega}{K_{\Omega 1}} \qquad K_{\Omega 3} > \frac{2N_\Omega}{\kappa_{\Omega 1}} + 1 + \frac{3\left[A_{dM}\sqrt{N_c}\right]^2}{\kappa_{c1}K_{S\max}^2}$$

$$K_{K\min} > 1 \qquad K_{S\min} > \frac{\Pi_{\max}^2}{K_{K\min}} + 4 \qquad (51)$$

the first nine terms in (49) are discovered to be less than zero. It follows that $\dot{V}_{UAV\,\Xi}$ is less than zero when controller gains are selected according to (51) and when the following inequalities hold:

$$\left\|\tilde{X}\right\| > \sqrt{\frac{B_{UAV}}{K_{S\max}^2 K_{\tilde{X}}}} \qquad \text{or} \qquad \left\|\tilde{\Theta}_{d\Xi}\right\| > \sqrt{\frac{B_{UAV}}{K_{S\max}^2 K_{\tilde{\Theta}d}}} \qquad \text{or} \qquad \|e_K\| > \sqrt{\frac{2B_{UAV}}{K_{ek}}}$$

or

$$\left\|\tilde{V}\right\| > \sqrt{\frac{2B_{UAV}}{K_{S\max}^2 K_{\tilde{V}}}} \qquad \text{or} \qquad \left\|\tilde{\omega}_{d\Xi}\right\| > \sqrt{\frac{2B_{UAV}}{K_{S\max}^2 K_{\tilde{\omega}d}}} \qquad \text{or} \qquad \left\|e_S\right\| > \sqrt{\frac{2B_{UAV}}{K_{es}}}$$

or

$$\left\|\tilde{W}_{o\Xi}\right\|_F > \sqrt{\frac{B_{UAV}}{K_{Wo}K_{S\max}^2}} \quad \text{or} \quad \left\|\tilde{W}_{\Omega\Xi}\right\|_F > \sqrt{\frac{B_{UAV}}{K_{W\Omega}K_{S\max}^2}} \quad \text{or} \quad \left\|\tilde{W}_{c\Xi}\right\|_F > \sqrt{\frac{B_{UAV}}{K_{Wc}}} \quad (52)$$

where $B_{UAV} = \eta_{UAV} + \Xi_{UAV}$. It can, therefore, be concluded that $\dot{V}_{UAV\,\Xi}$ is less than zero [15] and that all signals in the closed-loop are locally UUB.

Remark 4. By defining the augmented vector

$$\zeta = \left[\left\|\tilde{X}\right\|, \left\|\tilde{V}\right\|, \left\|\tilde{\Theta}_{d\Xi}\right\|, \|\tilde{\omega}_{d\Xi}\|, \|e_K\|, \|e_S\|, \left\|\tilde{W}_{o\Xi}\right\|_F, \left\|\tilde{W}_{\Omega\Xi}\right\|_F, \left\|\tilde{W}_{c\Xi}\right\|_F\right]^T,$$

it is easy to see how (49) can be written in the form $\dot{V}(\zeta) < -\Delta(\|\zeta\|) + \Lambda(\|\eta_{UAV}\|, \|\Xi_{UAV}\|)$, where the positive part, Λ, is viewed as an input to the closed-loop system and is a function of bounded measurement and NN reconstruction errors. It can, therefore, be concluded that the continuously sampled, closed-loop system generates a local ISS-like Lyapunov function. Together with the assumption that the system (3) is locally Lipschitz, this result satisfies all conditions necessary to show that there exists positive, nonzero inter-event periods [6]. This provision is necessary in order to ensure the avoidance of Zeno behavior.

As previously mentioned, the results of Theorem 2 are contingent on the boundedness of the event-sampling measurement errors. However, in order to implement the event-sampled controller, these results, by themselves, are not sufficient. In addition, it is necessary to demonstrate the boundedness of the measurement errors. The following theorem addresses the boundedness of measurement errors by considering two cases: The first case analyzes the dynamics and influences of $\dot{V}_{c\Xi}$ and $\dot{V}_{o\Xi}$ when the measurement errors are

zero and the second case considers the system with nonzero measurement errors. It is in the analysis of the second case where an event-execution law is designed.

Theorem 3. *(Boundedness of Measurement Errors):* Consider the dynamics described by (3). Let the NN observer be defined by (6) and let the observer NN weights be updated at event-sampling instants with (10) with initial weights in a compact set; additionally, let the event-sampled virtual controller be defined by (19) and let the virtual control NN weights be updated at event-sampling instants with (20) with initial weights in a compact set. Moreover, consider the event-sampled desired virtual control inputs and actual control inputs, (26), (32), (37), and (41), respectively, that are designed to stabilize the event-sampled tracking error dynamics given by (27), (33), and(43). Furthermore, let the NN weights corresponding to the actual control be updated at event-sampling instants with (44) with initial weights in a compact set. Finally, let the event-sampling measurement errors satisfy the condition $\|\Xi_{XUAV}\| + \|\Xi_{VUAV}\| \le \gamma_{SX}\mu_{SX} \|e_K\|^2 + \gamma_{SV}\mu_{SV} \|e_S\|^2$, where Ξ_{XUAV} and Ξ_{VUAV} are augmented measurement error vectors corresponding to the quadrotor's measured output and its estimated velocity, respectively; e_K and e_S are the augmented tracking error vectors corresponding to the quadrotor's measured output and its estimated velocity; and $0 < \gamma_{SX}, \gamma_{SV}, \mu_{SX}, \mu_{SV} < 1$ are all design constants. Then, there exist positive design constants K_{o1}, K_{o2}, K_{o3}, $K_{\Omega1}$, $K_{\Omega2}$, and $K_{\Omega3}$, and positive-definite design matrices K_ρ, K_Θ, K_v, and K_ω, such that the observer estimation errors, $\tilde{X}$ and $\tilde{V}$, the NN weight estimation errors, $\tilde{W}_{o\Xi}$, the desired virtual control estimation errors, $\tilde{\Theta}_{d\Xi}$ and $\tilde{\omega}_{d\Xi}$, the virtual control NN estimation errors, $\tilde{W}_{\Omega\Xi}$, the actual control NN weight estimation errors, $\tilde{W}_{c\Xi}$, and the position, orientation, and translational and rotational velocity tracking errors, e_ρ, e_Θ, and e_S, respectively, are all locally UUB. Moreover, given an appropriately designed event-execution law, the measurement errors that result from event-sampling remain bounded for all time.

Proof. The two cases for this proof are as follows:

Case 1. First, consider the definitions given in (50). When the measurement errors are taken to be zero, only a few modifications need to be made in (50) for this first case. At the event-sampling instants, the last three terms in (47) are absent and, as a result, it becomes unnecessary to invoke Young's inequality to separate the measurement errors from the tracking errors. As a result, the coefficients corresponding the the tracking errors become $K_{ek} = K_{K\min}$ and $K_{es} = K_{S\min} - \frac{\Pi_{\max}^2}{K_{K\min}} - 2$. With these considerations in mind, observe that

$$\dot{V}_{c\Xi} \leq -\frac{1}{2} K_{ek} \|e_K\|^2 - \frac{1}{2} K_{es} \|e_S\|^2 - K_{Wc} \left\| \tilde{W}_{c\Xi} \right\|_F^2 + \frac{1}{2} \left[K_{S\max}^2 + 3 \frac{\left[A_{dM} \sqrt{N_c} \right]^2}{\kappa_{c1}} \right] \|\tilde{V}\|^2$$

$$+ \frac{1}{2} \left[K_{S\max}^2 + 3 \frac{\left[A_{dM} \sqrt{N_c} \right]^2}{\kappa_{c1}} \right] \|\tilde{\omega}_{d\Xi}\|^2 + \eta_c. \quad (53)$$

Additionally, incorporating the results from *Lemma 1, Case 1,* the terms corresponding to the observer need to be updated with $K_{\tilde{V}} = K_{o3} - [2N_o] / \kappa_{o1} - 1 - \left[3 \left[A_{dM} \sqrt{N_c} \right]^2 \right] / \left[\kappa_{c1} K_{S\max}^2 \right]$ and $\eta_o = \kappa_{o1} W_{Mo}^2 + \xi_{1M}^2 / [2 [K_{o1} - K_{o3}]] + \xi_{2M}^2 / [2K_{o3}]$. Finally, the third change that needs to be made is in setting $\Xi_{UAV} = 0$. With the changes in the coefficients (50) that are made for this case, the closed-loop dynamics can be expressed with the same expression given by (49). Similarly, the bounds on the control gains remain identical to (51) provided that the condition on K_{o3} as well as the last two conditions are altered, giving a new set of conditions on the control gains

$$K_{o1} > K_{o3} + \frac{2N_o}{\kappa_{o1}} \qquad\qquad K_{o3} > \frac{2N_o}{\kappa_{o1}} + 1 + \frac{3 \left[A_{dM} \sqrt{N_c} \right]^2}{\kappa_{c1} K_{S\max}^2}$$

$$K_{\Omega1} > K_{\Omega3} + \frac{N_\Omega}{K_{\Omega1}} \qquad\qquad K_{\Omega3} > \frac{2N_\Omega}{\kappa_{\Omega1}} + 1 + \frac{3 \left[A_{dM} \sqrt{N_c} \right]^2}{\kappa_{c1} K_{S\max}^2}$$

$$K_{K\min} > 0 \qquad\qquad K_{S\min} > \frac{\Pi_{\max}^2}{K_{K\min}} + 2 \qquad\qquad (54)$$

With all of these modifications made, and provided that the inequalities (52) hold, it can be concluded that $\dot{V}_{UAV\,\Xi}$ is less than zero and that all signals in the closed-loop are locally UUB [15].

Case 2. Now, consider the inter-event period, $t \in [t_l, t_{l+1})$, during which time there is a nonzero event-sampling error, but with constant NN weights; in other words, in this case, $\Xi(t) \neq 0$ and $\dot{\hat{W}} = 0$ for all NN weights. The analyses corresponding to the observer and the virtual control stability with constant NN weight estimates are easy to perform. For the observer dynamics, the results from *Lemma 1, Case 2* can be used here. For the virtual controller dynamics, it is discovered

$$\dot{V}_{\Omega\Xi} \leq -[K_{\Omega 1} - K_{\Omega 3}]\left\|\tilde{\Theta}_d\right\|^2 - \frac{1}{2}[K_{\Omega 3} - 1]\|\tilde{\omega}_d\|^2 + \frac{N_\Omega}{2}\left\|\tilde{W}_\Omega\right\|_F^2 + \eta_\Omega \qquad (55)$$

where $\eta_\Omega = \xi_{\Omega M}^2 / [2K_{\Omega 3}]$ is a constant bounded term. Next, revisiting (46) with $\dot{\tilde{W}}_{c\Xi} = 0$, it is found that

$$\dot{V}_{c\Xi} = -e_\rho^T K_\rho e_\rho + e_\rho^T R e_v - e_\Theta^T K_\Theta e_\Theta - e_S^T K_S e_S - e_S^T K_S \tilde{V} + e_S^T K_S \tilde{\omega}_d + e_\rho^T K_\rho \Xi_\rho$$
$$+ e_S^T \xi_c + \text{tr}\left\{\tilde{W}_{c\Xi}^T \hat{\sigma}_{c\Xi} [A_d e_S]^T\right\} + e_\Theta^T K_\Theta \Xi_\Theta + e_S^T K_{X\Xi}^V \Xi_{SX} + e_S^T K_{V\Xi} \hat{\Xi}_{SV}. \qquad (56)$$

Then, by using properties of the matrix trace operation and completion of squares with respect to $\|e_K\|$ and $\|e_S\|$, it is revealed

$$\dot{V}_{c\Xi} \leq -\frac{1}{2}[K_{K\min} - 1]\|e_K\|^2 - \frac{1}{2}\left[K_{S\min} - \frac{\Pi_{\max}^2}{K_{K\min}} - \left[A_{dM}\sqrt{N_c}\right]^2 - 4\right]\|e_S\|^2$$
$$+ \frac{1}{2}\left\|\tilde{W}_{c\Xi}\right\|^2 + \frac{1}{2}K_{S\max}^2\left\|\tilde{V}\right\|^2 + \frac{1}{2}K_{S\max}^2\|\tilde{\omega}_{d\Xi}\|^2 + \frac{1}{2}\left[K_{K\max}^2 + \left[K_{X\Xi\max}^V\right]^2\right]\|\Xi_{SX}\|^2$$
$$+ \frac{1}{2}K_{V\Xi\max}^2\left\|\hat{\Xi}_{SV}\right\|^2 + \eta_c \qquad (57)$$

where $\eta_c = \xi_{Mc}^2/[2K_{S\min}]$ is a constant bounded term. It is noted here that, since the NN weight estimates are held constant, $\left\|\tilde{W}_\Xi\right\| = \|W\| - \left\|\hat{W}_\Xi\right\|$ remains bounded subject to the weight estimates at the previous event, $\hat{W}_\Xi(t_l)$ for all NN weights.

It is at this point that the event-execution law is derived. Recall that the measurement errors from *Lemma 1, Case 2* still need to be addressed. For clarity, the measurement errors from the observer are shown together with the measurement errors in (57) in the following expression

$$
\begin{aligned}
\Xi_{UAV} =& \frac{1}{2}\left[K_{K\max}^2 + \left[K_{X\Xi\max}^V\right]^2\right]\|\Xi_{SX}\|^2 + \frac{1}{4}K_{S\max}^2 L_\sigma \|\Xi_{SX}\|^4 \\
& + \frac{1}{4}K_{S\max}^2 L_\sigma \left\|\hat{\Xi}_{SX}\right\|^4 + \frac{1}{2}K_{V\Xi\max}^2 \left\|\hat{\Xi}_{SV}\right\|^2 + \frac{1}{4}K_{S\max}^2 L_\sigma \left\|\dot{\Xi}_{SV}\right\|^4.
\end{aligned} \tag{58}
$$

For sake of brevity, (58) will be rearranged so that corresponding measurement errors can be grouped together. Therefore, define $C_X = \left[K_{K\max}^2 + \left[K_{X\Xi\max}^V\right]^2\right]/2$, $C_V = K_{V\Xi\max}^2/2$, $C_L = K_{S\max}^2 L_\sigma/4$, $\Xi_{XUAV} = \left[\|\Xi_{SX}\|^2, \|\Xi_{SX}\|^4, \left\|\hat{\Xi}_{SX}\right\|^4\right]$, and $\Xi_{VUAV} = \left[\left\|\hat{\Xi}_{SV}\right\|^2, \left\|\dot{\Xi}_{SV}\right\|^4\right]$. With these, (58) can be rewritten with

$$
\Xi_{UAV} \leq \|[C_X, C_L, C_L]\| \, \|\Xi_{XUAV}\| + \|[C_V, C_L]\| \, \|\Xi_{VUAV}\|. \tag{59}
$$

Next, the execution law is designed such that the measurement errors satisfy the condition

$$
\|\Xi_{XUAV}\| + \|\Xi_{VUAV}\| \leq \gamma_{SX}\mu_{SX}\|e_K\|^2 + \gamma_{SV}\mu_{SV}\|e_S\|^2 \tag{60}
$$

with $0 < \gamma_{SX}, \gamma_{SV} < 1$ constant design parameters and the terms μ_{SX} and μ_{SV} are chosen such that the number of terms in $\dot{V}_{o\Xi} + \dot{V}_{c\Xi}$ is reduced. To this effect, observe that

$$
\|[C_X, C_L, C_L]\| \, \|\Xi_{XUAV}\| + \|[C_V, C_L]\| \, \|\Xi_{VUAV}\|
$$
$$
\leq \|[C_X, C_L, C_L]\| \, \gamma_{SX}\mu_{SX}\|e_K\|^2 + \|[C_V, C_L]\| \, \gamma_{SV}\mu_{SV}\|e_S\|^2 \tag{61}
$$

Then, selecting

$$\mu_{SX} = \frac{1}{\|[C_X, C_L, C_L]\|} \qquad\qquad \mu_{SV} = \frac{1}{\|[C_V, C_L]\|} \qquad (62)$$

the expression (61) can be rewritten

$$\|[C_X, C_L, C_L]\| \, \|\Xi_{XUAV}\| + \|[C_V, C_L]\| \, \|\Xi_{VUAV}\| \le \gamma_{SX} \|e_K\|^2 + \gamma_{SV} \|e_S\|^2. \qquad (63)$$

Finally, combining (57) and (63) yields

$$\begin{aligned}
\dot{V}_{c\Xi} \le\ & -\frac{1}{2} \left[K_{K\min} - \gamma_{SX} - 1 \right] \|e_K\|^2 \\
& -\frac{1}{2} \left[K_{S\min} - \frac{\Pi_{\max}^2}{K_{K\min}} - \left[A_{dM} \sqrt{N_c} \right]^2 - \gamma_{SV} - 4 \right] \|e_S\|^2 \\
& +\frac{1}{2} \left\| \tilde{W}_{c\Xi} \right\|^2 + \frac{1}{2} K_{S\max}^2 \left\| \tilde{V} \right\|^2 + \frac{1}{2} K_{S\max}^2 \|\tilde{\omega}_{d\Xi}\|^2 + \eta_c \qquad (64)
\end{aligned}$$

Note that, for the expression found in (64), the measurement errors from the observer in *Lemma 1, Case* 2 have been incorporated in the design of the event-execution law. As a final step, the upper bound on $\dot{V}_{c\Xi}$ (64) is combined with the upper bounds (17) and (55) corresponding to the observer and the virtual controller, respectively. In an effort to follow the approach that was taken previously, begin by updating the parameters (50) with

$$K_{\tilde{\Theta}d} = K_{\Omega 1} - K_{\Omega 3}, \qquad K_{\tilde{X}} = \frac{[K_{o1} - K_{o3}]}{2}, \qquad K_{ek} = K_{K\min} - \gamma_{SX} - 1,$$

$$K_{es} = K_{S\min} - \frac{\Pi_{\max}^2}{K_{K\min}} - \left[A_{dM} \sqrt{N_c} \right]^2 - \gamma_{SV} - 4, \qquad K_{\tilde{V}} = K_{o3} - 3, \qquad K_{\tilde{\omega}d} = K_{\Omega 3} - 2,$$

$$K_{Wo} = -\frac{N_o}{2}, \qquad\qquad K_{W\Omega} = -\frac{N_\Omega}{2}, \qquad\qquad K_{Wc} = -\frac{1}{2},$$

$$\eta_{UAV} = K_{S\max}^2 \eta_o + K_{S\max}^2 \eta_\Omega + \eta_c, \qquad\qquad \Xi_{UAV} = 0. \quad (65)$$

One important remark that will be made here is that, with $K_{Wo} = -\frac{N_o}{2}$ and $K_{W\Omega} = -\frac{N_\Omega}{2}$, the bounds in (52) corresponding to the observer and virtual controller NN weight estimates cannot be evaluated and should be disregarded; however, this is not a concern because these terms are altogether absent from the expression for $\dot{V}_{UAV\,\Xi}$ in Case 2. Due to the fact that all NN weight estimates are known to remain bounded during inter-event periods subject to their values at the previous event-sampling instants, the absence of these terms is of no concern.

With the updated parameters (65), the closed-loop dynamics of the UAV system during inter-event periods are described by (49). Then, by selecting controller gains satisfying the conditions

$$K_{o1} > K_{o3}, \qquad K_{o3} > 3, \qquad K_{\Omega 1} > K_{\Omega 3}, \qquad K_{\Omega 3} > 2,$$

$$K_{K\min} > \gamma_{SX} + 1, \qquad\qquad K_{S\min} > \frac{\Pi_{\max}^2}{K_{K\min}} + \gamma_{SV} + 4, \qquad (66)$$

it can be shown that the first nine terms in $\dot{V}_{UAV\,\Xi}$ are less then zero when the inequalities (52) are satisfied, provided that the definitions given by (65) are assumed.

In Case 1, the stability of the system was demonstrated at moments when the measurement errors are zero and when the NN's are updated and it was shown that all signals remain bounded. Then, in Case 2, it was shown how all signals in the system remain bounded during periods of time when there are nonzero measurement errors and when the NN weight estimates are held. In connecting these two cases, one may consider the dynamics that exist at the moments of transition. In other words, the results from Case 1 only show that the dynamics that exist at a single event-sampling instant are bounded; however, by considering "jump dynamics" that may exist in the transitions in the dynamics described

by Cases 1 and 2, it may also be shown that these bounded effects do not accumulate over time and, ultimately, result in instability.

This can be accomplished by extending the results for Case 2 and by considering, not only the estimation error and tracking error dynamics, but also the dynamics of the NN weight estimation errors at event-sampling instants. Since the observer estimation errors and tracking errors have already been shown to be stable for Case 2, it is sufficient to consider discritized NN weight update laws and to demonstrate that they, too, remain bounded in the jump dynamics for all time [16]. As an additional remark, note that, in Case 2, the results were given in terms of the ideal and estimated NN weights; however, with the results summarized here, it is easy to show that the bounds on the NN weight estimation errors are decreasing. Hence, the bounds that exist for the observer estimation errors, the tracking errors, and the NN weight estimation errors are decreasing during the inter-event periods as well as in the jump dynamics.

Finally, the results from Cases 1 and 2 are combined. By considering the intersection of the conditions on the controller gains (54) and (66), from Cases 1 and 2, respectively, and by choosing coefficients from Case 1 and Case 2 such that the bounds (52) are maximized, it can easily be shown that $\dot{V}_{UAV\,\Xi}$ is less than zero and, hence, all signals in the closed-loop are locally UUB [15] for all time. Therefore, it can be concluded that, by designing the event-execution law according to (60) and (62), the measurement errors introduced by event-sampling remain bounded for all time.

With the derivations complete, simulation results may now be presented. The effectiveness of the proposed event-sampled controller will be illustrated and its performance will be compared to that of its time-sampled counterpart.

5 RESULTS AND DISCUSSION

5.1 SIMULATION RESULTS

The objective of the simulations is to illustrate the effects of event-sampling. With this in mind, simulations were performed using the proposed event-sampled controller as well as its time-sampled counterpart presented in [1]. For sake of brevity, only figures for event-sampled results will be presented. In order to evaluate the controller's performance, the averages of the control inputs, tracking errors, and observer estimation errors for both time- and event-sampled controllers will be summarized. Additionally, the effects of varying the parameters γ_{SX} and γ_{SV} will be considered.

The simulations performed in [1] took into account disturbances such as unknown aerodynamic effects, blade flapping, and signal noise. Moreover, it introduced a parameter, α, which describes how thrust is redirected as a result of, in part, wind conditions; by taking this parameter to be initially zero and then suddenly increasing it to $20°$ at $t = 20\,\mathrm{s}$, the effects of an external influence on the system, such as a gust of wind, can be illustrated. All of the considerations that were taken in [1] are taken here.

In general, event-triggering mechanisms for strict-feedback systems can be implemented in numerous ways. In this work, the event-sampling scheme employed is one such that the measurement errors and tracking errors corresponding to the UAV's position and velocity are combined and the combinations become the basis by which an event occurs; specifically, an event takes place when there is a failure in the condition $\|\Xi_{XUAV}\|^2 + \|\Xi_{VUAV}\|^2 \leq \gamma_{SX}\mu_{SX}\|e_K\|^2 + \gamma_{SV}\mu_{SV}\|e_S\|^2$.

Identical simulation parameters and controller gains were used in both simulations. The gains selected in [1] were used here with the following exceptions: The orientation control gains were chosen to be $K_\Theta = \mathrm{diag}\{40,40,40\}$ and the angular velocity control gains were selected as $K_\omega = \mathrm{diag}\{35,35,35\}$. Additionally, the desired trajectory remained identical to what was considered in [1], with the only changes being $\omega_x = \omega_y = 0.06\pi$,

$r_x = r_y = 0.1$, $r_z = 0.5$, and $\omega_\psi = 0.03\pi$. Finally, for the results that are illustrated in the figures, the event-execution parameters were chosen to be $\gamma_{SX} = \gamma_{SV} = 0.95$.

The event-sampled quadrotor UAV trajectory is shown in Figure 5.1. The effects of the sudden disturbance at $t = 20\,\text{s}$ can be clearly seen in the UAV position error. Although the effects of the disturbances are clearly visible, the controller's ability to compensate and recover is also evident. The recovery, however, is not without expense: Figure 5.2 clearly shows an increase in the total thrust and the rotational torque control inputs when the value of α jumps from $0°$ to $20°$.

The results shown in Figures 5.1 and 5.2 demonstrate the stability of the event-sampled controller. However, with regards to the effects of event-sampling, these results are not tremendously revealing. In an effort to illustrate these effects, consider the results shown in Figure 5.3. First, the effectiveness of the event-execution law is demonstrated by showing that the measurement errors are upper bounded by the adaptive threshold. Note the restricted range of simulated time that is displayed: Following the initial spike in the threshold, its magnitude very quickly drops and remains close to zero for the remainder of the simulation. Next, the occurence of events is shown. By normalizing the total number of available samples on the $x-$axis to one and by scaling the number of events with an equivalent factor, it can be seen that about 60% of the total samples are event-sampling instants. In other words, the remaining 40% of the samples are instants when it was unnecessary to update the controller. These results can be summarized by stating that the implementation of the event-sampled controller yielded a 40% reduction in the amount of sampling instants used by the controller.

EFFECTS OF EVENT-SAMPLING. As a final assessment on the effectiveness of event-sampling, consider the information provided in Tables 5.1 and 5.2. Firstly, the effects of changing the event-execution parameters, γ_{SX} and γ_{SV}, are explored and, secondly, the relationship between the number of events and controller performance is assessed. Whereas previous results spoke only to the stability of the controller, the information in Tables 5.1

and 5.2 will allow the perfomance of the event-sampled controller to be compared to that of the time-sampled controller.

Before considering the data, a few remarks will be made concerning the notations in the tables. Firstly, the selection of $\gamma_{SX} = \gamma_{SV} = 0$ is equivalent to implementing the time-sampled controller; hence, the first row will serve as a standard to which the event-sampled cases can be compared. Secondly, the number of events that occur out of the total available samples is given by $\Gamma = (Number\ of\ Events)\ /\ (Total\ Samples\ Available)$; for the time-sampled case, the value for this parameter is unity. Thirdly, as a basis for comparisons, the mean squared errors, $MSE\ (\bullet)$, are considered for the tracking and observer estimation errors corresponding to the position, orientation, and translational and angular velocities. The values summarized in Table 5.1 are calculated with $\aleph_j = \sum\limits_{i=x,y,z} MSE\ (j_i)$ for $j = e_\rho, e_\Theta, e_v, e_\omega, \tilde{\rho}, \tilde{\Theta}, \tilde{v}, \tilde{\omega}$. Finally, in order to analyze control efforts under the influence of event-sampling, the means of the control inputs, $\bar{u}$, are considered in Table 5.2.

First, observe that the number of events increases as γ_{SX} and γ_{SV} are increased; in other words, the number of computations executed by the controller decreases with increasing γ's. This behaviour is explained by noting that, with smaller γ's, the upper bounding threshold on the measurement errors is decreased; with smaller thresholds, it takes less amount of time for the measurement errors to grow, reach its threshold, and trigger an event. If the threshold is made zero by selecting $\gamma_{SX} = \gamma_{SV} = 0$, an event is triggered every instant that finite measurement errors exist and, practically, the event-sampled controller exhibits time-sampled behaviour.

Next, concerning tracking errors, there appears to be marginal differences in the mean squared errors corresponding the position and orientation. With respect to translational and angular velocities, it is clear that the performance of the time-sampled controller is better; this, however, is not to say that the event-sampled controller performs poorly in these areas. As a matter of fact, given the exceptional position and orientation tracking error performances, it would seem that the effects of event-sampling on the velocities are

inconsequential. These conclusions can be very easily made for the observer estimation errors as well. Especially in the case of the observer estimation errors corresponding to translational velocity, it appears that event-sampling has very little effect. Finally, it can be seen that, with event-sampling, the amount of control effort that is needed does not change substantially. It is evident that, especially with the rotational torques, that greater control effort is required, but the additional amount is insignificant relative to the total.

The effects of event-sampling are summarized by the information in Tables 5.1 and 5.2: The use of event-sampling gives flexibility in the amount of computations executed by the controller; moreover, while the reduction in computations does come at a cost with regards to performance, the fidelity of the controller is not significantly compromised.

Table 5.1   Effects of Event-Sampling on Mean Squared Errors

γ_{SX}, γ_{SV}	Γ	$\aleph_{e\rho}$	$\aleph_{e\Theta}$	$\aleph_{ev}$	$\aleph_{e\omega}$	$\aleph_{\tilde{\rho}}$	$\aleph_{\tilde{\Theta}}$	$\aleph_{\tilde{v}}$	$\aleph_{\tilde{\omega}}$
0	1	0.0026	0.0019	0.2608	6.094	3.29×10^{-4}	0.0029	0.0033	0.3117
0.01	0.8050	0.0293	0.0218	2.936	95.93	2.89×10^{-4}	0.0127	0.0040	3.787
0.1	0.7003	0.0249	0.0236	2.448	92.69	3.06×10^{-4}	0.0106	0.0040	2.470
0.5	0.6254	0.0152	0.0189	1.516	48.72	3.35×10^{-4}	0.0081	0.0042	1.467
0.95	0.5705	0.0155	0.0252	1.630	38.97	3.08×10^{-4}	0.0103	0.0042	1.115

Table 5.2   Effects of Event-Sampling on Control Effort Means

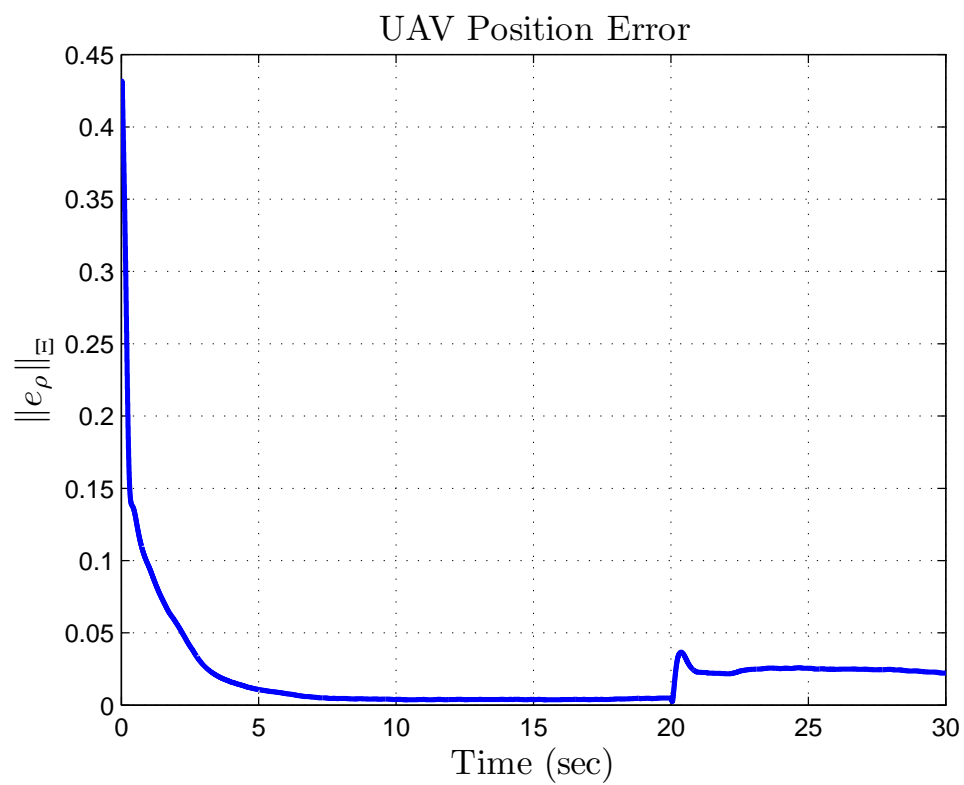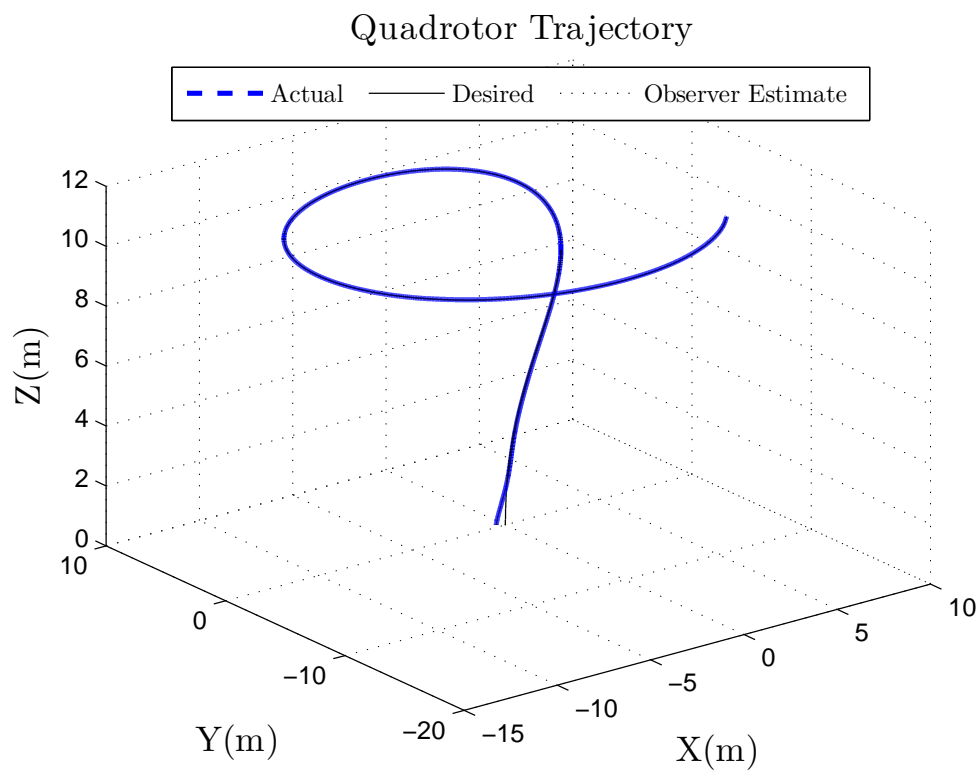| γ_{SX}, γ_{SV}	$\bar{u}_1$	$\bar{u}_{21}$	$\bar{u}_{22}$	$\bar{u}_{23}$
0	9.430	0.7554	1.014	1.155
0.01	9.430	0.7554	1.015	1.136
0.1	9.426	0.6790	1.005	1.089
0.5	9.425	0.6090	0.9772	1.002
0.95	9.426	0.6618	0.9345	0.9668

Quadrotor Trajectory

UAV Position Error

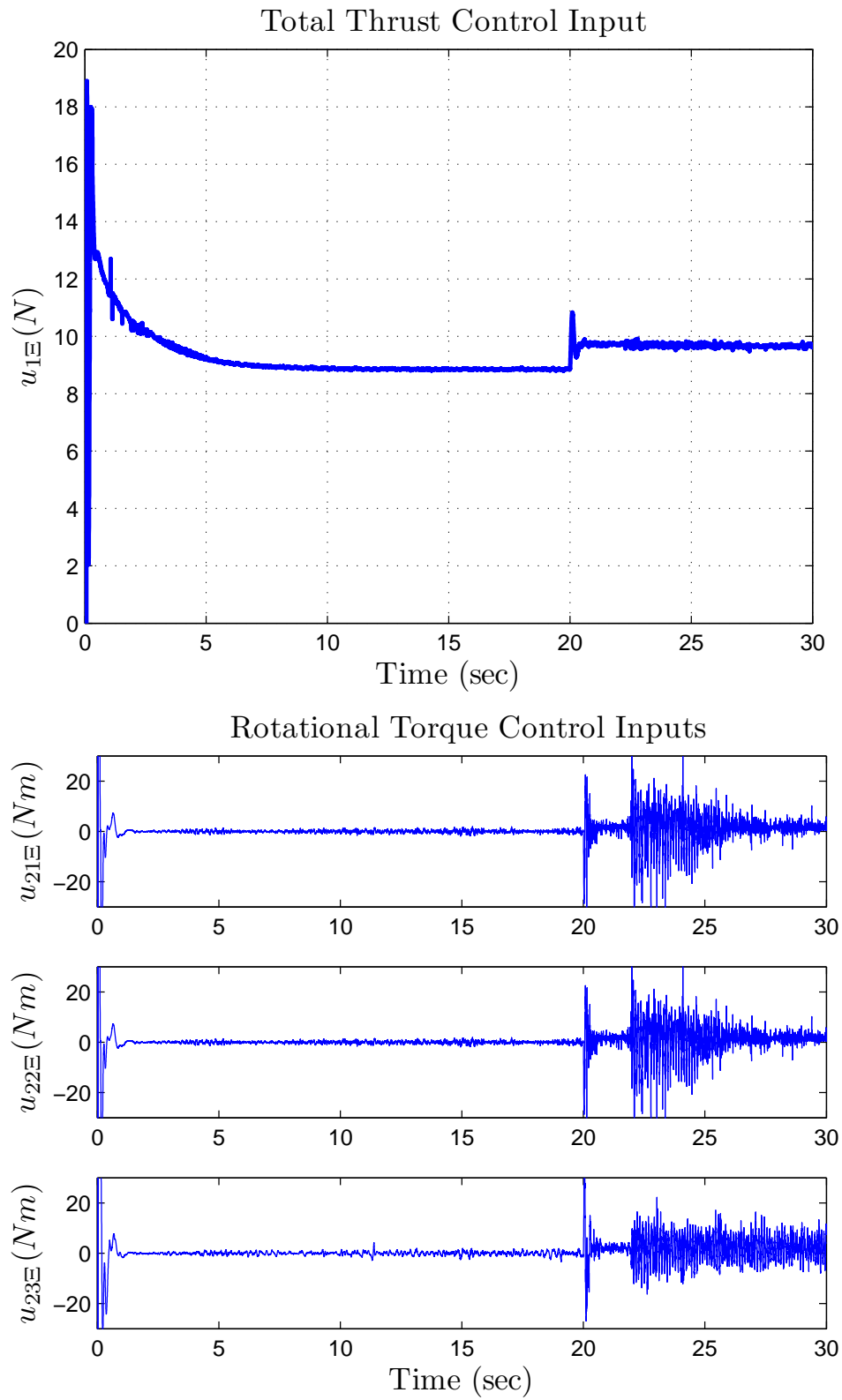Fig. 5.1   UAV Trajectory Tracking
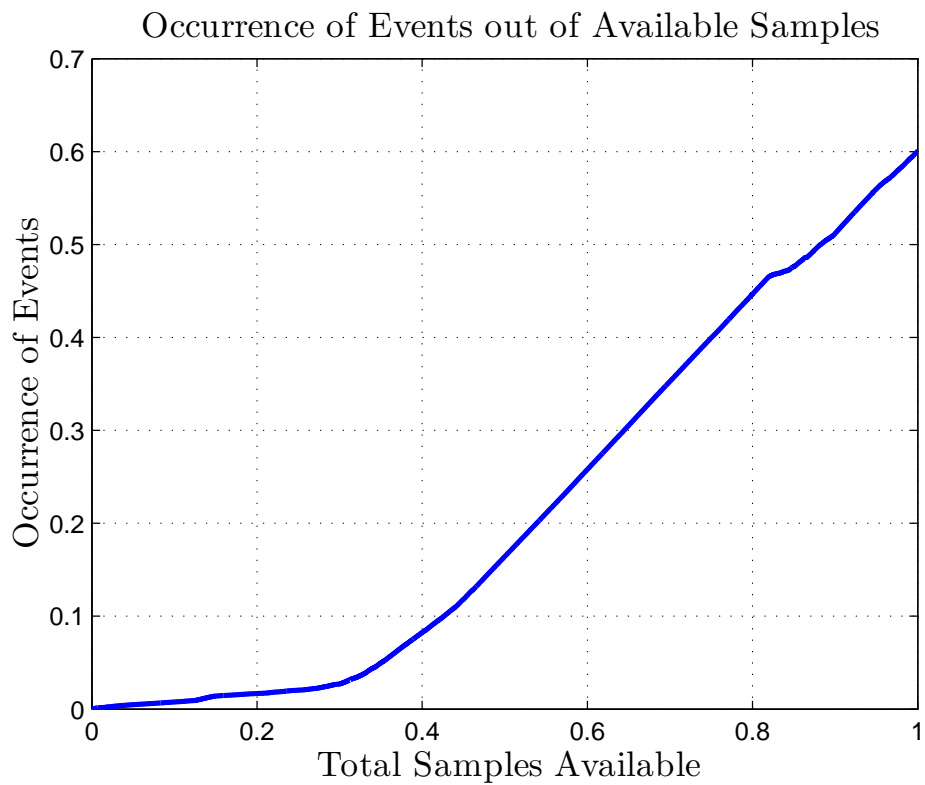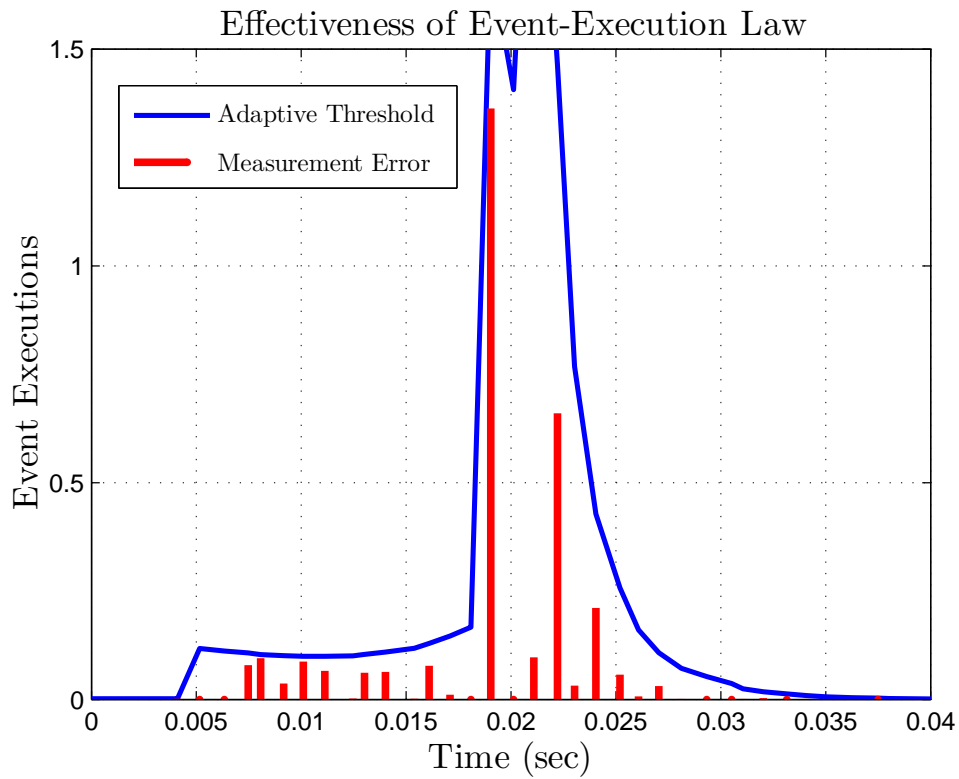
Fig. 5.2   Control Inputs

Fig. 5.3   Effectiveness of Event-Sampling

5.2 HARDWARE IMPLEMENTATION

In order to fully evaluate the effects of event-sampling in the control of a quadrotor, the notions presented in this paper were implemented in hardware. Rather than building a quadrotor from scratch, an Iris+ quadrotor was purchased from 3D Robotics – this decision was made in order to save in hardware development time. The Iris+ utilizes a Pixhawk controller which is an industry standard autopilot that supports the PX4 flight stack and is used in many UAV applications. The Iris+ can be seen alongside the Pixhawk in Fig. 5.4.

The versatility of the Pixhawk controller allows for minimal hardware development. The controller's Inertial Measurement Unit (IMU) comes equipped with a gyroscope, accelerometer, magnetometer, and a barometer; with these sensors, it is possible to measure, among other things, the quadrotor's attitude as well as it's angular velocity. Moreover, the interfaces supported by the Pixhawk include UART, CAN, I2C, and SPI; these options allow for a Global Positioning System (GPS) to provide information on the quadrotor's coordinate position. Furthermore, the controller's PWM outputs are used to apply the generated control inputs to the motors. Additionally, an SD card slot provides an option for easy data logging during flight. Finally, firmware development for the Pixhawk was expedited by making use of the Pilot Support Package (PSP) published by the Pilot Engineering Group from MathWorks. The PSP provides Simulink blocks that access the Pixhawk's sensors, interface ports, and PWM outputs. The measurements can be used in custom algorithms, which are designed using standard Simulink blocks, and then applied to the actuators. Once the controller is created in a Simulink project, MathWorks's Embedded Coder toolbox is utilized to generate code in C and to deploy the firmware onto the Pixhawk. A high-level view of the Simulink project can be seen in Fig. 5.5.

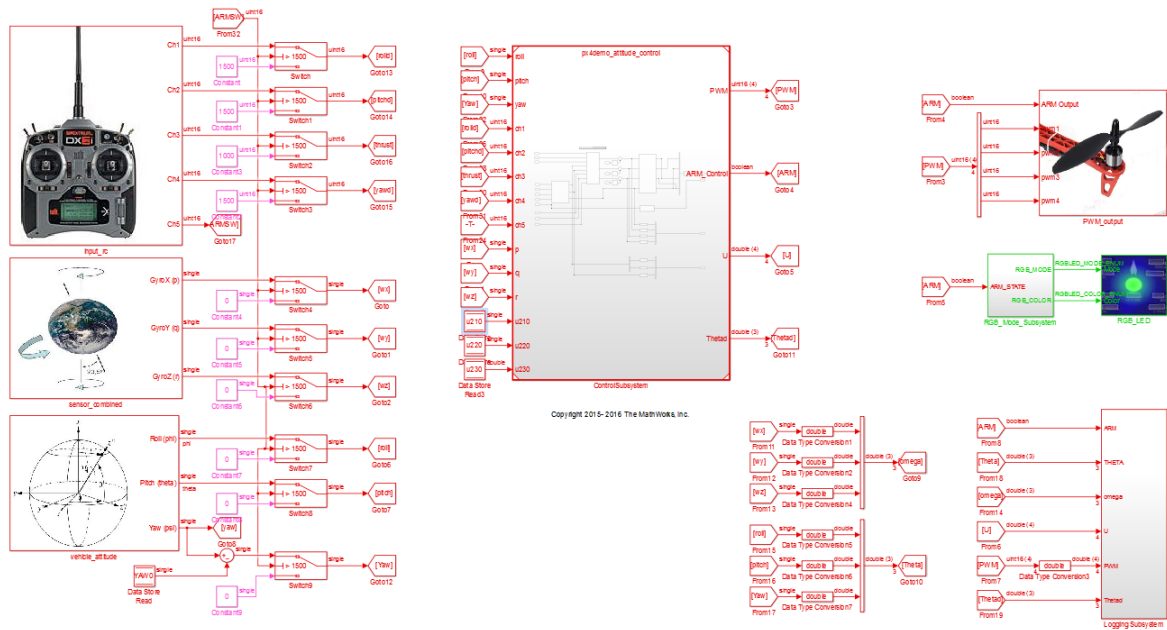Fig. 5.4   Iris+ Quadrotor and Pixhawk Controller

Fig. 5.5   Simulink Project for Quadrotor

Observing Fig. 5.5, inputs are read on the left, the controller is implemeneted in the center-block, and outputs are applied and data is logged on the right. The inputs from the RC controller are 16-bit unsigned integers that range in value from 1000 to 2000; inside the main controller block, these values are normalized to be between -1 and +1. The sensor measurements corresponding to the vehicle's attitude are given in radians and the measurements corresponding to its angular velocity are in radians per second. Inside the controller block, the input data is used to generate control inputs. Then, using a standard motor-mixing formula, the control inputs are converted to four PWM signals; these PWM signals are the output of the main controller block and are applied to the motors. With event-sampling, the rotational torques that are used to calculate the PWM signals which are applied to the motors are held until there is an event; when an event occurs, the controller is updated with the most recent measurements and, ultimately, the PWM values are recalculated and applied to the motors until the next event occurs.

For simplicity, instead of implementing the autonomous NN-based controller which was presented in this paper, an event-based PID controller was evaluated. The approach to

deriving a suitable event-execution law for the PID controller is identical to what has been presented in this work. However, since the desired attitude and thrust of the vehicle are known inputs from the RC transmitter, the derivations became much simpler. Additionally, the control objective was simplified to only track roll, pitch, and yaw trajectories and not to track a specified coordinate position trajectory. In order to accomplish this, the only sensor measurements that are necessary are those corresponding to the quadrotor's orientation and rotational velocity; both of these measurements are readily available from the Pixhawk's IMU.

Since the controller relies on the vehicle's orientation and rotational velocity, the introduction of event-sampling introduces measurement errors corresponding to those sensor readings. Using the Lyapunov-based approach presented in this paper, an event-execution law was derived in order to address these measurement errors. Begin by defining the positive-definite proportional, integral, and derivative gain matrices, $K_{P\Theta} = \text{diag}\left\{k_{P\varphi}, k_{P\theta}, k_{P\psi}\right\}$, $K_{I\Theta} = \text{diag}\left\{k_{I\varphi}, k_{I\theta}, k_{I\psi}\right\}$, and $K_{D\Theta} = \text{diag}\left\{k_{D\varphi}, k_{D\theta}, k_{D\psi}\right\}$, corresponding to the PID controller used to stabilize the vehicle's attitude. Moreover, the gain matrices corresponding to the PID controller which stabilizes the angular rates are defined as $K_{P\omega} = \text{diag}\left\{k_{P\omega x}, k_{P\omega y}, k_{P\omega z}\right\}$, $K_{I\omega} = \text{diag}\left\{k_{I\omega x}, k_{I\omega y}, k_{I\omega z}\right\}$, and $K_{D\omega} = \text{diag}\left\{k_{D\omega x}, k_{D\omega y}, k_{D\omega z}\right\}$. Next, define the augmented vectors $E_{\Theta} = \left[\Xi_{\Theta}^2, \left[\int_0^t \Xi_{\Theta}\, d\tau\right]^2\right]$ and $E_{\omega} = \left[\Xi_{\omega}^2, \left[\int_0^t \Xi_{\omega}\, d\tau\right]^2\right]$ corresponding to orientation and rotational velocity measurement errors, respectively. The coefficient vectors corresponding to these measurement error vectors are $C_{\Theta} = [T_M / [1 + 2\, \|K_{D\Theta}\|\, T_m]]^2 \left[\|K_{P\Theta}\|^2, \|K_{I\Theta}\|^2\right]$ and $C_{\omega} = [1 + 2T_M\, \|K_{D\omega}\|]^2 \left[\|K_{P\omega}\|^2, \|K_{I\omega}\|^2\right]$, where T_M and T_m are the maximum and minimum singular values of the rotation translational matrix, T, respectively. With these, the event-execution law is given by

$$\|E_{\Theta}\| + \|E_{\omega}\| \leq \gamma_{\Theta}\mu_{\Theta} \|e_{\Theta}\|^2 + \gamma_{\omega}\mu_{\omega} \|e_{\omega}\|^2$$

where $0 < \gamma_\Theta, \gamma_\omega < 1$ are design parameters and μ_Θ and μ_ω are chosen to be $\mu_\Theta = 1/\|C_\Theta\|$ and $\mu_\omega = 1/\|C_\omega\|$.

In the results that follow, gains were selected as $K_{P\Theta} = \text{diag}\{4, 3, 3\}$, $K_{I\Theta} = \text{diag}\{0.2, 0.8, 0.6\}$, $K_{D\Theta} = \text{diag}\{0.01, 0.01, 0.01\}$, $K_{P\omega} = \text{diag}\{0.3, 0.4, 0.2\}$, $K_{I\omega} = \text{diag}\{0.1, 0.2, 0.3\}$, and $K_{D\omega} = \text{diag}\{0.01, 0.01, 0.02\}$ and the event-execution parameters were chosen to be $\gamma_\Theta = \gamma_\omega = 0.008$. Figure 5.6 shows the measured and desired roll, pitch, and yaw and it can be seen that the tracking objective was met. Next, Fig. 5.7 illustrates the effectiveness of the proposed event-execution law. Finally, the effectiveness of event-sampling is shown in Fig. 5.8, where it can be seen that, out of a total of 8,000 samples, the control objectives were accomplished with only 5,500 samples.
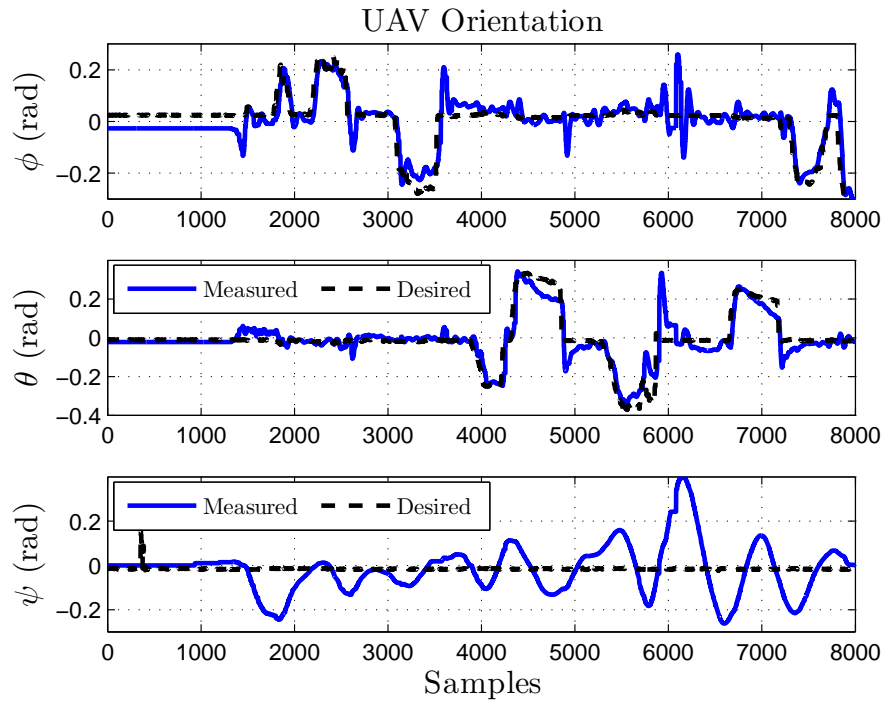

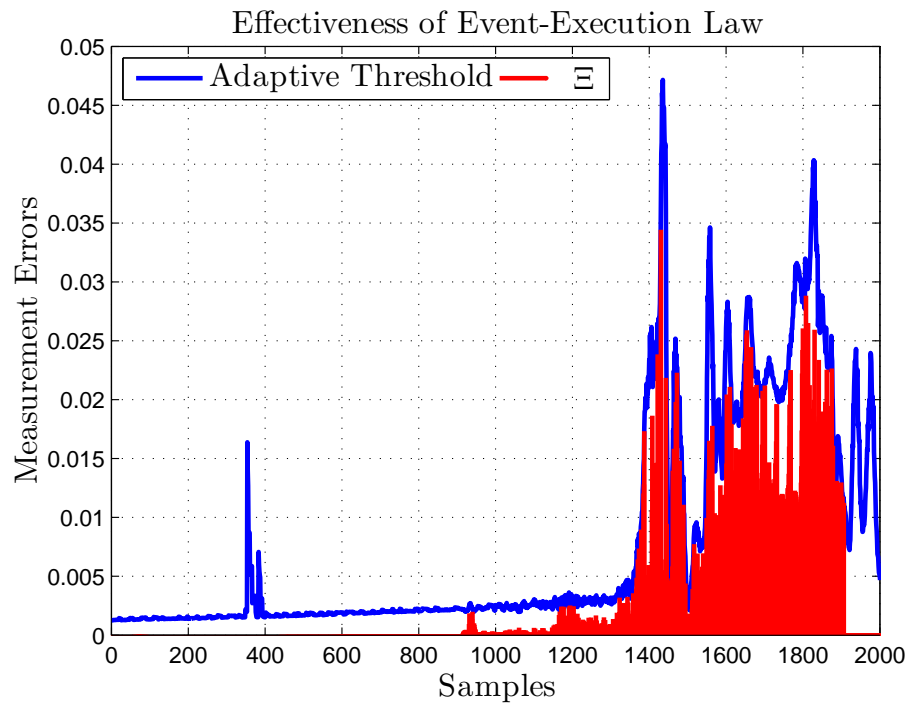Fig. 5.6   Measured and Desired Orientation

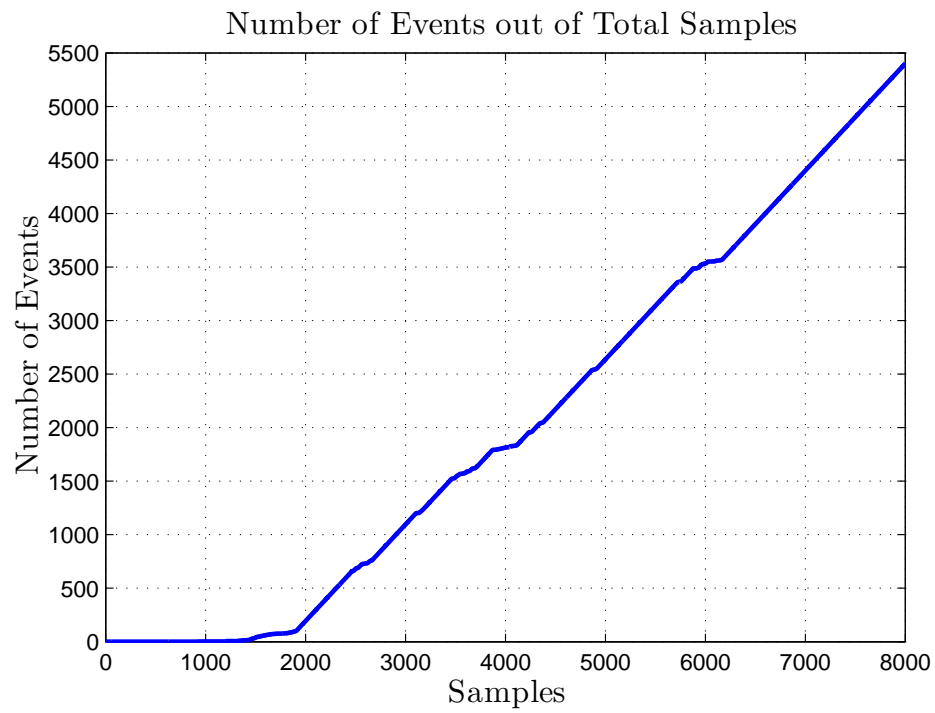Fig. 5.7   Boundedness of Measurement Errors

Fig. 5.8   Number of Events

Finally, by averaging the results from several flights, the information comparing the effects of the event-execution parameters on the number of events and on the mean squared errors corresponding to the orientation tracking errors can be seen in Table 5.3. It can be seen that by increasing γ_Θ and γ_ω, the number of events is reduced; consequently, with fewer events, in general, the tracking performance suffers. These results coincide with the simulation results.

Table 5.3   Effects of Event-Sampling on Number of Events and Mean Squared Errors

$\gamma_\Theta, \gamma_\omega$	Γ	$\aleph_{e\Theta}$
0.001	0.8403	0.0068
0.008	0.7588	0.0263
0.01	0.6158	0.0105
0.03	0.5487	0.0525
0.05	0.1522	0.0520

6 CONCLUSIONS

An event-sampled output-feedback NN controller was developed for an underactuated quadrotor UAV system. Additionally, the overall stability of the quadrotor system was demonstrated in the presence of measurement errors introduced by event-sampling. Finally, the effectiveness of the event-sampled controller was discussed with simulations. The event-sampled controller was found to be effective in reducing the number of computations while maintaining stable performance. Not only was the controller shown to be stable, it was found to perform comparatively well with respect to its time-sampled counterpart. Based on the simulation results, the engineering decision involved with the implementation of event-sampling became apparent: In order to improve the computational efficiency, it becomes necessary to sacrifice tracking and estimation performance. However, depending on how critical performance is, this sacrifice may not be one that is substantial. In the end, the proposed event-sampled controller was found to be effective in providing a greater degree of engineering flexibility.

BIBLIOGRAPHY

[1] T. Dierks and S. Jagannathan, "Output feedback control of a quadrotor UAV using neural networks," *IEEE Trans. Neural Netw.*, vol. 21, no. 1, pp. 50-66, 2010.

[2] H. Voos, "Nonlinear state-dependent Riccati equation control of a quadrotor UAV," *2006 IEEE Conference on Computer Aided Control System Design, 2006 IEEE International Conference on Control Applications, 2006 IEEE International Symposium on Intelligent Control*, 2006.

[3] T. Madani and A. Benallegue, "Sliding mode observer and backstepping control for a quadrotor unmanned aerial vehicles," *2007 American Control Conference*, 2007.

[4] K. Issam and G. Qingbo, "Research on control strategies for the stabilization of quadrotor UAV," *Fifth International Conference on Intelligent Control and Information Processing*, 2014.

[5] D. Lee, T. Burg, B. Xian and D. Dawson, "Output feedback tracking control of an underactuated quad-rotor UAV," *2007 American Control Conference*, 2007.

[6] P. Tabuada, "Event-triggered real-time scheduling of stabilizing control tasks," *IEEE Transactions on Automatic Control*, vol. 52, no. 9, pp. 1680-1685, 2007.

[7] M. Mazo Jr. and P. Tabuada, "Input-to-state stability of self-triggered control systems," in *Joint 48th IEEE Conference on Decision and Control*, Shanghai, P.R. China, 2009, pp. 928-933.

[8] M. Mazo and P. Tabuada, "Decentralized event-triggered control over wireless sensor/actuator networks," *IEEE Transactions on Automatic Control*, vol. 56, no. 10, pp. 2456-2461, 2011.

[9] D. Lehmann and J. Lunze, "A state-feedback approach to event-based control," *Automatica*, vol. 46, no. 1, pp. 211-215, 2010.

[10] D. Lehmann and J. Lunze, "Event-based output-feedback control," *in 19th Mediterranean Conference on Control and Automation*, Corfu, Greece, 2011, pp. 982-987.

[11] P. Tallapragada and N. Chopra, "On event triggered tracking for nonlinear systems," *IEEE Transactions on Automatic Control*, vol. 58, no. 9, pp. 2343-2348, 2013.

[12] A. Sahoo, H. Xu and S. Jagannathan, "Neural network-based event-triggered state feedback control of nonlinear continuous-time systems," *IEEE Trans. Neural Netw. Learning Syst.*, pp. 1-1, 2015.

[13] N. Persson and F. Gustafsson, "Event based sampling with application to vibration analysis in pneumatic tires," *2001 IEEE International Conference on Acoustics, Speech, and Signal Processing*. Proceedings (Cat. No.01CH37221).

[14] H. Wang, Y. Tian and N. Christov, "Event-triggered sampling observer based control design with application to networked visual servoing control systems," *Control Conference (CCC), 2013 32nd Chinese*, pp. 6710-6715, 2013.

[15] F. Lewis, S. Jagannathan and A. Yeşildirek, *Neural Network Control of Robot Manipulators and Nonlinear Systems*. London: Taylor & Francis, 1999.

[16] X. Zhong and H. He, "An Event-Triggered ADP Control Approach for Continuous-Time System With Unknown Internal States," *IEEE Trans. Cybern.*, pp. 1-12, 2016.

SECTION

2   CONCLUSIONS AND FUTURE WORK

In this thesis, event-sampling was incorporated in two different contexts. First, a general strict-feedback system having unknown dynamics was considered and, second, an output-feedback quadrotor UAV controller that was developed in a previous work was revisited. In both these scenarios, event-sampling was considered in the context of neural networks that were implemented in order to compensate for unknown nonlinearities. Moreover, an assumption on full knowledge of the state-vector was relaxed by incorporating NN observers.

In the first scenario, the standard backstepping approach was used. Each subsystem was considered separately and NNs were introduced to compensate for nonlinear uncertainties. First, Lyapunov theory was used to show that the system exhibited ISS-like behaviour with respect to bounded measurement errors. Then, it was shown how Lyapunov analysis can be used to design an event-execution law that guarantees the boundedness of measurement errors introduced by event-sampling. As a corollary, the derivation for a state-feedback controller was also summarized. The effectivness of both controllers was demonstrated with simulation results. As an assessment on the effects of periodic sampling, simulations were performed with the proposed event-sampled controllers as well as their time-sampled counterparts. It was found that, with appropriately selected control gains and event-execution parameters, the number of computations could be substantially reduced without having to sacrifice controller fidelity with respect to tracking performance as well as control effort.

Subsequently, an output-feedback quadrotor UAV controller was revisited. Similar to the first case, Lyapunov theory was first used to demonstrate that the system exhibited ISS-like behavior with respect to bounded measurement errors. Next, the derivation for an event-execution law was demonstrated. Finally, the effectiveness of the proposed event-sampled controller was demonstrated with simulations. It was found that the controller was

able to achieve performance very comparable to that of its time-sampled counterpart all the while reducing the number of computations. To reinforce the notion of event-sampling in a quadrotor control application, an event-based PID controller was implemented in hardware and the results were found to support the theoretical conclusions.

Future work may include the extension of the concepts presented in this work for several different contexts. With the considerations given to the strict-feedback system presented in the first chapter, the conclusions on event-sampling will be able to be applied to a number of applications. Furthermore, the results in this work may extended by considering multi-agent systems. The incorporation of event-sampling in formation control applications may present interesting results in the computational reductions with regards to individual robots as well as to the whole system. Finally, there are still many opportunities to implement the growing number of theoretical results in hardware and to demonstrate the effectiveness of event-sampling in real-world applications. In this work, an event-based quadrotor PID controller was implemented in hardware, however, the implementation of the proposed NN-based controller has yet to be done and the demonstration of event-sampled autonomous flight still needs to be accomplished.

BIBLIOGRAPHY

[1] S. Ge and Cong Wang, "Direct adaptive NN control of a class of nonlinear systems," *IEEE Trans. Neural Netw.*, vol. 13, no. 1, pp. 214-221, 2002.

[2] T. Dierks and S. Jagannathan, "Output feedback control of a quadrotor UAV using neural networks," *IEEE Trans. Neural Netw.*, vol. 21, no. 1, pp. 50-66, 2010.

[3] Zhi Liu, Fang Wang, Yun Zhang, Xin Chen and C. Chen, "Adaptive fuzzy output-feedback controller design for nonlinear systems via backstepping and small-gain approach," *IEEE Trans. Cybern.*, vol. 44, no. 10, pp. 1714-1725, 2014.

[4] S. Tong and Y. Li, "Adaptive fuzzy output feedback tracking backstepping control of strict-feedback nonlinear systems with unknown dead zones," *IEEE Trans. Fuzzy Syst.*, vol. 20, no. 1, pp. 168-180, 2012.

[5] S. Tong, Y. Li and P. Shi, "Observer-based adaptive fuzzy backstepping output feedback control of uncertain MIMO pure-feedback nonlinear systems," *IEEE Trans. Fuzzy Syst.*, vol. 20, no. 4, pp. 771-785, 2012.

[6] S. Shanwei, "Output-feedback tracking control for a class of nonlinear non-minimum phase systems via backstepping method," *in 34th Chinese Control Conference*, 2015, pp. 475-480.

[7] P. Tabuada, "Event-triggered real-time scheduling of stabilizing control tasks," *IEEE Transactions on Automatic Control*, vol. 52, no. 9, pp. 1680-1685, 2007.

[8] M. Mazo Jr. and P. Tabuada, "Input-to-state stability of self-triggered control systems," in *Joint 48th IEEE Conference on Decision and Control*, Shanghai, P.R. China, 2009, pp. 928-933.

[9] M. Mazo and P. Tabuada, "Decentralized event-triggered control over wireless sensor/actuator networks," *IEEE Transactions on Automatic Control*, vol. 56, no. 10, pp. 2456-2461, 2011.

[10] D. Lehmann and J. Lunze, "A state-feedback approach to event-based control," *Automatica*, vol. 46, no. 1, pp. 211-215, 2010.

[11] D. Lehmann and J. Lunze, "Event-based output-feedback control," *in 19th Mediterranean Conference on Control and Automation*, Corfu, Greece, 2011, pp. 982-987.

[12] P. Tallapragada and N. Chopra, "On event triggered tracking for nonlinear systems," *IEEE Transactions on Automatic Control*, vol. 58, no. 9, pp. 2343-2348, 2013.

[13] A. Sahoo, H. Xu and S. Jagannathan, "Neural network-based event-triggered state feedback control of nonlinear continuous-time systems," *IEEE Trans. Neural Netw. Learning Syst.*, pp. 1-1, 2015.

[14] N. Persson and F. Gustafsson, "Event based sampling with application to vibration analysis in pneumatic tires," *2001 IEEE International Conference on Acoustics, Speech, and Signal Processing*. Proceedings (Cat. No.01CH37221).

[15] H. Wang, Y. Tian and N. Christov, "Event-triggered sampling observer based control design with application to networked visual servoing control systems," *Control Conference (CCC), 2013 32nd Chinese*, pp. 6710-6715, 2013.

VITA

Nathan Szanto was born in Portland, Oregon in 1992. He earned a Bachelor of Science degree in Electrical Engineering while attending Missouri University of Science and Technology in May 2014. He earned a Master of Science degree in Electrical Engineering in December 2016 while attending Missouri University of Science and Technology.